

**NASA Contractor Report 180809**

**EVALUATION OF COATED COLUMBIUM TEST  
PANELS HAVING APPLICATION TO A  
SECONDARY NOZZLE EXTENSION FOR THE  
RL10 ROCKET ENGINE SYSTEM; PARTS I  
AND II**

**FINAL REPORT**

*Pratt & Whitney  
Government Engine Business  
P.O. Box 109600  
West Palm Beach, Florida 33410-9600*

**December 1988**

**Prepared for:  
Lewis Research Center  
Under Contract NAS3-25052**



National Aeronautics and  
Space Administration



**NASA Contractor Report 180809**

**EVALUATION OF COATED COLUMBIUM TEST  
PANELS HAVING APPLICATION TO A  
SECONDARY NOZZLE EXTENSION FOR THE  
RL10 ROCKET ENGINE SYSTEM; PARTS I  
AND II**

**FINAL REPORT**

*Pratt & Whitney  
Government Engine Business  
P.O. Box 109600  
West Palm Beach, Florida 33410-9600*

**December 1988**

**Prepared for:  
Lewis Research Center  
Under Contract NAS3-25052**



National Aeronautics and  
Space Administration

## FOREWORD

This report summarizes the activity performed by Pratt & Whitney on the screening and evaluation of various coatings for application on columbium alloy test panels representative of a radiation-cooled nozzle extension for the RL10 rocket engine. This evaluation was conducted in two parts during the period from September 1984 through June 1986. Efforts under Part I entailed the evaluation of vendors and processes of candidate coatings, while Part II consisted of post engine test evaluation of the two coatings selected in Part I. The program was performed in compliance with the requirements stipulated under NASA Lewis Research Center Contract NAS3-25052 where various methods of improving the performance of the RL10 engine were investigated.

The principal investigators responsible for this effort were Kenneth S. Murphy, Senior Materials Engineer and Joaquin H. Castro, Senior Experimental/Test Engineer. Technical Monitoring was performed by Richard L. DeWitt of the NASA Lewis Research Center.

PRECEDING PAGE BLANK NOT FILMED

**PART I  
COATING VENDOR/PROCESS  
EVALUATION**

**PRECEDING PAGE BLANK NOT FILMED**

**v**

**PAGE iv INTENTIONALLY BLANK**

## CONTENTS

<i>Section</i>		<i>Page</i>
1.0	BACKGROUND .....	I-1
2.0	AS-COATED PANEL EVALUATION .....	I-3
2.1	Silicide Coatings .....	I-4
2.1.1	R512-E: Hitemco .....	I-4
2.1.2	W3-Mod: Chromalloy .....	I-4
2.1.3	VH-109: Vac Hyd .....	I-5
2.2	Aluminide Coatings .....	I-5
2.2.1	VH-9: Vac Hyd .....	I-5
2.2.2	R505-F: Hitemco .....	I-5
2.2.3	VH-2: Vac Hyd .....	I-5
2.2.4	RT-40: Chromalloy .....	I-6
3.0	DISCUSSION .....	I-7
4.0	CONCLUSIONS .....	I-8

PRECEDING PAGE BLANK NOT FILMED

## ILLUSTRATIONS

<i>Figure</i>		<i>Page</i>
1-1	Typical Test Panel Attachment to RL10 Exhaust Nozzle .....	I-9
2-1	Standard Panel Sectioning Diagram .....	I-10
2-2	Backscattered Electron Image Identifying the Coating Locations (Phases) Analyzed .....	I-11
2-3	Side 1 of Hitemco R512-E (Flame Side) .....	I-12
2-4	Side 2 of Hitemco R512-E .....	I-13
2-5	Hitemco R512-E Coating and Substrate Thickness Distribution .....	I-14
2-6	Hitemco R512-E Microstructure (Etch: 60% Lactic; 20% HNO <sub>3</sub> ; 20% Hf; Thickness: $3.1 \pm 0.5$ mils) .....	I-15
2-7	Elemental X-ray Maps of Hitemco R512-E — Side 1 (Sheet 1 of 2) ..	I-16
2-8	Side 1 of Chromalloy W3-Mod. CVD Si (Flame Side) .....	I-18
2-9	Side 2 of Chromalloy W3-Mod. CVD Si .....	I-19
2-10	Chromalloy W3-Mod. CVD Si Coating and Substrate Thickness Distributions .....	I-20
2-11	Chromalloy W3-Mod. Sample (Etch: 60% Lactic; 20% HNO <sub>3</sub> ; 20% Hf; Thickness: $1.4 \pm 0.2$ mils) .....	I-21
2-12	Elemental X-ray Maps of Chromalloy W3-Mod. (Sheet 1 of 2) .....	I-22
2-13	Side 1 of Vac Hyd VH-109 Coated Sample (Flame Side) .....	I-24
2-14	Side 2 of Vac Hyd VH-109 Coated Sample .....	I-25
2-15	Vac Hyd VH-109 Coating and Substrate Thickness Distribution .....	I-26
2-16	Vac Hyd VH-109 Microstructure (Etch: 60% Lactic; 20% HNO <sub>3</sub> ; 20% Hf; Thickness: $4.1 \pm 0.4$ mils) (Sheet 1 of 2) .....	I-27
2-17	Elemental X-ray Maps of Vac Hyd VH-109 (Sheet 1 of 2) .....	I-29
2-18	Side 1 of Vac Hyd VH-9 Coated Sample (Flame Side) .....	I-31
2-19	Side 2 of Vac Hyd VH-9 Coated Sample .....	I-32
2-20	Vac Hyd VH-9 Coating and Substrate Thickness Distributions .....	I-33
2-21	Vac Hyd VH-9 Microstructure (Etch: 60% Lactic; 20% HNO <sub>3</sub> ; 20% Hf; Thickness: $2.6 \pm 1.5$ mils) (Sheet 1 of 2) .....	I-34

## ILLUSTRATIONS (Continued)

<i>Figure</i>		<i>Page</i>
2-22	Elemental X-ray Maps of Vac Hyd VH-9 (Sheet 1 of 2) .....	I-36
2-23	Side 1 of Hitemco R505-F (Flame Side) .....	I-38
2-24	Side 2 of Hitemco R505-F .....	I-39
2-25	Hitemco R505-F Coating and Substrate Thickness Distributions .....	I-40
2-26	Hitemco R505-F Microstructure (Etch: 10% HCL; 90% H <sub>2</sub> O; Thickness 3.4±1.0 mils) (Sheet 1 of 2) .....	I-41
2-27	Elemental X-ray Maps of Hitemco R505-F (Sheet 1 of 2) .....	I-43
2-28	Side 1 of Vac Hyd VH-2 Coating Sample (Flame Side) .....	I-45
2-29	Side 2 of Vac Hyd VH-2 Coating Sample .....	I-46
2-30	Vac Hyd VH-2 Coating and Substrate Thickness Distributions .....	I-46
2-31	Vac Hyd VH-2 Microstructure (Etch: 60% Lactic; 20% HNO <sub>3</sub> ; 20% Hf; Thickness: 5.3±0.8 mils) (Sheet 1 of 2) .....	I-47
2-32	Elemental X-ray Maps of Vac Hyd VH-2 .....	I-49
2-33	Side 1 of Chromalloy RT-40 (Flame Side) .....	I-50
2-34	Side 2 of Chromalloy RT-40 .....	I-51
2-35	Chromalloy RT40 Coating and Substrate Thickness Distributions .....	I-51
2-36	Chromalloy RT-40 Microstructure (Etch: 60% Lactic; 20% HNO <sub>3</sub> ; 20% Hf; Thickness: 0.5±0.1 mil) .....	I-52
2-37	Elemental X-ray Maps of Chromalloy RT-40 (Sheet 1 of 2) .....	I-53

## **SECTION 1.0 BACKGROUND**

To increase the specific impulse of the RL10 liquid hydrogen/liquid oxygen rocket engine, a nozzle extension has been proposed. The extension will translate between stowed and deployed positions. When stowed, the extension will be nested with the regeneratively cooled RL10 nozzle. Two versions of the extension are planned for different models of the RL10. One version will be designed for the RL10A-3-3A and be 20 inches long, while the other version will be for the RL10-IIB, 55 inches long.

A commercially available columbium (niobium) alloy, C-103, has been chosen as the structural material for the nozzle extension. This alloy has the necessary high-temperature strength properties that are estimated to be required for the longer version of the nozzle. However, C-103 is susceptible to both hydrogen and oxygen embrittlement as well as high temperature oxidation. Therefore, a coating must be applied to C-103 to protect the alloy from the deleterious effects of the  $H_2O/H_2/O_2$  environment created by the RL10.

At the onset of the screening effort, several guidelines were established:

- The coating would be vendor applied and fully developed
- The vendor must possess equipment and facilities capable of coating the large diameter nozzles
- The vendor shall apply  $3.0 \pm 1.0$  mils of coating to test panels for screening evaluation
- The test panels will be tested in the engine environment by attachment to an RL10 nozzle during test firing (Figure 1-1).

After a literature search of possible coatings and coating vendors, contact was made with candidate vendors to explain the RL10 C-103 nozzle extension requirements. Vendors who could not comply with the above guidelines were no longer considered for this effort. Vendors that could comply with the guidelines were supplied with 15-mil C-103 sheet test panels.

Various coatings were recommended by P&W's Materials Engineering and Technology laboratory and the vendors. The coatings selected are of two basic types, aluminides and silicides. A summary of the coatings is given in Table 1-1.

**TABLE 1-1. — SELECTED VENDOR AND COATINGS**

<i>Vendor</i>	<i>Coating</i>	<i>Constituents</i>	<i>Application Technique</i>
Chromalloy	RT-40	Si + Al	CVD + Pack
Chromalloy	W3-Mod	Si	CVD
Hitemco	R512-E	Si,Cr,Fe	Slurry
Hitemco	R505-F	Al,Sn,Mo	Slurry
Vac-Hyd	VH-2	Al	Slurry
Vac-Hyd	VH-9	Al,Ti	Slurry
Vac-Hyd	VH-109	Si,Cr,Hf,Zr,Fe	Slurry

R20482/1



## SECTION 2.0 AS-COATED PANEL EVALUATION

All panel test samples were color photographed, rough cut with a drummel tool to obtain the four standard sections (Figure 2-1), fine cut with a slow-speed, diamond blade saw, and nickel plated to minimize coating edge rounding and preserve as-coated features. All metallographic mounts were mechanically polished. The brittle nature of columbium silicide and aluminide coatings complicates metallographic preparation. Therefore, most microstructures have cracks and other damage that have been induced by metallography. Typical coating microstructures and significant deviations were documented via standard light photomicroscopy. Coating thickness and remaining substrate thickness distributions were determined to document the actual coating thickness applied and the extent of interdiffusion with the C-103 substrate. Table 2-1 summarizes the information gathered regarding each coating. Nominal coating compositions and elemental x-ray maps were obtained from microprobe analysis. All coating compositions are tabulated in Table 2-2.

TABLE 2-1. — SUMMARY OF COATING CHARACTERISTICS

<i>Coating Type</i>	<i>Vendor</i>	<i>Designation</i>	<i>Constituents (Target) (Actual)</i>	<i>Application Technique</i>	<i>Coating Thickness (mils)</i>	<i>Substrate Thickness (mils)</i>	<i>Comments</i>
Silicide	Hitemco	R512-E	Si-Cr-Fe Si-Cr-Fe	Slurry	3.1±0.5	14.9±1.7	Excellent integrity
Silicide	Vac-Hyd	VH-109	Si-Hf-Cr-Zr-Fe Si-Hf-Cr-Zr-Fe	Slurry	4.1±0.4	10.5±0.2	Excellent Integrity Slightly thicker than required
Silicide	Chromalloy	W3-Mod	Si Si	CVD	1.4±0.2	15.5±0.1	Excellent integrity One-half of thickness required
Aluminide	Vac-Hyd	VH-2	Al Al	Slurry	5.3±0.8	22.8±0.4	Questionable structural integrity — "pull-out" Incomplete coating coverage
Aluminide	Hitemco	R505-F	Sn-Al-Mo Sn-Al-Mo	Slurry	3.4±1.0	16.2±0.6	Questionable structural integrity — "pull-out" Nearly incomplete coating coverage at sample edges
Aluminide	Vac-Hyd	VH-9	Al-Ti Si-Cr-Al-Ti	Slurry	2.6±1.5	8.4±0.7	Unique layer coating profile Radical thickness variations — coating and substrate Significant substrate consumption during coating process Unexpected detection of Si and Cr
Aluminide	Chromalloy	RT-40	Si-Al Si-Cr-Fe	CVD/Pack	0.5±0.1	16.1±0.1	No Al in coating Coating origin unknown Coating thickness well under design goal

R20482/1

TABLE 2-2. — COATING COMPOSITIONS (BY WEIGHT IN PERCENT)

Coating	Location	Cb	Si	Cr	Fe	Hf	Al	Mo	Sn
*R512-E	1	64.2	22.0	1.5	4.4	8.4	—	—	—
	2	49.0	34.9	3.8	7.8	4.5	—	—	—
	3	36.7	28.6	10.6	16.7	7.3	—	—	—
	4	53.0	44.6	2.0	—	0.3	—	—	—
*VH-109	1	68.0	21.2	1.8	0.3	8.7	—	—	—
	2	55.5	40.5	0.9	0.2	2.9	—	—	—
	3	31.4	24.9	22.6	1.7	19.5	—	—	—
	4	49.3	42.1	3.9	0.2	4.5	—	—	—
	5	13.0	26.4	44.5	1.7	14.4	—	—	—
W3-Mod	General	54.0	40.0	0.2	0.2	6.0	—	—	—
VH-2	General	49.5	—	—	—	5.5	45.0	—	—
R505-F	Matrix	—	—	—	—	—	—	—	100
	Precipitates	—	—	—	—	—	8.0	92.0	—
	Interface	48.2	—	—	—	—	45.5	—	6.4
VH-9	Outer Zone(Si)	53.3	38.6	2.1	0.2	2.6	2.6	—	—
	Inner Zone(Al)	50.5	11.1	—	—	4.8	33.6	—	—
RT-40	Outer Zone	—	37.6	28.8	33.7	—	—	—	—
	Inner Zone	55.0	38.7	0.6	0.6	5.0	—	—	—

\*Refer to Figure 2-2 to correlate analysis location to phase of microstructure.

R20482/1

## 2.1 SILICIDE COATINGS

### 2.1.1 R512-E: Hitemco

Hitemco has extensive experience coating C-103 material with R512-E (Si-20Cr-20Fe). This coating/substrate combination is presently used in parts for the augmentor of the P&W F100 jet engine. No visually obvious surface flaws were detected on the as-received panels (Figures 2-3 and 2-4). Metallographic examination showed that the nominal  $3.0 \pm 1.0$ -mil goal was achieved with approximately 1.0 mil of interdiffusion. Coating and substrate thicknesses averaged  $3.1 \pm 0.5$  and  $14.9 \pm 1.7$  mils respectively (Figure 2-5). The microstructure was typical for R512-E (Figure 2-6). Through-thickness cracks were present, but are common in the typical R512-E microstructure. These cracks are usually attributed to metallographic preparation. Microprobe results were typical of R512-E. The backscattered image (BSI) and elemental maps illustrated the interaction of the coating elements (Si, Cr, and Fe) with the substrate elements (Cb, Hf, and Ti) (Figure 2-7).

### 2.1.2 W3-Mod: Chromalloy

Chromalloy has acquired a CVD system capable of coating RL10 nozzle extensions. The general appearance of the coated panels was good (Figure 2-8 and 2-9). The coating appeared to be uniformly applied to all regions of the panel. Metallographic documentation of the coating and substrate thicknesses are illustrated in Figure 2-10. The coating thickness averaged  $1.4 \pm 0.2$  mils, which is much thinner than the target thickness of 3.0 mils. Chromalloy speculates that as Si is deposited and reacts with Cb, the resultant CbSi phase retards further reaction, thus limiting the coating thickness that can be attained in a reasonable time frame. The substrate thickness was very consistent at 15.5 mils. Chromalloy indicates that the coating is

more of a buildup type than an interdiffusion type; therefore, limited or no substrate conversion to coating would be expected. The microstructure was consistent with occasional through-thickness cracks (Figure 2-11). These cracks were attributed to metallographic preparation. Characteristic x-ray elemental maps identified the presence of substrate elements (Cb, Hf and Ti) in addition to Si in the coating (Figure 2-12).

### **2.1.3 VH-109: Vac Hyd**

The general appearance of the VH-109 coating was good. However, minor discolorations and surface roughness variations were evident in the vicinity of the panel edges (Figures 2-13 and 2-14). The average coating thickness,  $4.1 \pm 0.4$  mils, was slightly thicker than the target thickness of  $3.0 \pm 1.0$  mils (Figure 2-15). This small thickness variation should not affect the coating performance. The substrate thickness is 4.5 mils below the original 15-mil-thick sheet. However, variations in sheet thickness combined with 1.0 mil of interdiffusion per panel face could result in 10 mils of substrate after coating. The typical microstructure had through-thickness cracks (probably induced by metallography), and a phase at the coating midplane that was intermittently present (Figure 2-16). Also, a significantly thick oxide layer had formed on the coating. Microprobe analysis resolved the intermittent precipitates as Hf- and Cr-rich (Figure 2-17). These elements were also present in the apparent interdiffusion zone. Observations from the x-ray maps indicated that the oxide was Hf-rich with Si and Cb.

## **2.2 ALUMINIDE COATINGS**

### **2.2.1 VH-9: Vac Hyd**

The as-received VH-9 panel was dark gray with many surface protuberances near the panel edges (Figures 2-18 and 2-19). The panel was visually thinner than uncoated panels, and metallography confirmed this observation (Figures 2-20 and 2-21). The coating thickness was inconsistent, ranging between 7.0 mils at protuberances to 1.5 mils in other locations. The substrate thickness was thin, ranging from 7.0 to 9.5 mils. No logical explanation for the large deviation from the original 15-mil panel thickness can be determined. The microstructures in Figure 2-21 readily depict the inconsistent nature of this coating/substrate system. Microprobe analysis showed the coating was layered (Figure 2-22). The outer region was rich in Si with some Cr. The apparent interdiffusion zone was rich in Al. Locally high concentrations of Si, Cr, Ti, Hf and Al were present throughout the coating. The detection of Si and Cr was unexpected in the microstructure. No plausible explanation was offered by the vendor.

### **2.2.2 R505-F: Hitemco**

The R505-F coated panel had visual streaks and surface discolorations (Figures 2-23 and 2-24). Coating average thickness was  $3.6 \pm 1.5$  mils. However, Region 4 showed a consistently thicker coating of about 5.0 mils (Figure 2-25). The substrate thickness averaged  $16.2 \pm 0.6$  mils. The typical coating had globular MoAl precipitates in a Sn matrix. A very thin interdiffusion zone was evident. Some regions show extensive voids in the coating. It was unclear whether the voids were entrapped gas or associated with metallographic pull-out. (Figure 2-26). Panel edges had thin coatings and may be problem areas for complete coating coverage. Microprobe results identified the interdiffusion zone as Al rich (Figure 2-27). Cb appeared to have interacted with the MoAl precipitates while Hf and Ti were barely detected in the coating. Sn was the predominant coating matrix material.

### **2.2.3 VH-2: Vac Hyd**

The VH-2 coating had a blue-gray color and was very smooth (Figures 2-28 and 2-29). The coating thickness was greater than requested,  $5.3 \pm 0.8$  mils (Figure 2-30). The substrate was

unusually thick, between 22.0 and 23.0 mils. Metallographically, the coating appears to be composed of spherical particles with very little interaction with the substrate (Figure 2-31). The particles were closely packed near the substrate and loosely held together near the external surface. Small voids in the coating about 0.6 mil above the coating/substrate interface evolved during metallographic polishing. Edge corners had unusual coating coverage. The coating did not cover corners uniformly and continuously. The microprobe detected only Al in the coating and discussions with Vac-Hyd confirmed the VH-2 composition as consisting essentially of Al (Figure 2-32).

#### **2.2.4 RT-40: Chromalloy**

The RT-40 coating had numerous surface discolorations on both panel faces (Figures 2-33 and 2-34). Metallurgical evaluation of the coating was conducted on a test coupon. The coating thickness was significantly under the  $3.0 \pm 1.0$ -mil requirement (Figure 2-35). The coating thickness averaged  $0.5 \pm 0.1$  mil. The substrate thickness was about 17 mils. Metallographic results showed that the coating was uniformly thin with numerous through-thickness cracks (Figure 2-36). Microprobe results detected no Al in the coating (Figure 2-37). Si, Cr and Fe were detected in addition to the substrate elements. The vendor has been contacted regarding the composition of the coating. No satisfactory response was offered to explain the lack of Al and the presence of Fe in the coating.

## SECTION 3.0 DISCUSSION

Three coating vendors applied seven different coatings for this screening effort. Only coating thickness was specified as a coating integrity requirement. As a result, each coating is unique and presents its own processing and microstructural problems. After review of the as-coated microstructures, observations from each coating have led to conclusions regarding coating integrity and, hence, have assisted in determining the likelihood of success in the engine test phase of this program.

Of the silicide coatings evaluated, R512-E, W3-Mod, and VH-109 appeared to be of the soundest integrity. The R512-E met all requirements with uniform coating coverage. The VH-109 was slightly thicker than required, but coating coverage was uniform. Intermittent precipitates were observed in this coating but appear to be typical. The W3-Mod coating was uniformly thin. The CVD technique employed for this coating may have hindered the development of a thicker coating. Further process modifications would be required to reach the 3.0-mil thickness goal, an operation which was not allowed by the original guidelines. However, the thinness associated with this coating may be beneficial for minimizing coating cracking and reducing coating mass.

Each aluminide coating has undesirable features in its microstructure.

The VH-9 coating is not recommended for additional testing: (1) the coating thickness varies to greatly for a quality coating, (2) substantial substrate thickness was consumed by the coating process, (3) target and measured coating chemistries did not agree. However, the resultant layered nature of this coating is unique and may be a good approach to protect columbium alloys.

The R505-F was chosen as a coating candidate to address low temperature considerations related to the regeneratively cooled nozzle. Thus, it would not be expected to perform well in high temperature applications. Coating thickness on panel faces was good but thickness control at edges and coating voids detracted from coating integrity. These features may prematurely expose the C-103 to the environment leading to hydrogen embrittlement and oxidation of the base alloy.

The VH-2 coating was thicker than desired and had very limited interaction with the substrate. Substantial metallographic pull-out questions the structural integrity of the coating. Sample edges were not thoroughly coated; again, this could lead to premature base alloy degradation.

The RT-40 coating is a combination of Chemical Vapor Deposited Si and Pack Deposited Al. However, no Al was detected and Cr and Fe were found in addition to Si. The vendor was unable to explain these chemistry discrepancies, thus, reproduction of this coating is unlikely. No further work on RT-40 is recommended.

## SECTION 4.0 CONCLUSIONS

Table 4-1 is a preference list for testing the various coatings. The list matches the coatings in descending order of preference with brief comments on the integrity of the coating.

TABLE 4-1. — ORDER OF PREFERENCE FOR TESTING COATS

	<i>Coating</i>	<i>Type</i>	<i>Comments</i>
1.	R512-E	Silicide	Excellent integrity
2.	VH-109	Silicide	Excellent integrity Slightly thicker than required
3.	W3-(Mod)	Silicide	Excellent integrity One-half of thickness required
4.	VH-2	Aluminide	Questionable structural integrity — "pull-out" Incomplete coating coverage at sample edges
5.	R505-F	Aluminide	Questionable structural integrity — "Entrapped gas or pull-out" Nearly incomplete coating coverage at sample edges
6.	VH-9	Aluminide	Unique layered coating profile Radical thickness variations — coating and substrate Significant substrate consumption during coating process Unexpected detection of Si and Cr
7.	RT-40	Aluminide	No Al in coating Coating origin unknown Coating thickness is well below design goal

R20482/1

The three silicide coatings (R512-E, VH-109, and W3-Mod) have the best coating integrity and are recommended for further testing. As discussed previously, R512-E met all requirements and is the primary candidate for coating the RL10 nozzle extension. The other coatings, VH-109 and W3-Mod, did not meet thickness requirements but warrant consideration for panel testing in the RL10 exhaust.

All aluminide coatings have characteristics which preclude recommendation for further testing. VH-2 and R505-F did not uniformly coat edges and may prematurely expose the base alloy to the environment. Although the layered structure of VH-9 was interesting, coating thickness control was lacking. The RT-40 coating chemistry did not agree with the vendor's processing history. The presence of Fe and Cr and the lack of Al in the coating chemistry, and the minimal coating thickness eliminate RT-40 from further consideration.

ORIGINAL PAGE IS  
OF POOR QUALITY

FD 358171

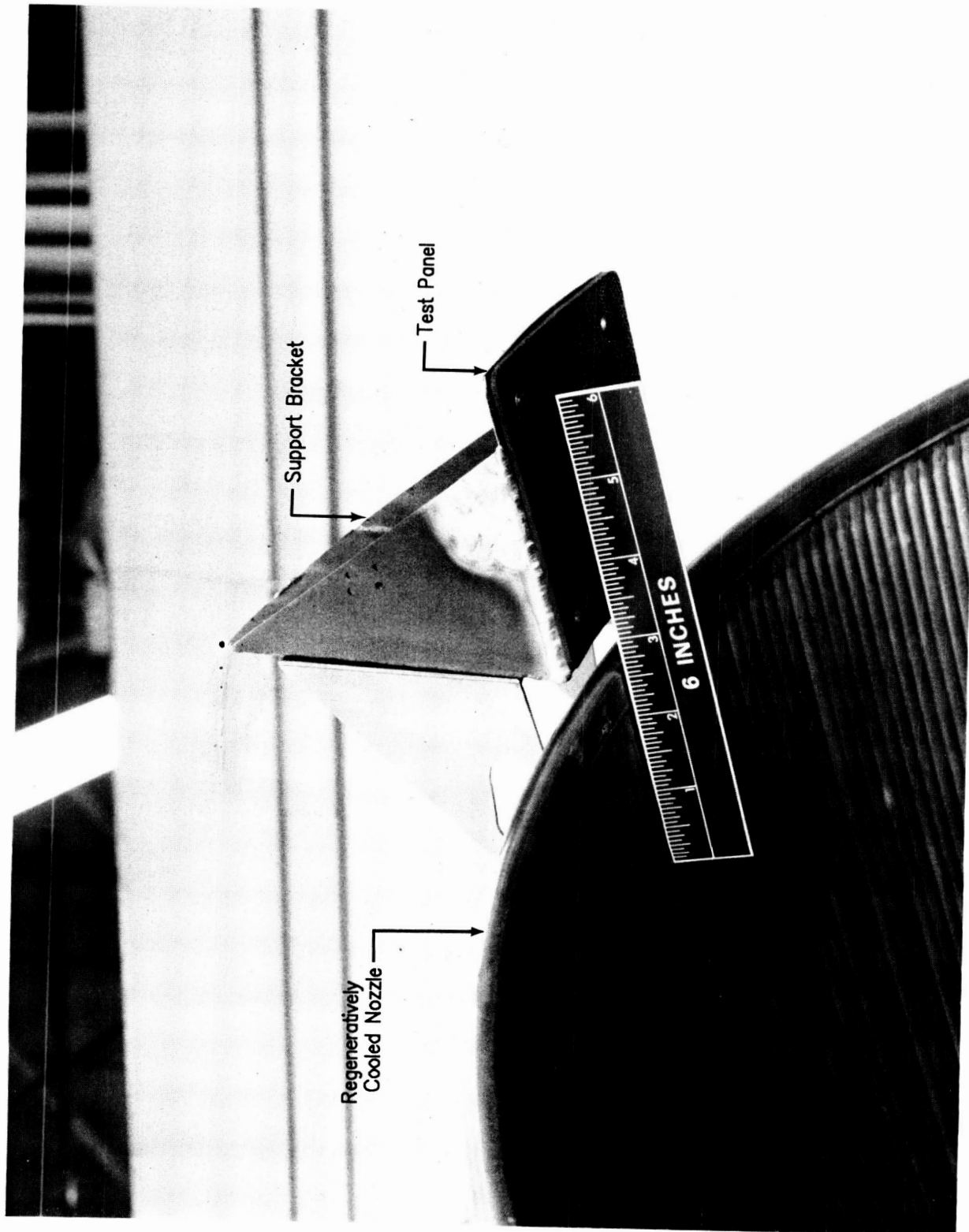
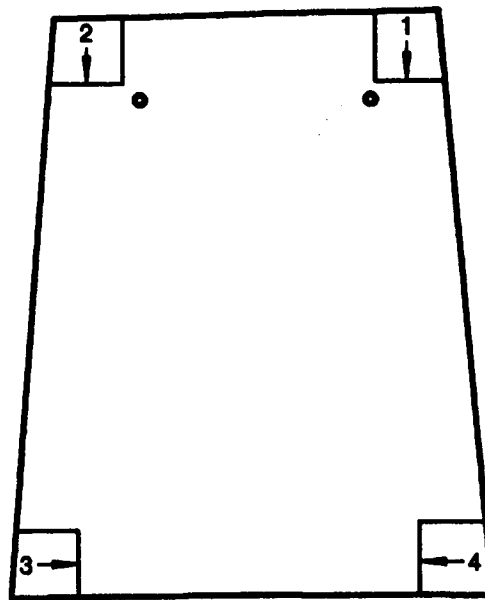


Figure 1-1. Typical Test Panel Attachment to RL10 Exhaust Nozzle



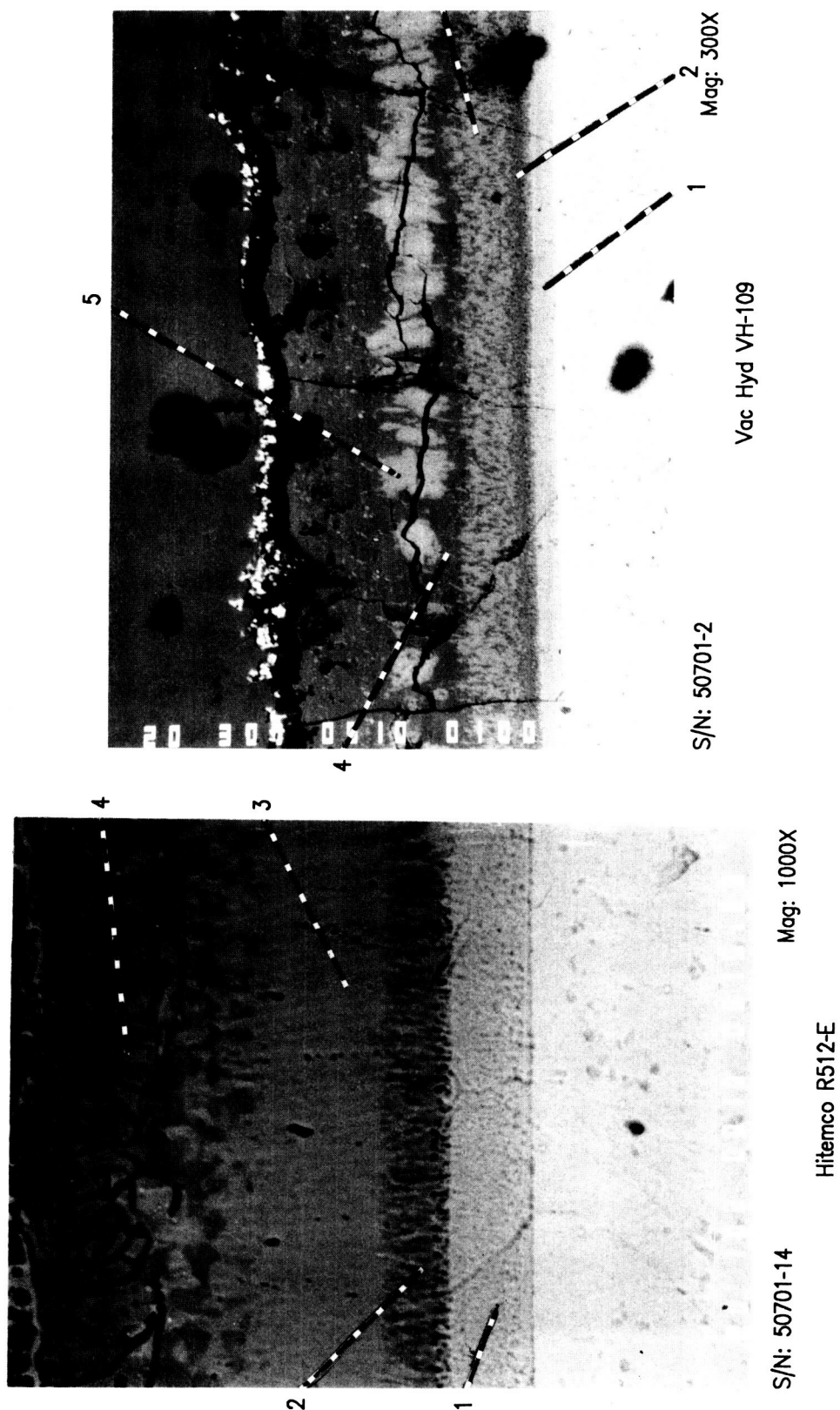
\*Arrows indicate Metallographic Plane of Polish

FD 358173

*Figure 2-1. Standard Panel Sectioning Diagram*



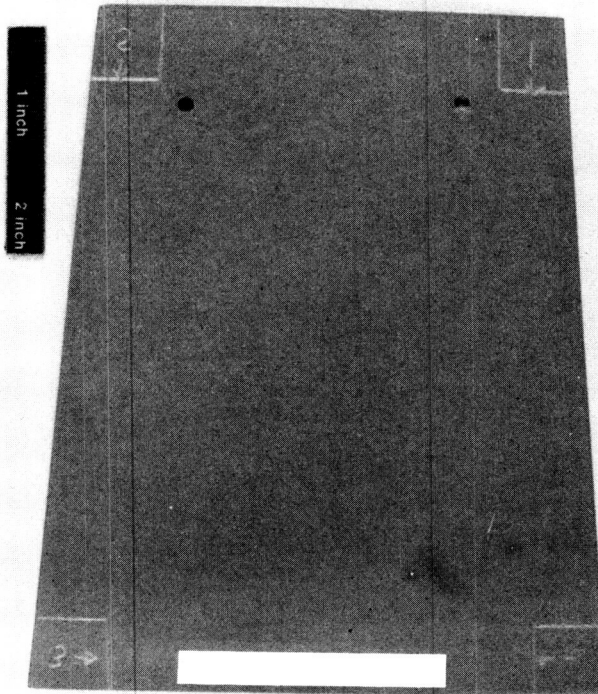
ORIGINAL PAGE IS  
OF POOR QUALITY



FD 358172

Figure 2-2. Backscattered Electron Image Identifying the Coating Locations (Phases)  
Analyzed

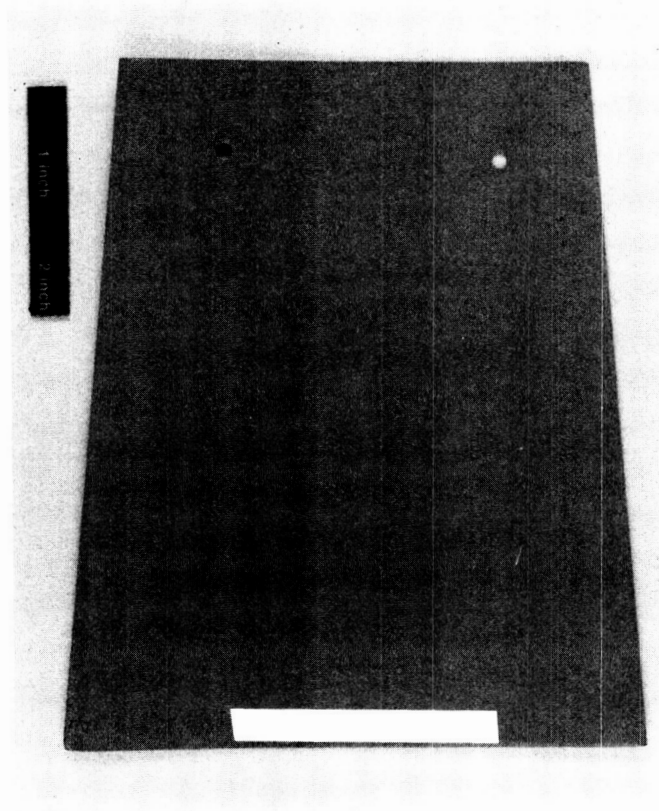
ORIGINAL PAGE IS  
OF POOR QUALITY



FD 358174

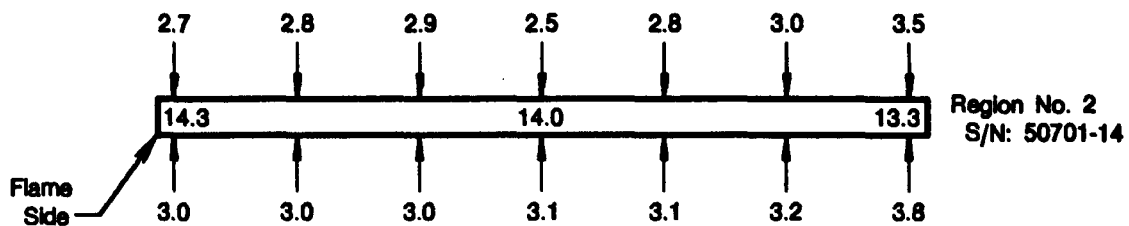
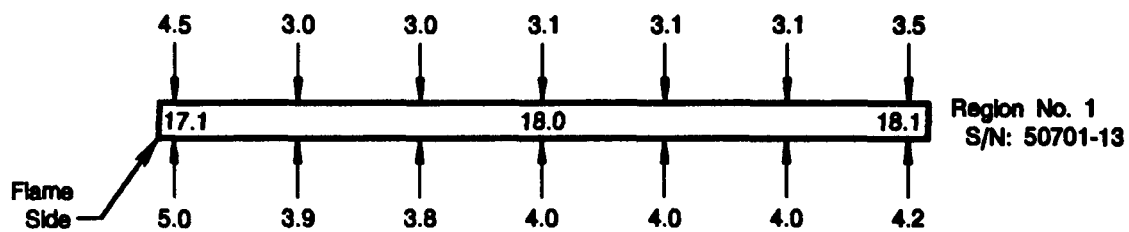
*Figure 2-3. Side 1 of Hitemco R512-E (Flame Side)*

ORIGINAL PAGE IS  
OF POOR QUALITY

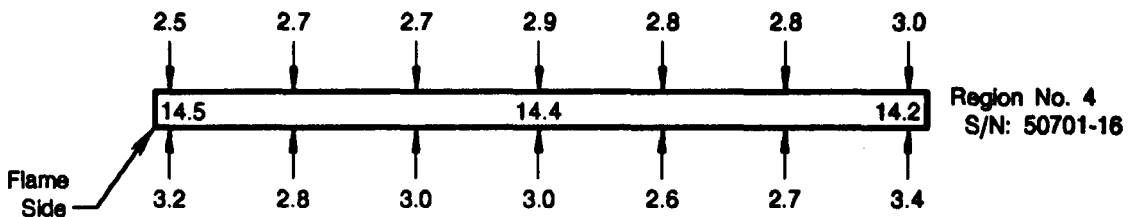
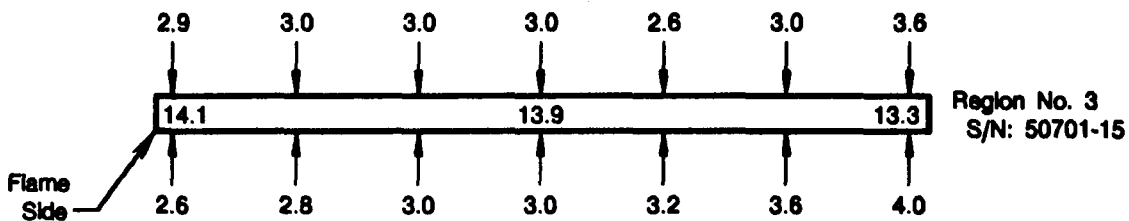


FD 358175

*Figure 2-4. Side 2 of Hitemco R512-E*



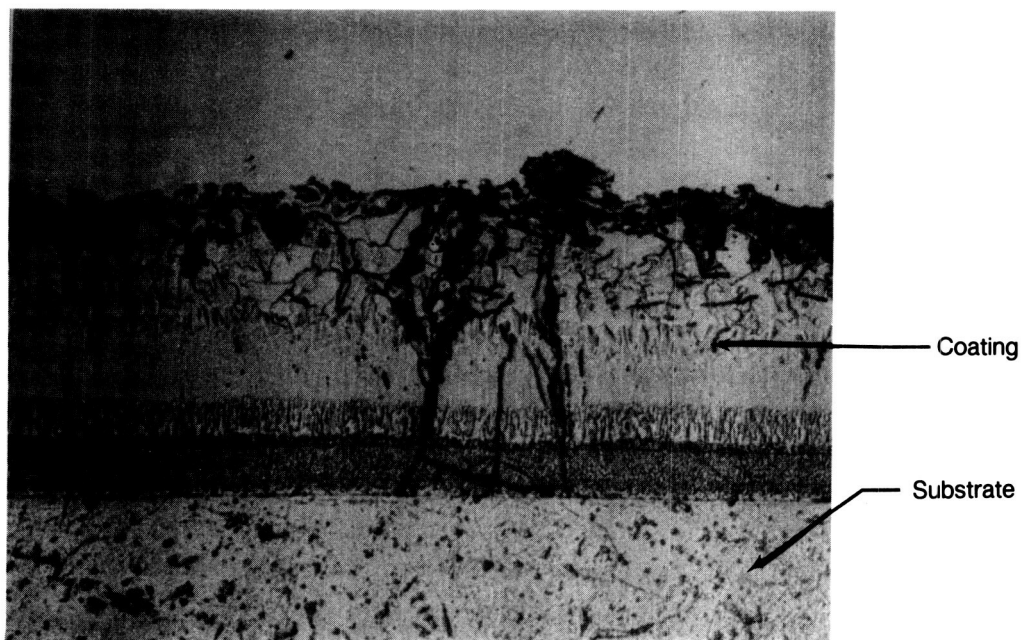
All Units Are In Mils



FD 358176

Figure 2-5. Hitemco R512-E Coating and Substrate Thickness Distribution

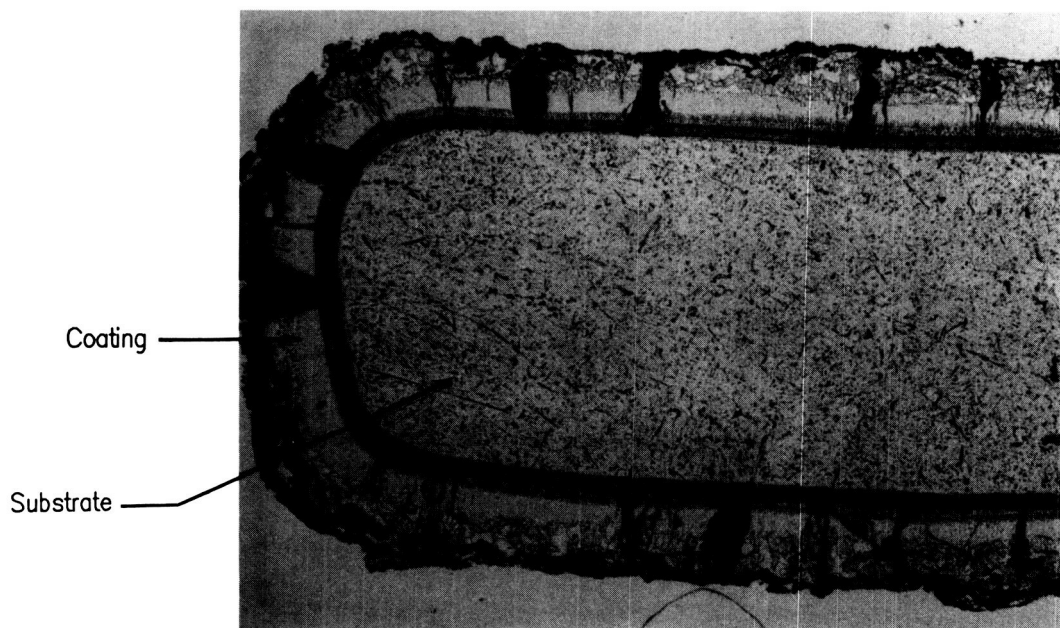
ORIGINAL PAGE IS  
OF POOR QUALITY



S/N: 50701-14

Mag: 500X

Side1 - Typical Coating From Region No. 2



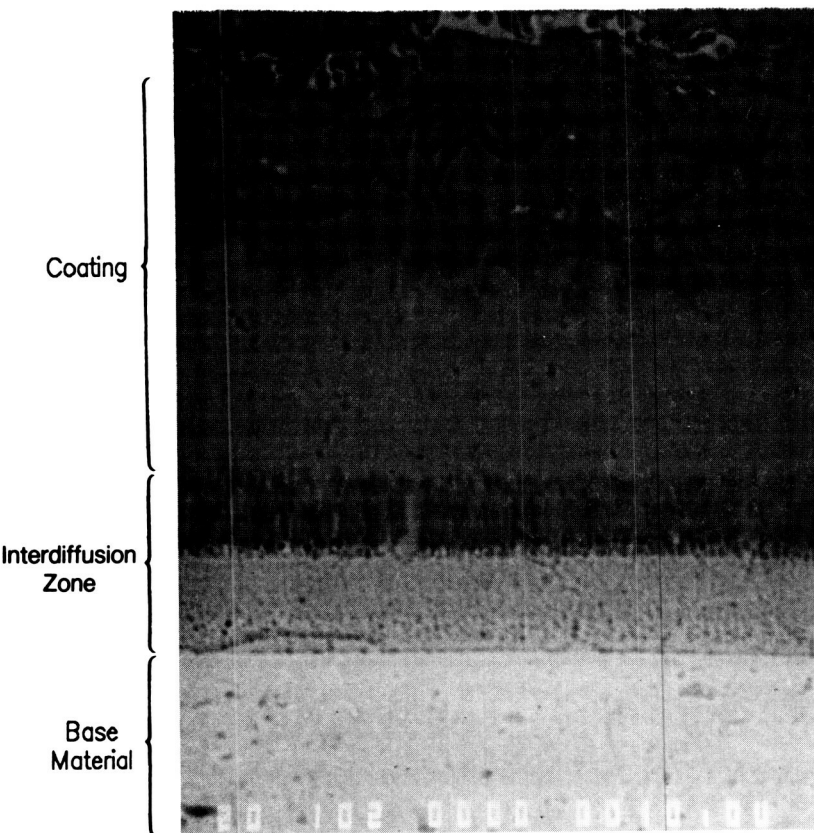
S/N: 50701-14

Mag: 126X

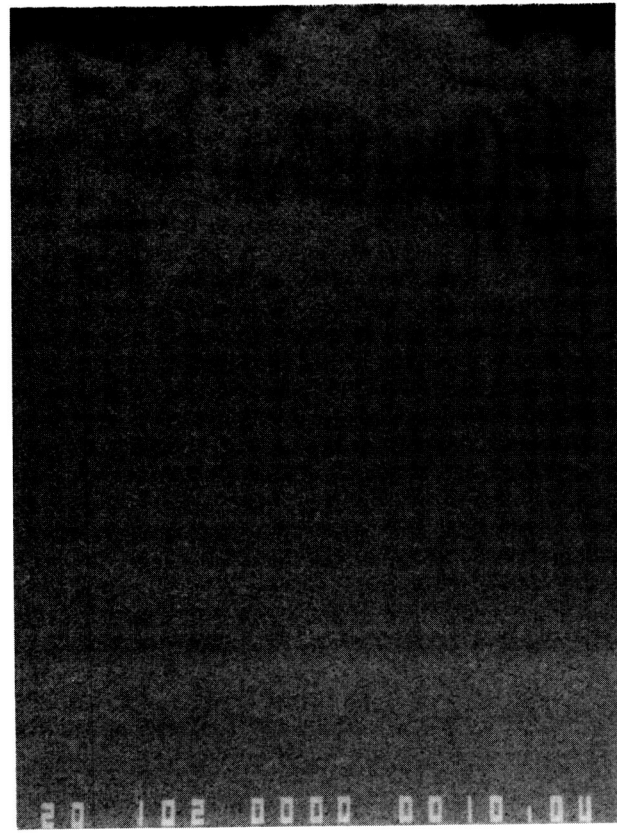
Typical Coating Edge Coverage on Lengthwise  
Panel Edge From Region No. 2

FD 358177

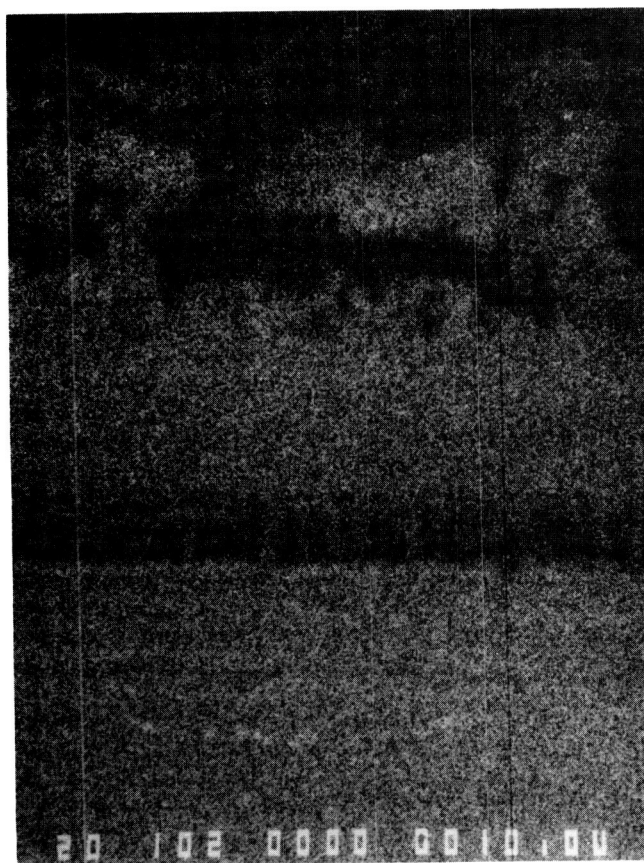
Figure 2-6. Hitemco R512-E Microstructure (Etch: 60% Lactic; 20%  $\text{HNO}_3$ ; 20%  $\text{Hf}$ ;  
Thickness:  $3.1 \pm 0.5$  mils)



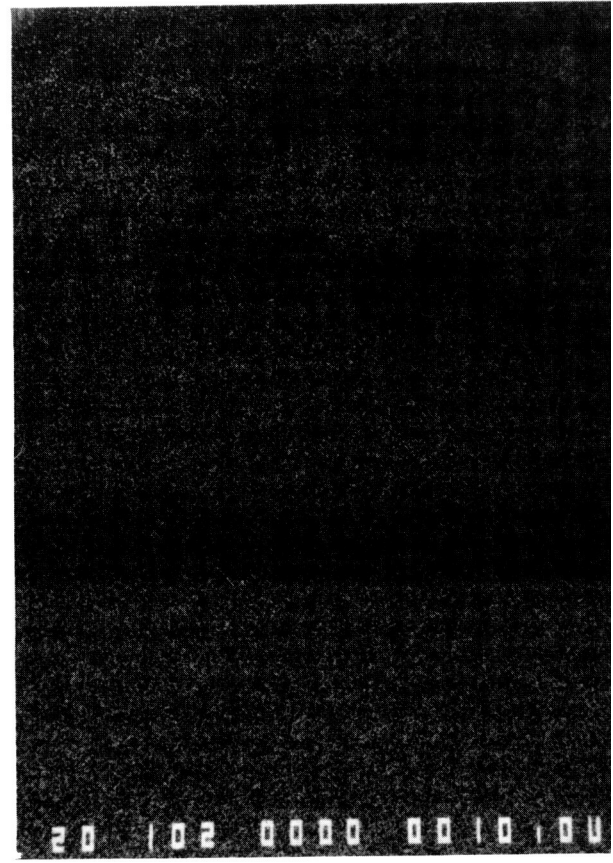
Backscattered Image



Element - Cb



Element - Hf



Element - Ti

Mag: 1000X

S/N: 50701-14

Side 1

FD 358171

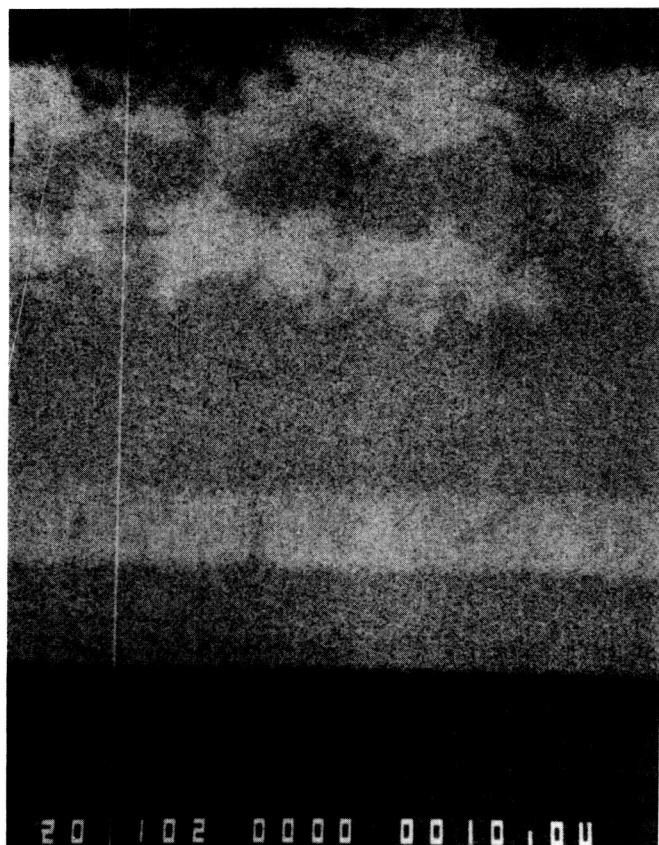
Figure 2-7. Elemental X-ray Maps of Hitemco R512-E — Side 1 (Sheet 1 of 2)

I-16

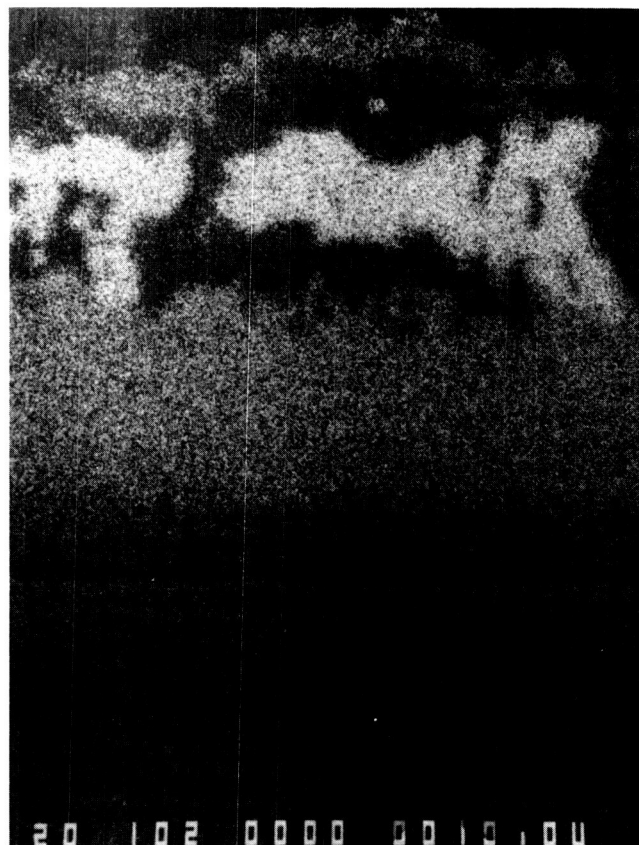
R20482/3

ORIGINAL PAGE IS  
OF POOR QUALITY

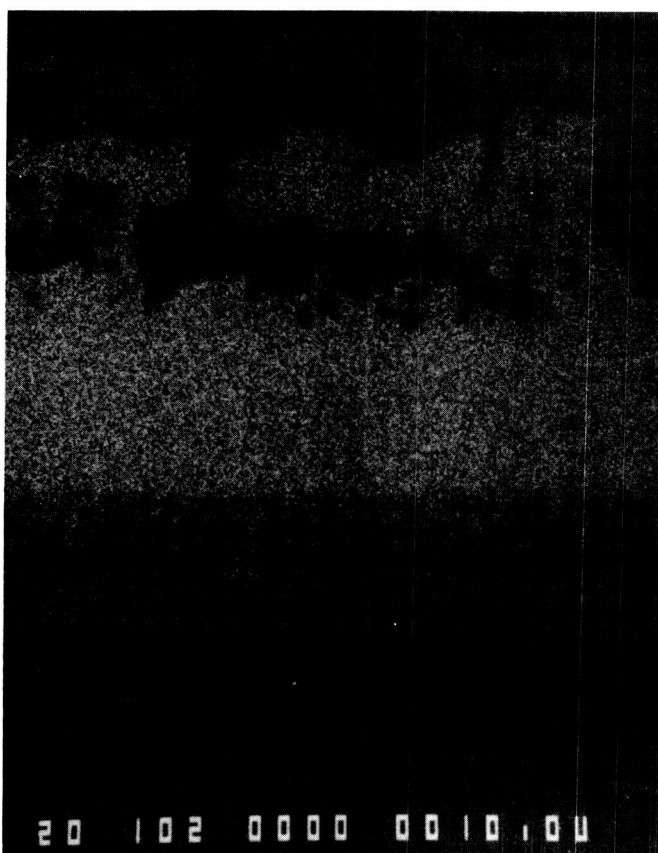




Element - Si



Element - Cr



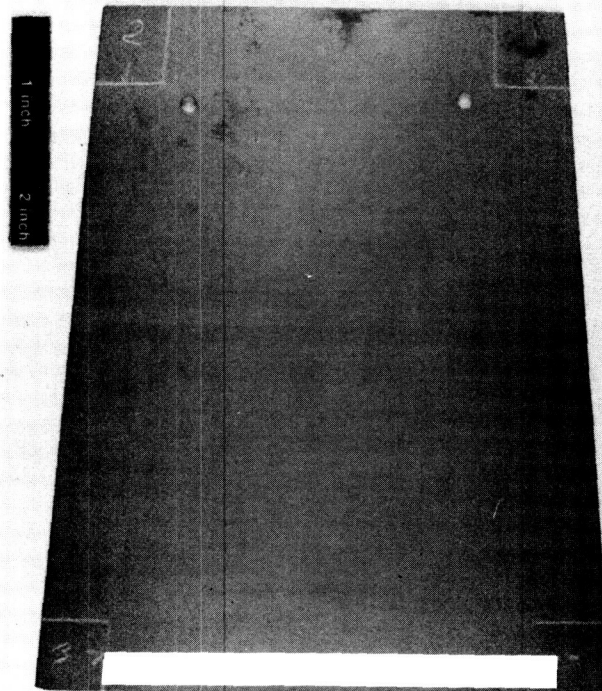
Element - Fe

ORIGINAL PAGE IS  
OF POOR QUALITY

ORIGINAL PAGE IS  
OF POOR QUALITY

Figure 2-7. Elemental X-ray Maps of Hitemco R512-E — Side 1 (Sheet 2 of 2)

ORIGINAL PAGE IS  
OF POOR QUALITY.

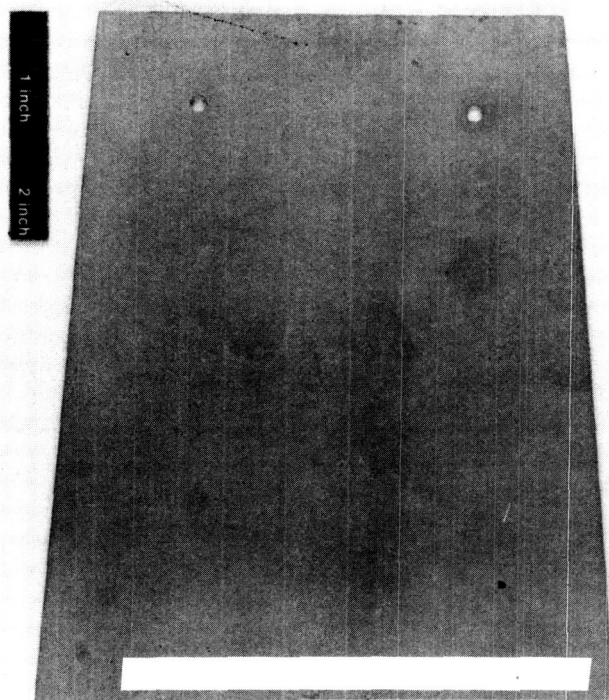


FD 358180

*Figure 2-8. Side 1 of Chromalloy W3-Mod. CVD Si (Flame Side)*

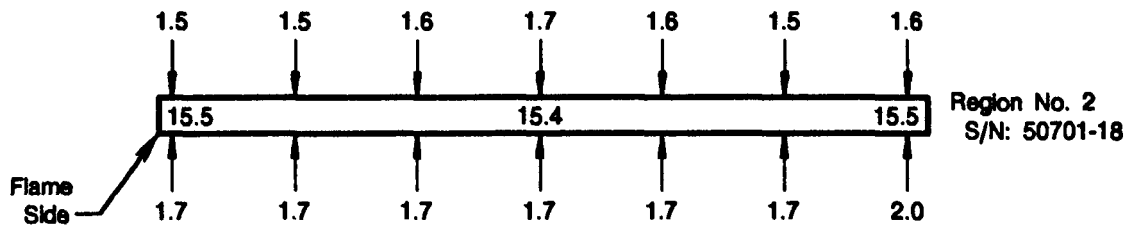
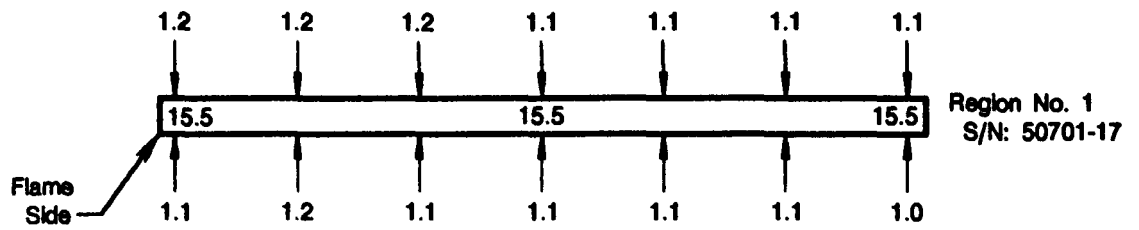


ORIGINAL PAGE IS  
OF POOR QUALITY.

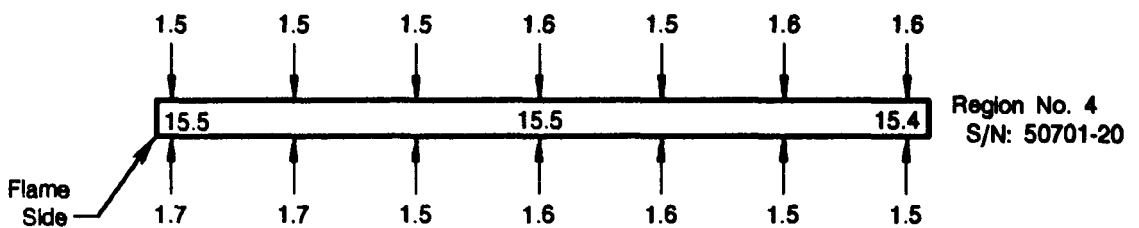
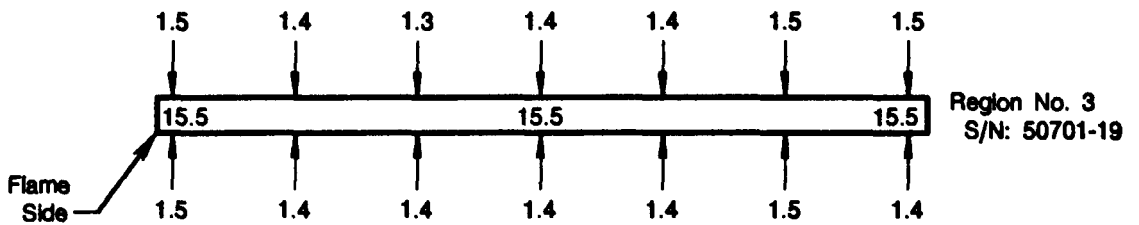


FD 358181

*Figure 2-9. Side 2 of Chromalloy W3-Mod. CVD Si*



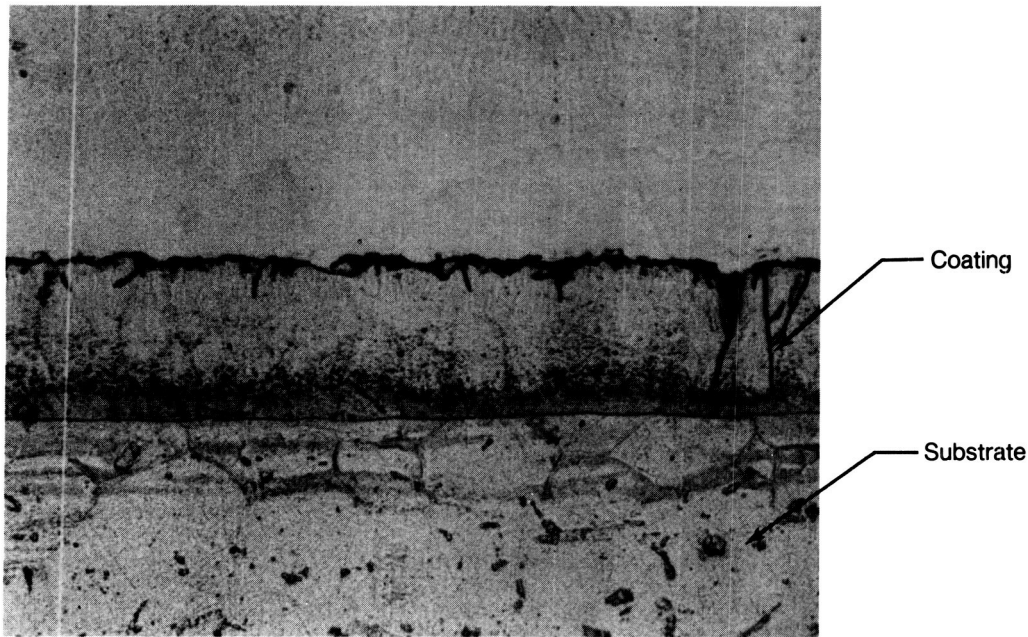
All Units Are In Mils



FD 358182

Figure 2-10. Chromalloy W3-Mod. CVD Si Coating and Substrate Thickness Distributions

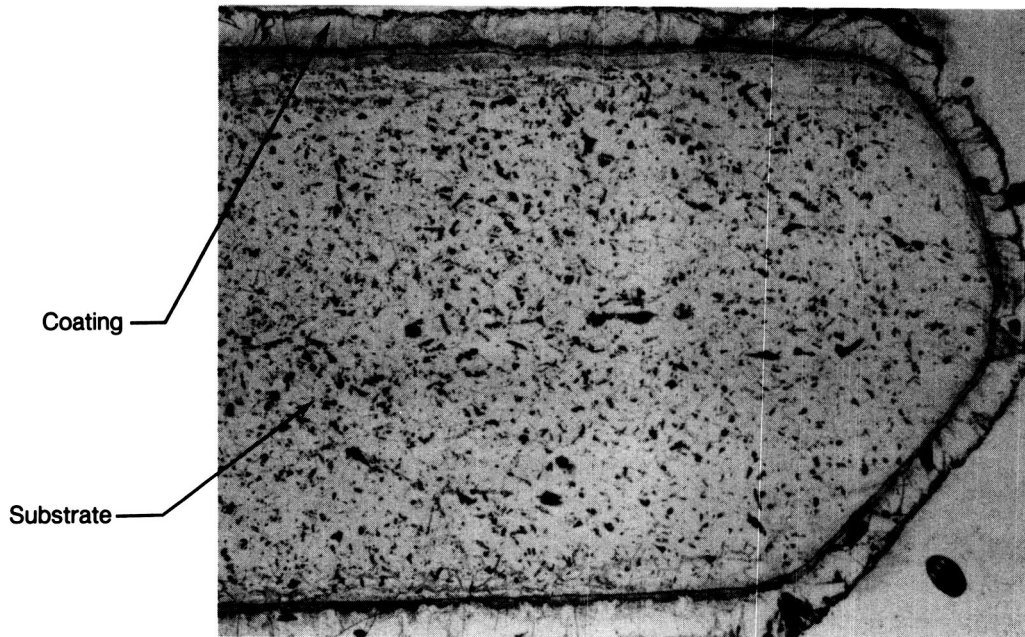
ORIGINAL PAGE IS  
OF POOR QUALITY



S/N: 50701-19

Mag: 500X

Side 1 - Typical Coating From Region No. 3



S/N: 50701-18

Mag: 126X

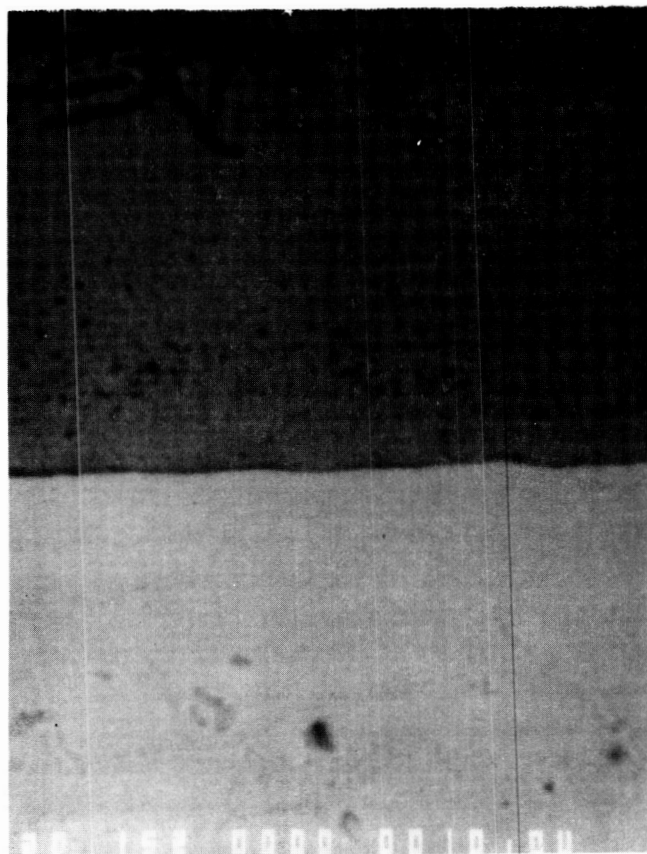
Typical Coating Edge Coverage on Lengthwise  
Panel Edge From Region No. 2

FD 358183

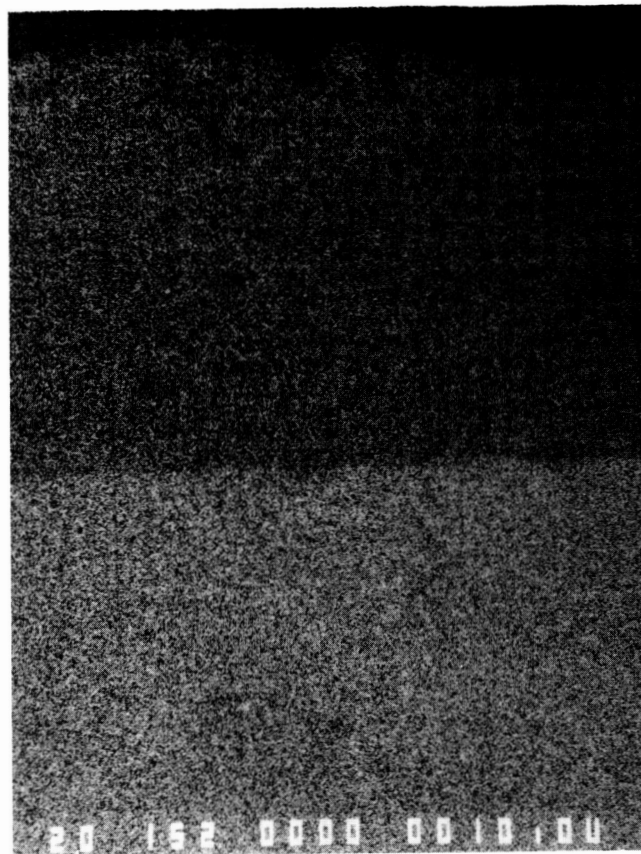
Figure 2-11. Chromalloy W3-Mod. Sample (Etch: 60% Lactic; 20%  $\text{HNO}_3$ ; 20%  $\text{Hf}$ ;  
Thickness:  $1.4 \pm 0.2$  mils)

Coating

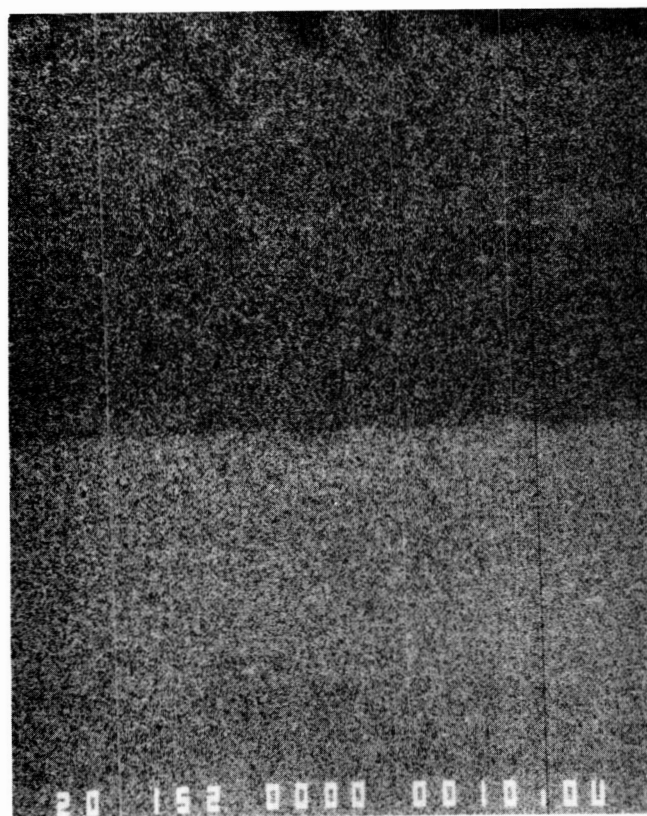
Substrate



Backscattered Image



Element - Cb



Element - Hf



Element - Ti

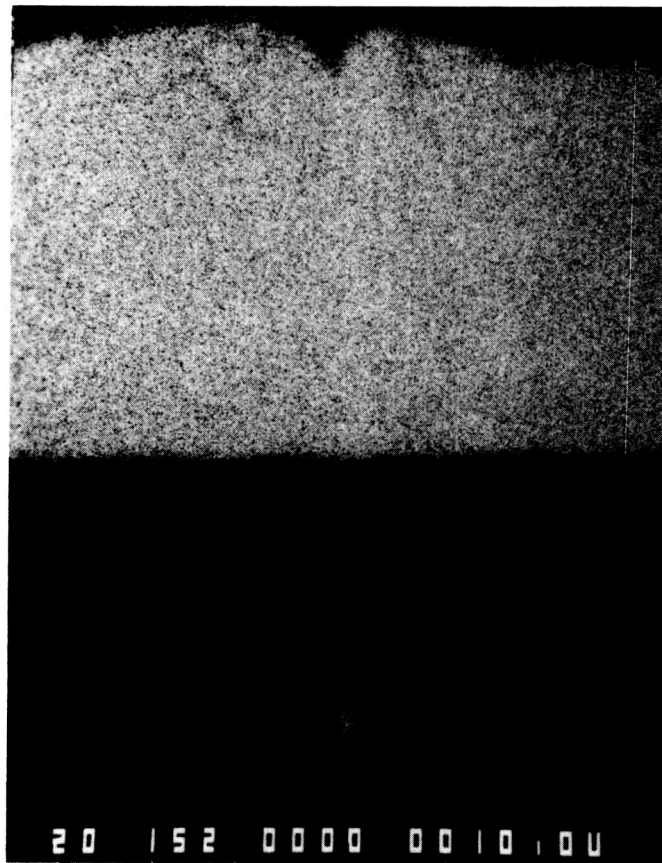
S/N: 50701-19

Mag: 1500

FD 35818

Figure 2-12. Elemental X-ray Maps of Chromalloy W3-Mod. (Sheet 1 of 2)

ORIGINAL PAGE IS  
OF POOR QUALITY



S/N: 50701-19

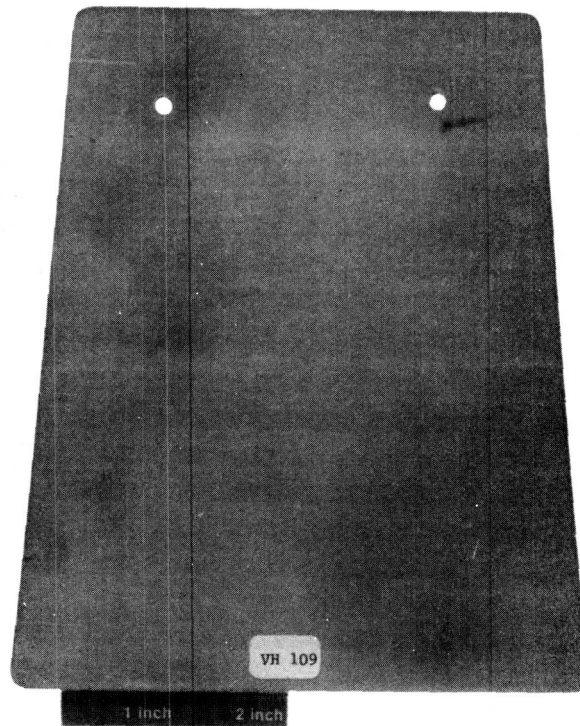
Mag: 1500X

Element - Si

FD 358185

*Figure 2-12. Elemental X-ray Maps of Chromalloy W3-Mod. (Sheet 2 of 2)*

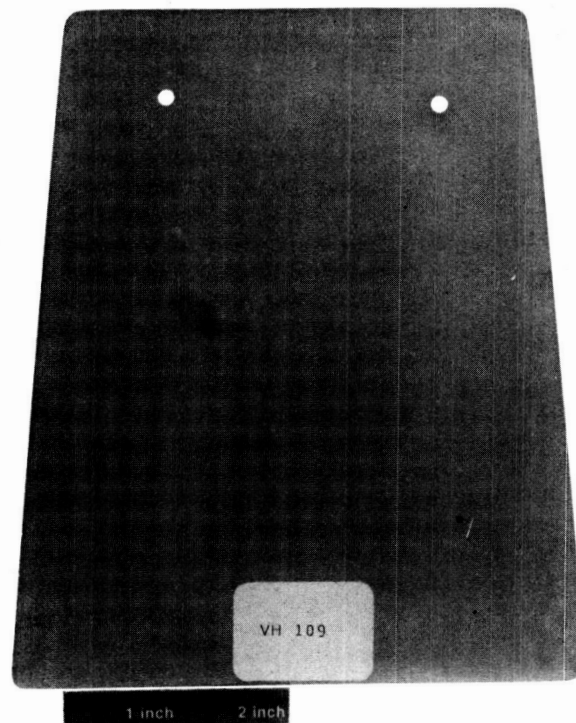
ORIGINAL PAGE IS  
OF POOR QUALITY



FD 358186

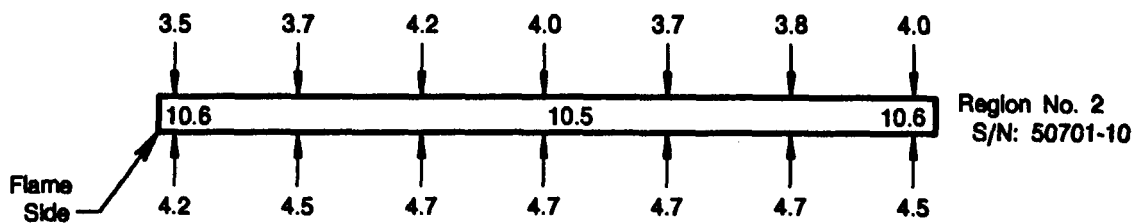
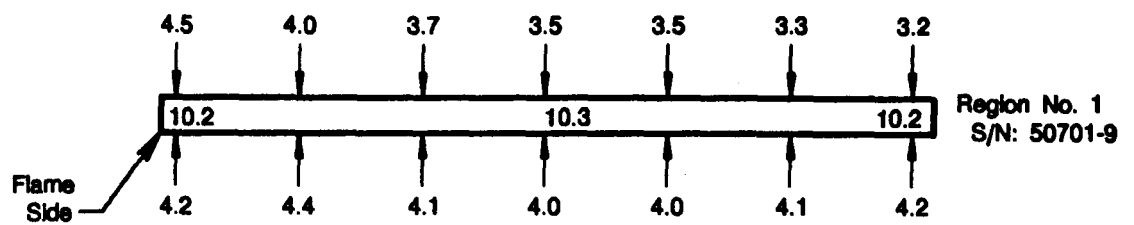
*Figure 2-13. Side 1 of Vac Hyd VH-109 Coated Sample (Flame Side)*

ORIGINAL PAGE IS  
OF POOR QUALITY

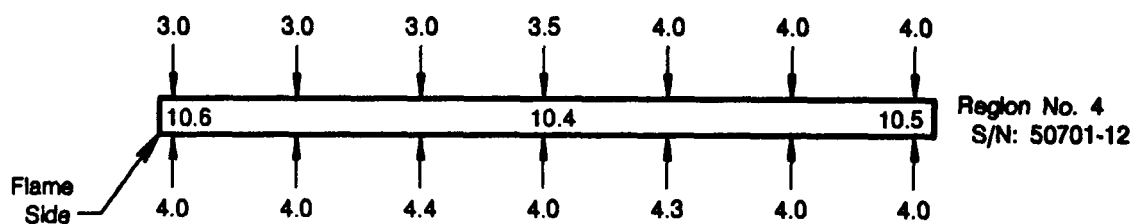
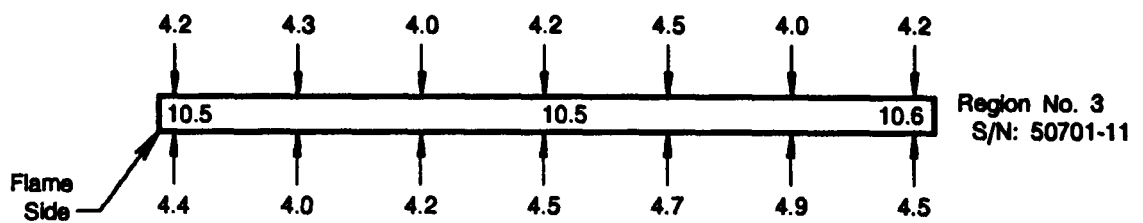


FD 358187

*Figure 2-14. Side 2 of Vac Hyd VH-109 Coated Sample*



All Units Are In Mils

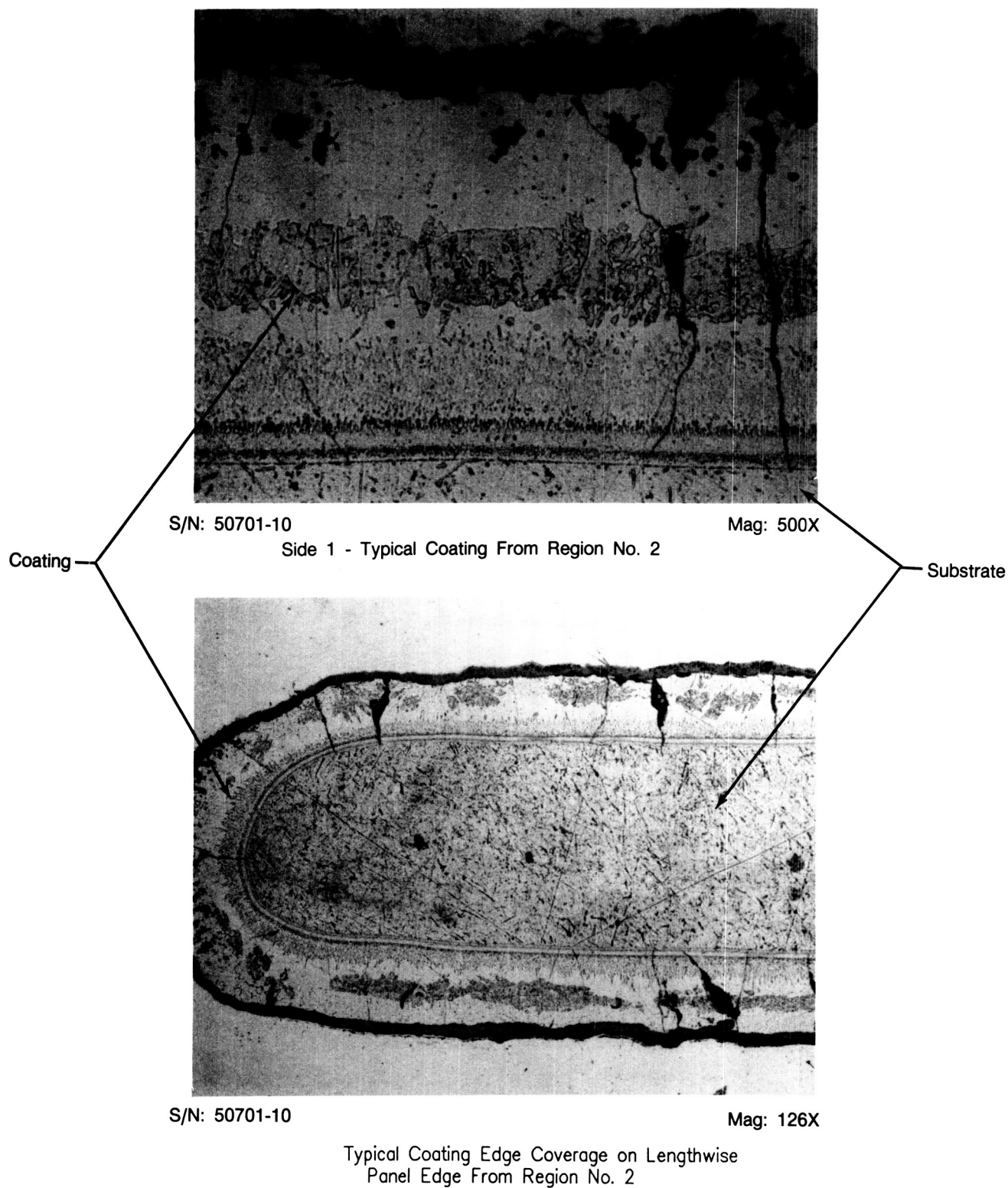


FD 358188

Figure 2-15. Vac Hyd VH-109 Coating and Substrate Thickness Distribution

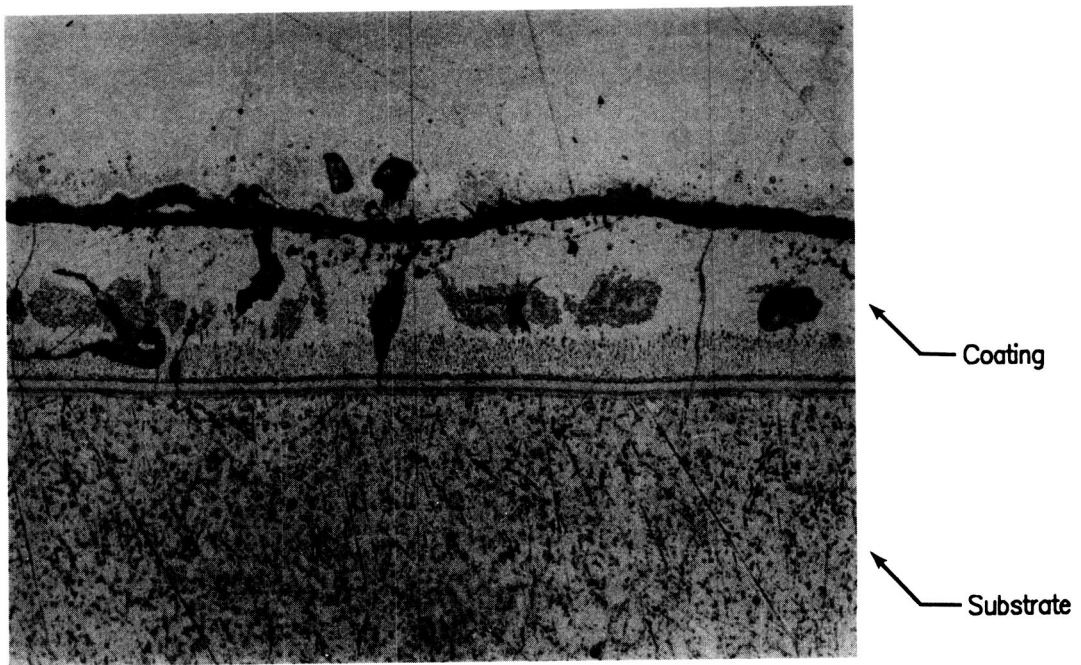


ORIGINAL PAGE IS  
OF POOR QUALITY



FD 358189

Figure 2-16. Vac Hyd VH-109 Microstructure (Etch: 60% Lactic; 20%  $\text{HNO}_3$ ; 20%  $\text{Hf}$ ;  
Thickness:  $4.1 \pm 0.4$  mils) (Sheet 1 of 2)



S/N: 50701-10

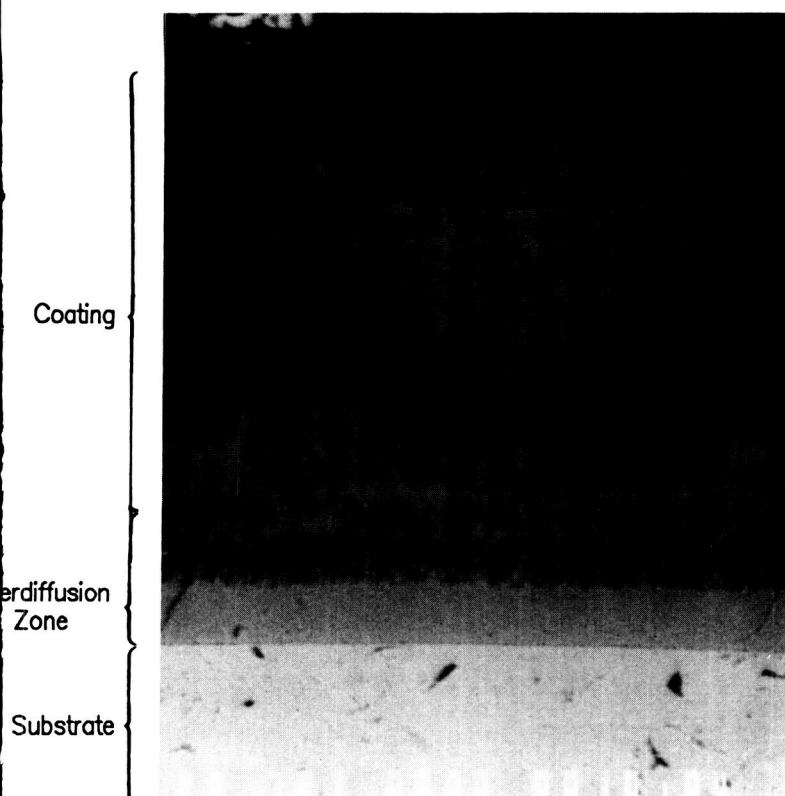
Mag: 200X

Side 1 - Typical Coating From Region No. 3 Showing  
Uneven Distribution of Phases in Coating

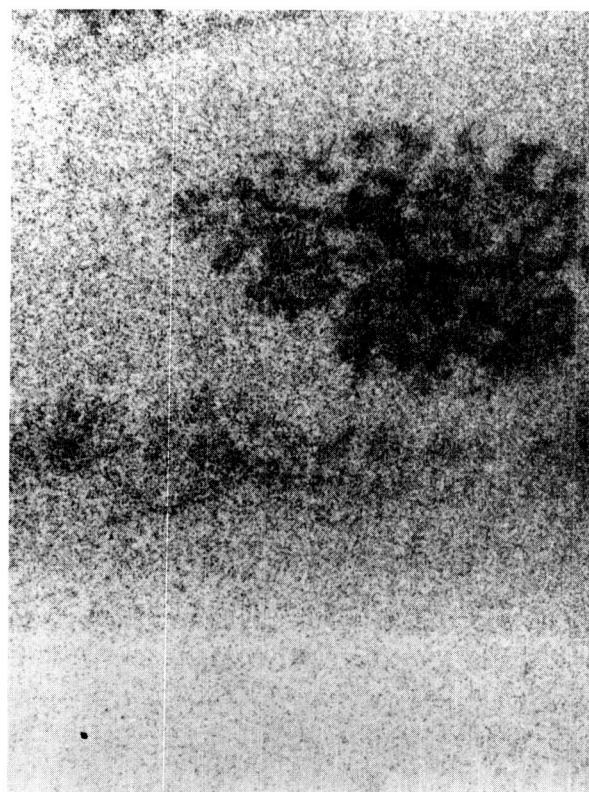
FD 358190

*Figure 2-16. Vac Hyd VH-109 Microstructure (Etch: 60% Lactic; 20%  $\text{HNO}_3$ ; 20%  $\text{Hf}$ ;  
Thickness:  $4.1 \pm 0.4$  mils) (Sheet 2 of 2)*

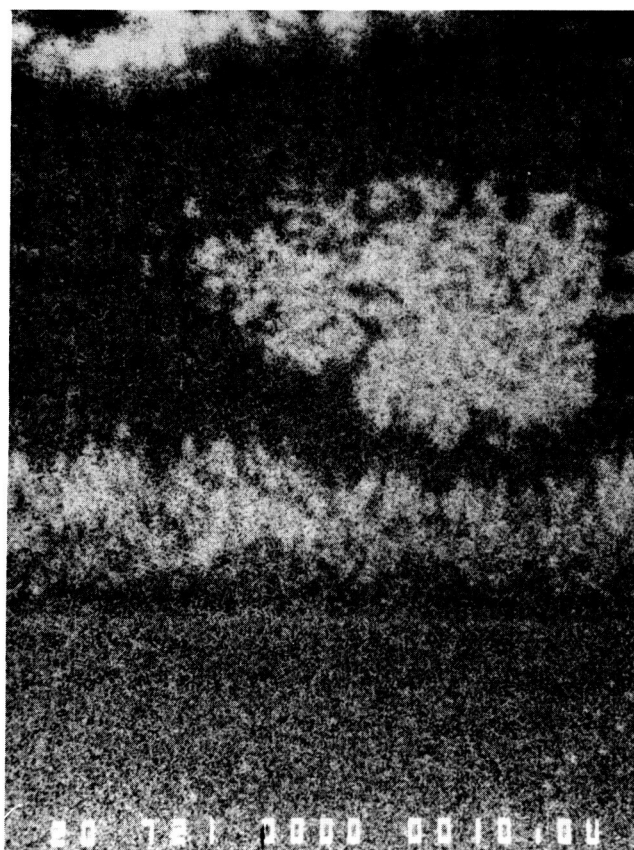
ORIGINAL PAGE IS  
OF POOR QUALITY



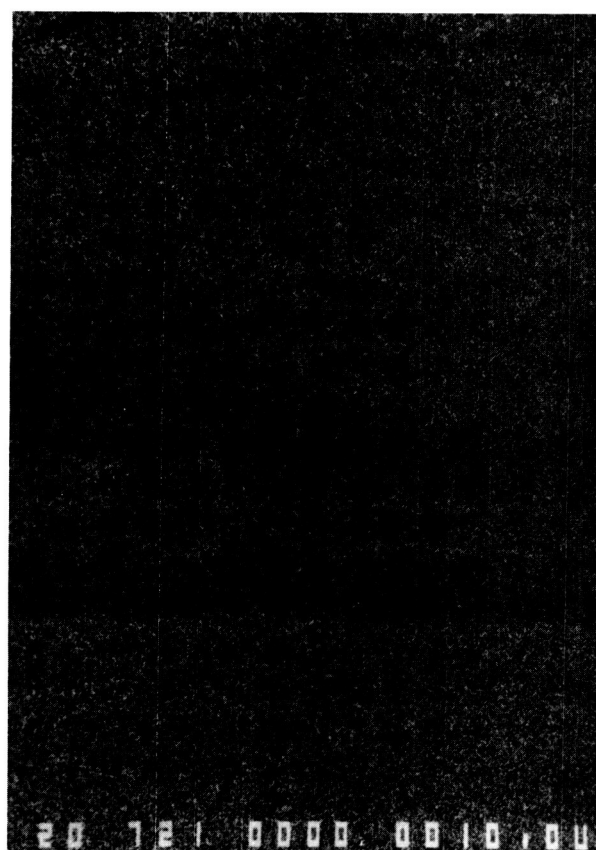
Backscattered Image



Element - Cb



Element - Hf



Element - Ti

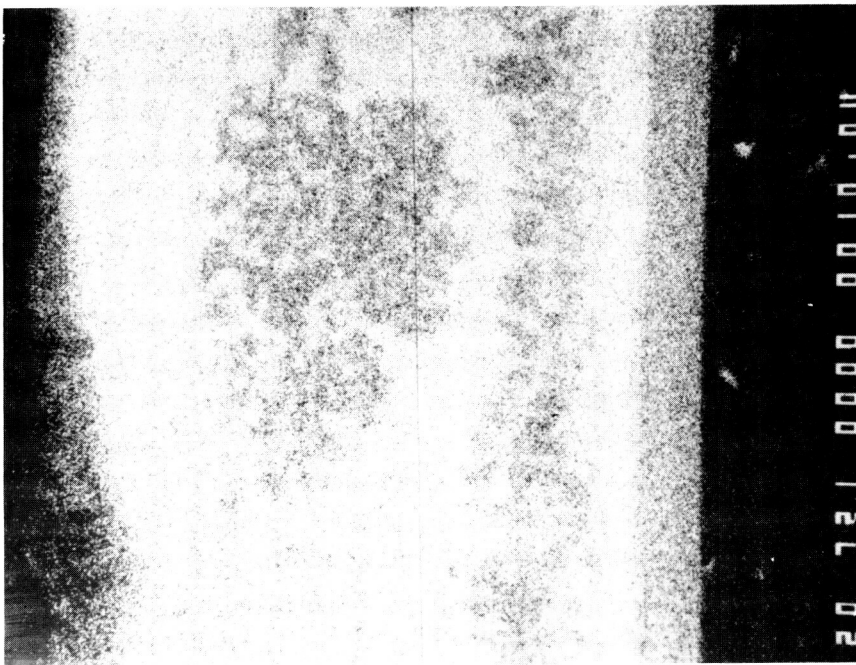
Mag: 720X

FD 358191

S/N: 50701-10

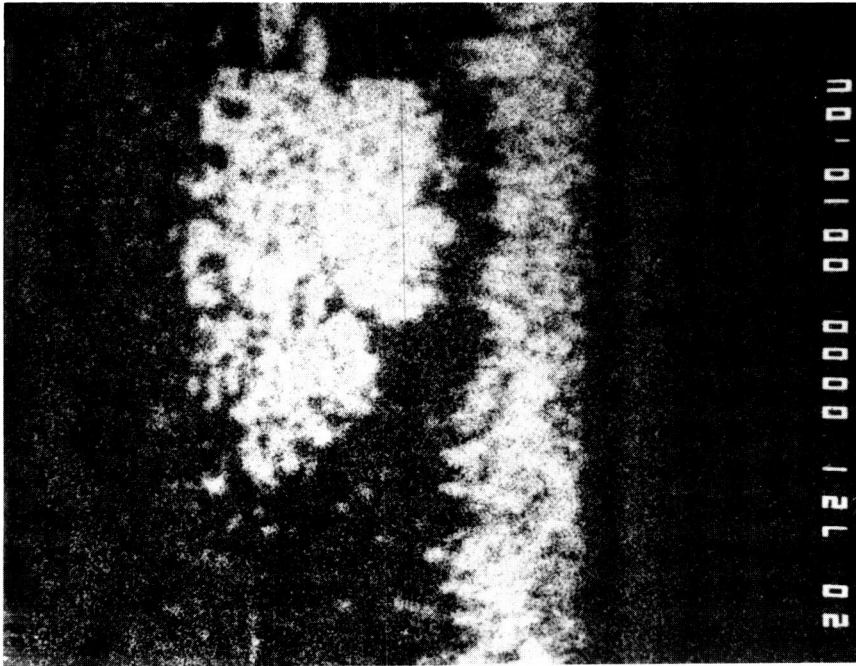
Figure 2-17. Elemental X-ray Maps of Vac Hyd VH-109 (Sheet 1 of 2)

ORIGINAL PAGE IS  
OF POOR QUALITY



Element - Si

S/N: 50701-10

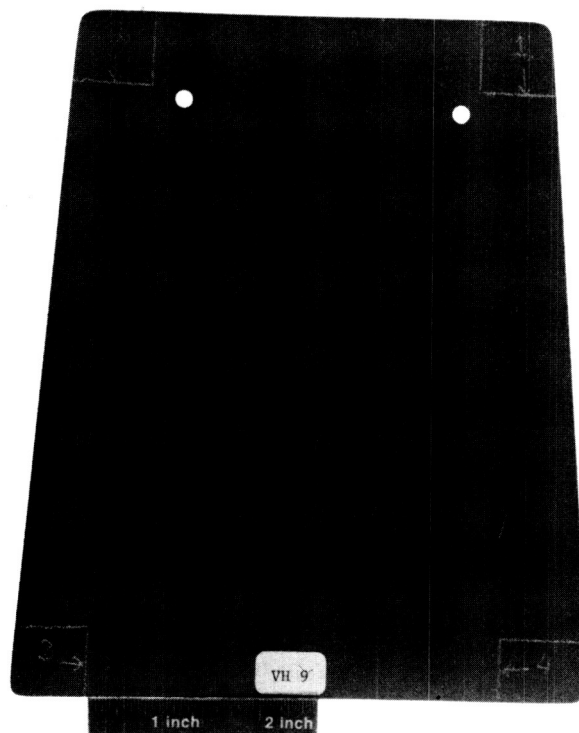


Element - Cr

Mag: 720X  
FD 358192

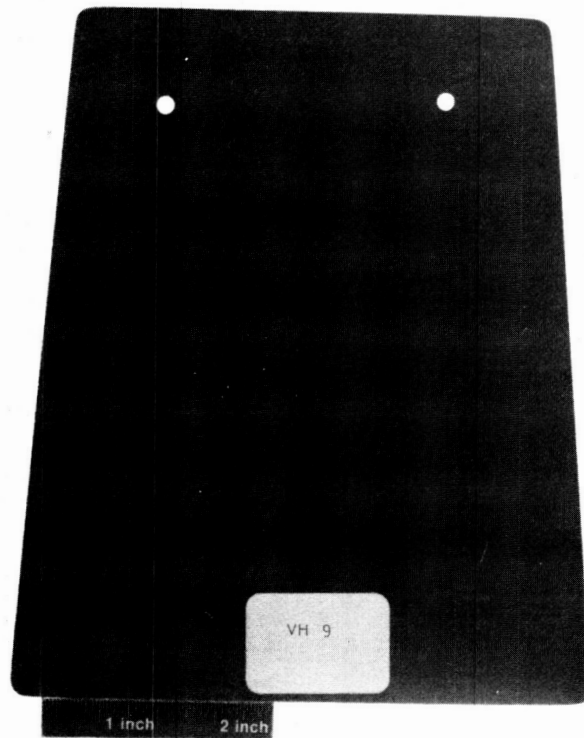
Figure 2-17. Elemental X-ray Maps of Vac Hyd VH-109 (Sheet 2 of 2)

ORIGINAL PAGE IS  
OF POOR QUALITY



FD 358193

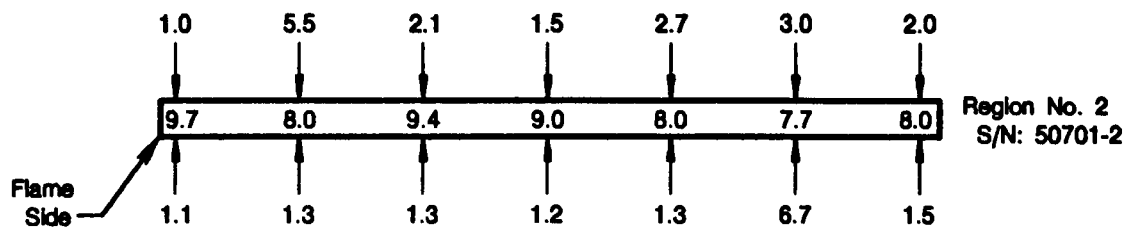
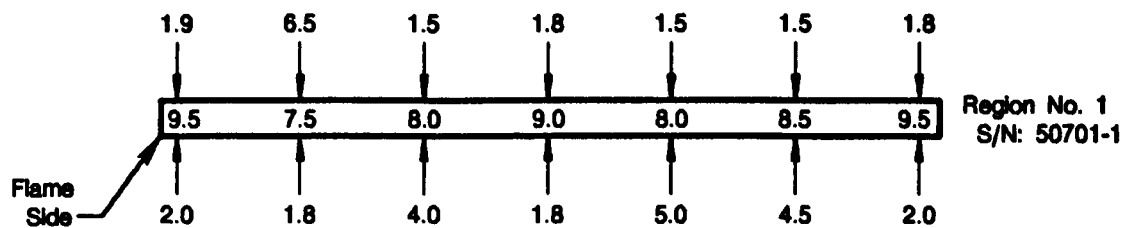
*Figure 2-18. Side 1 of Vac Hyd VH-9 Coated Sample (Flame Side)*



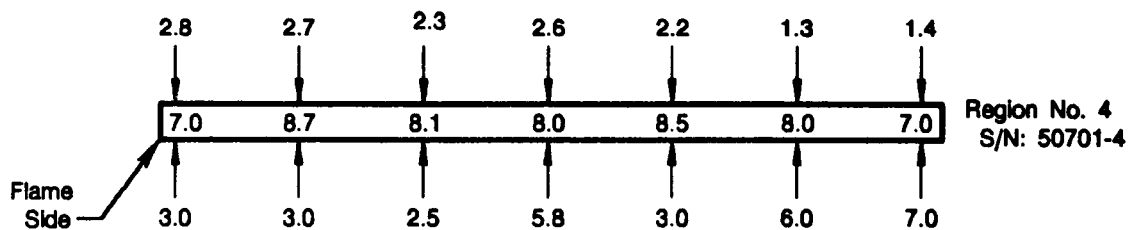
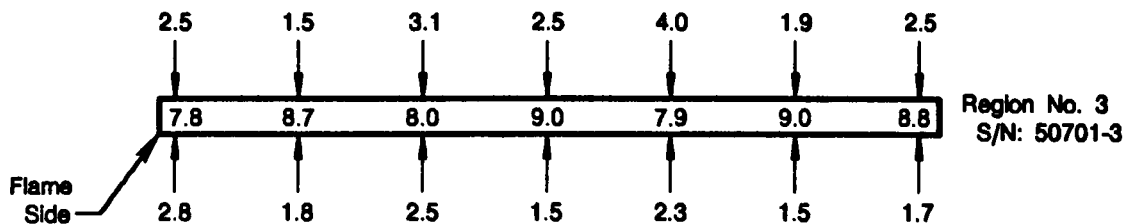
FD 358194

*Figure 2-19. Side 2 of Vac Hyd VH-9 Coated Sample*

ORIGINAL PAGE IS  
OF POOR QUALITY.



All Units Are In Mills

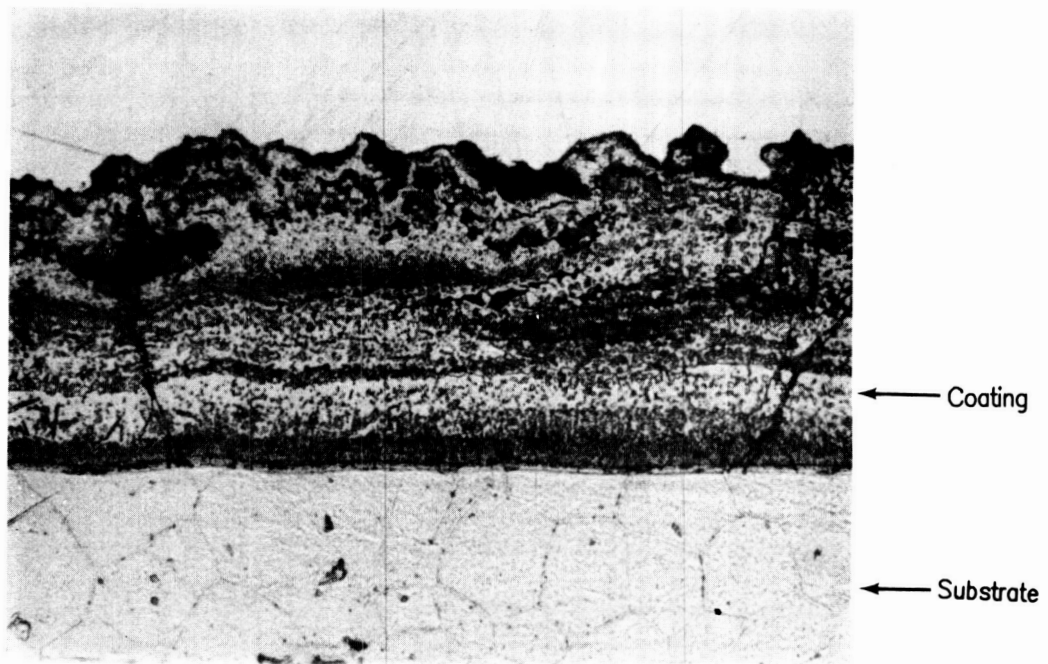


FD 358195

Figure 2-20. Vac Hyd VH-9 Coating and Substrate Thickness Distributions



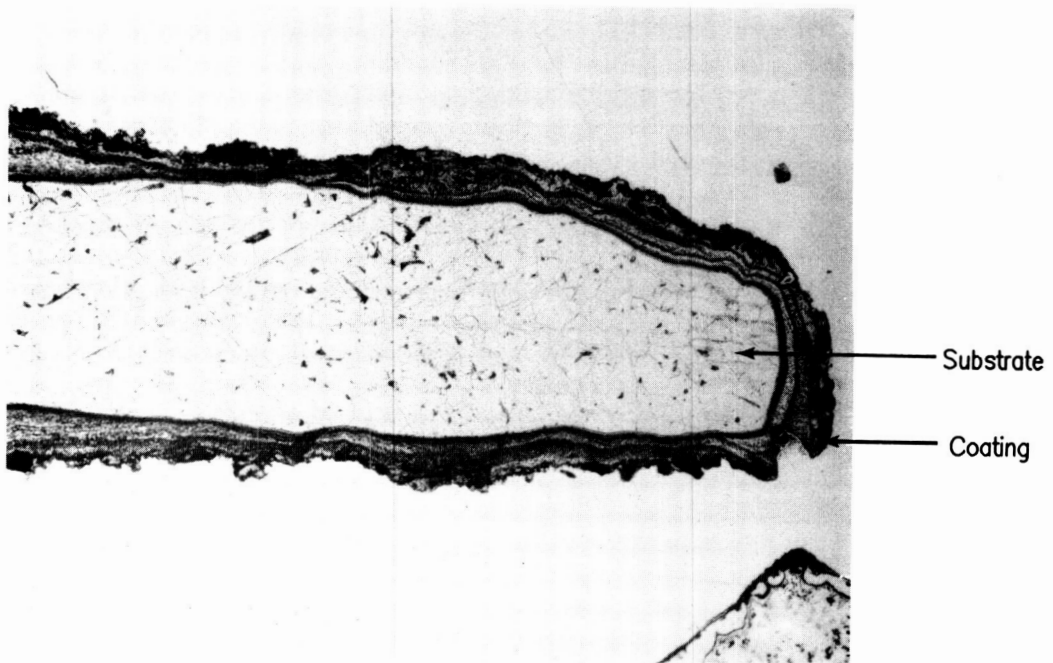
ORIGINAL PAGE IS  
OF POOR QUALITY



S/N 50701-2

Mag: 500X

Side 1: Typical Coating From Region No.2



S/N 50701-1

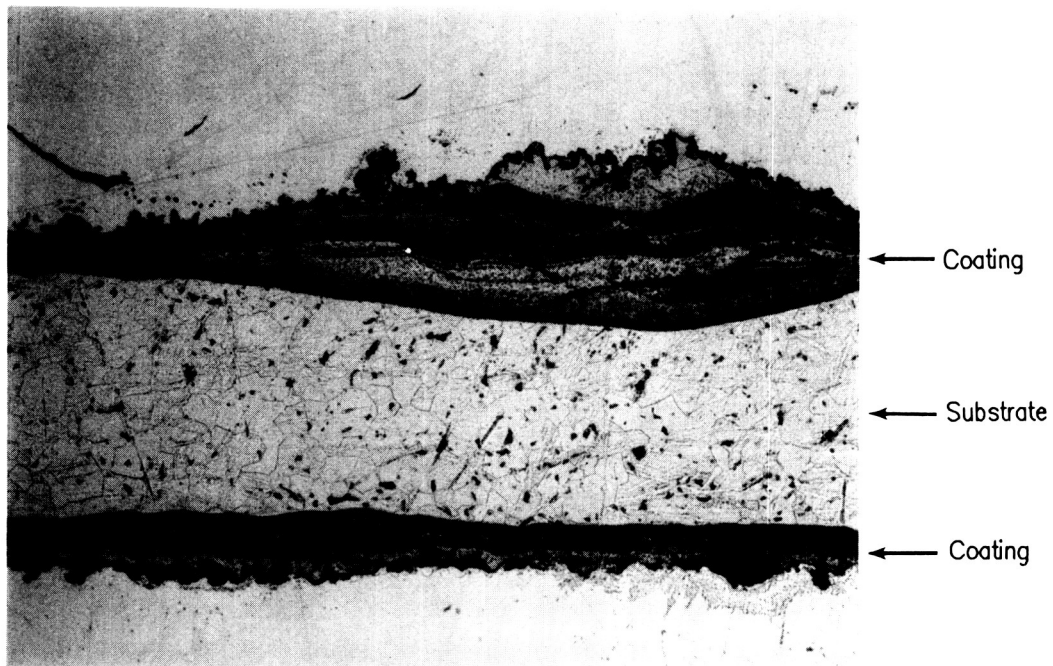
Mag: 126X

Typical Coating Edge Coverage on Lengthwise  
Panel Edge From Region No. 1

FD 358196

Figure 2-21. Vac Hyd VH-9 Microstructure (Etch: 60% Lactic; 20%  $\text{HNO}_3$ ; 20%  $\text{Hf}$ ;  
Thickness:  $2.6 \pm 1.5$  mils) (Sheet 1 of 2)

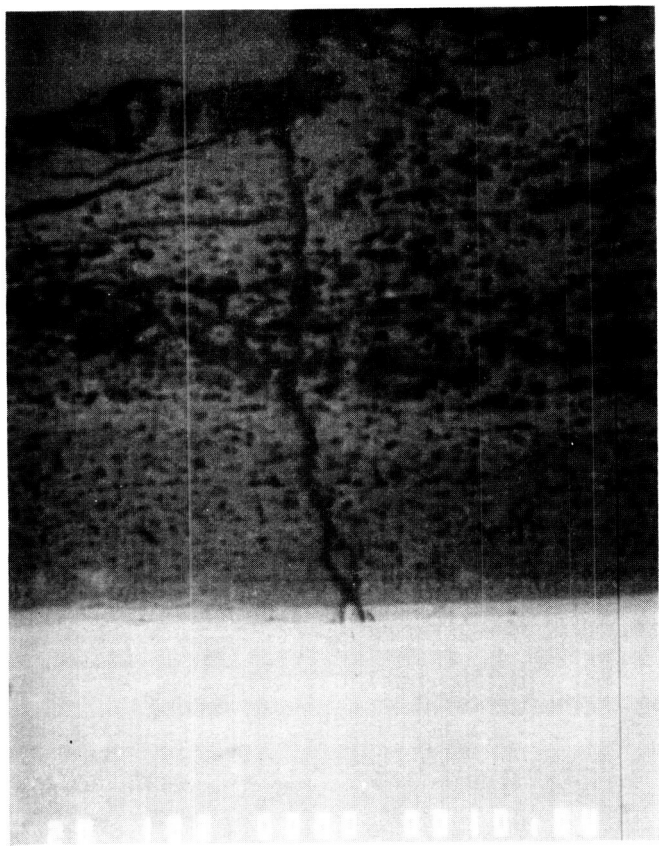




Non-Uniform Coating Thickness  
and Interaction With C-103 Substrate

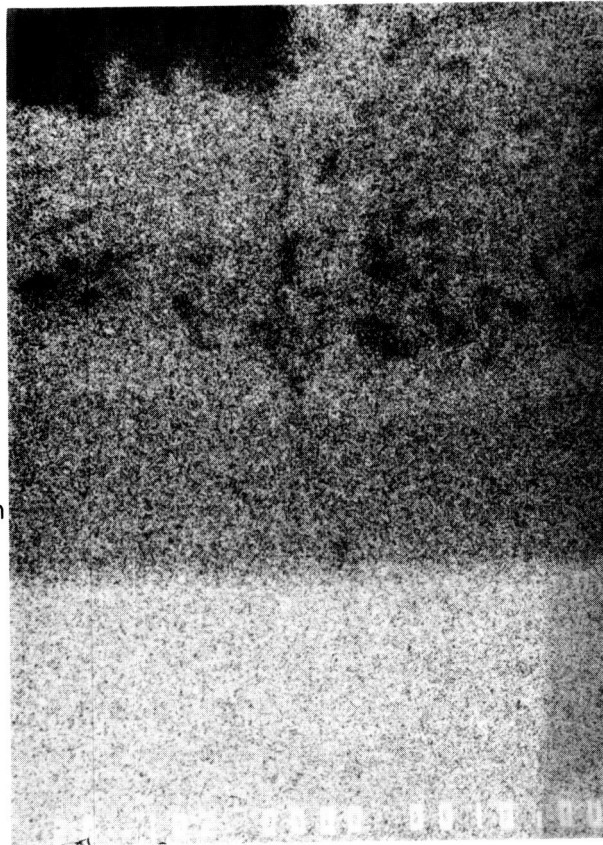
FD 358197

*Figure 2-21. Vac Hyd VH-9 Microstructure (Etch: 60% Lactic; 20%  $\text{HNO}_3$ ; 20%  $\text{Hf}$ ;  
Thickness:  $2.6 \pm 1.5$  mils) (Sheet 2 of 2)*

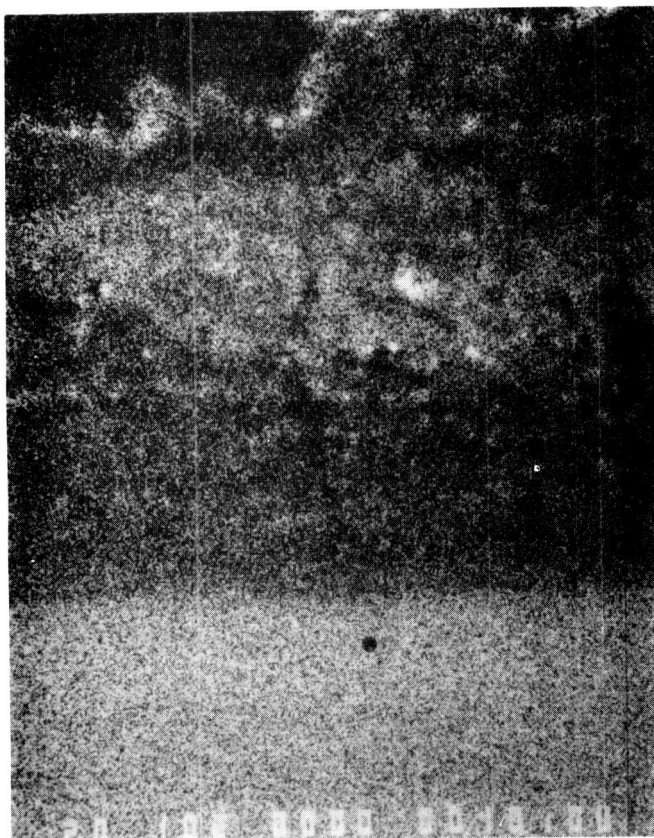


Backscattered Image

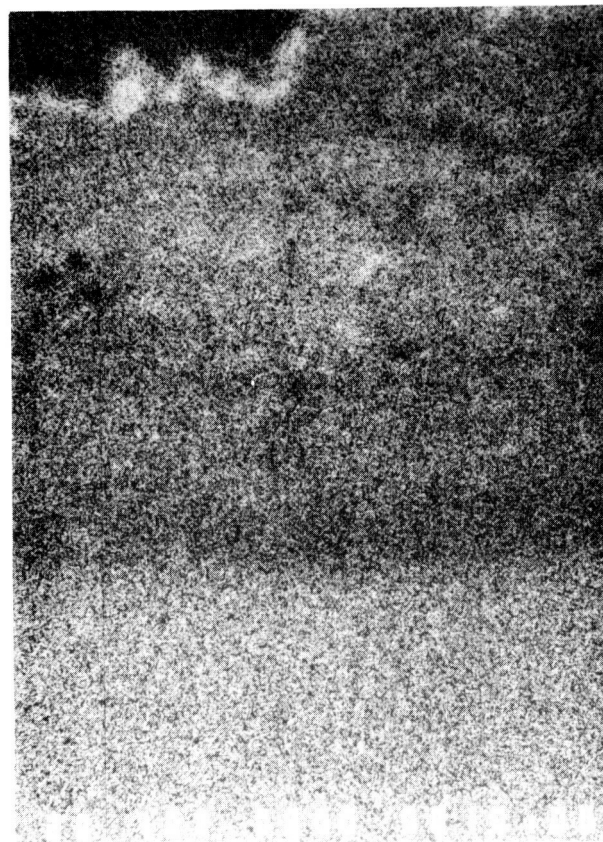
Coating  
Interdiffusion  
Zone  
Substrate



Element - Cb



Element - Hf



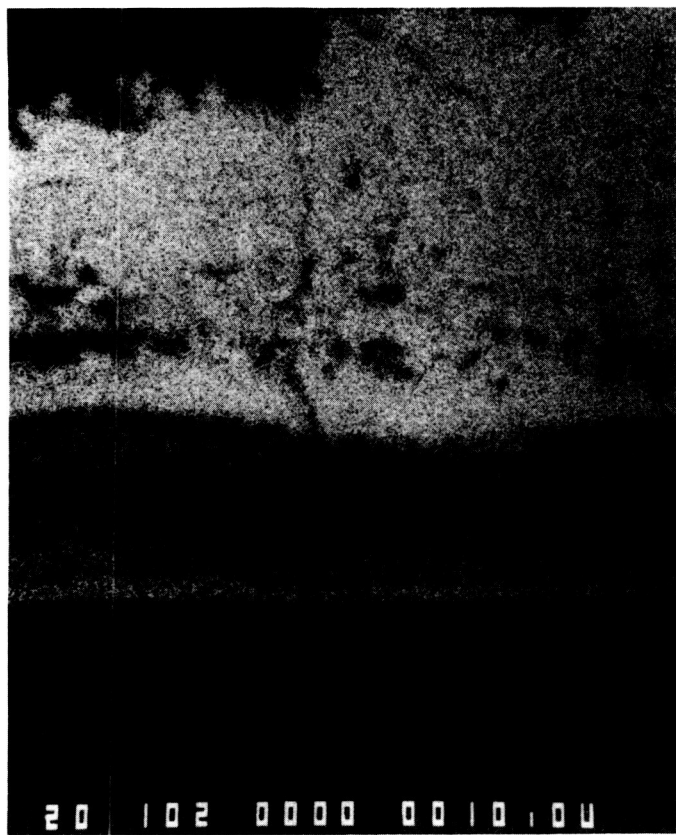
Element - Ti

Mag: 1000

FD 3581

S/N:50701-2

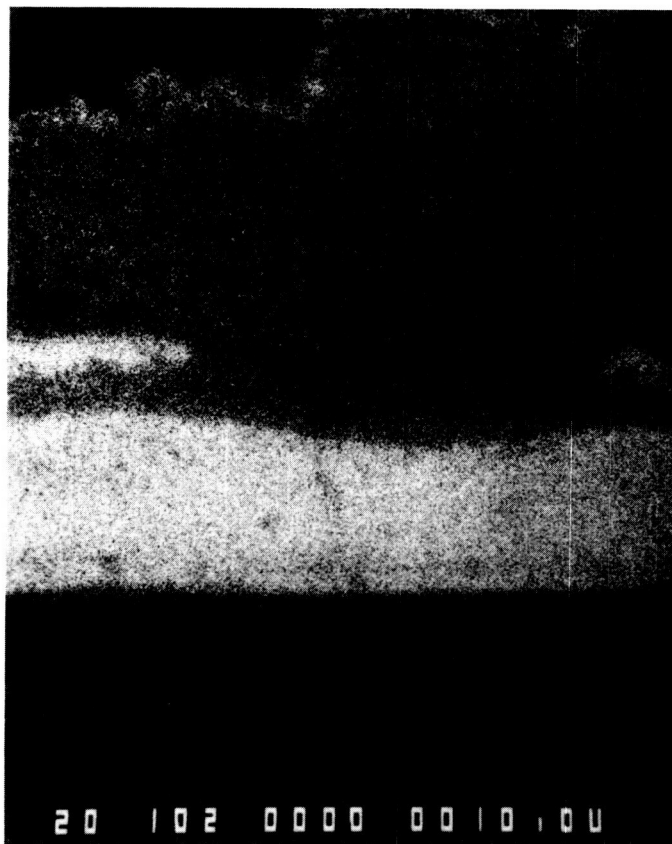
Figure 2-22. Elemental X-ray Maps of Vac Hyd VH-9 (Sheet 1 of 2)



Element Si



Element Cr



Element Al

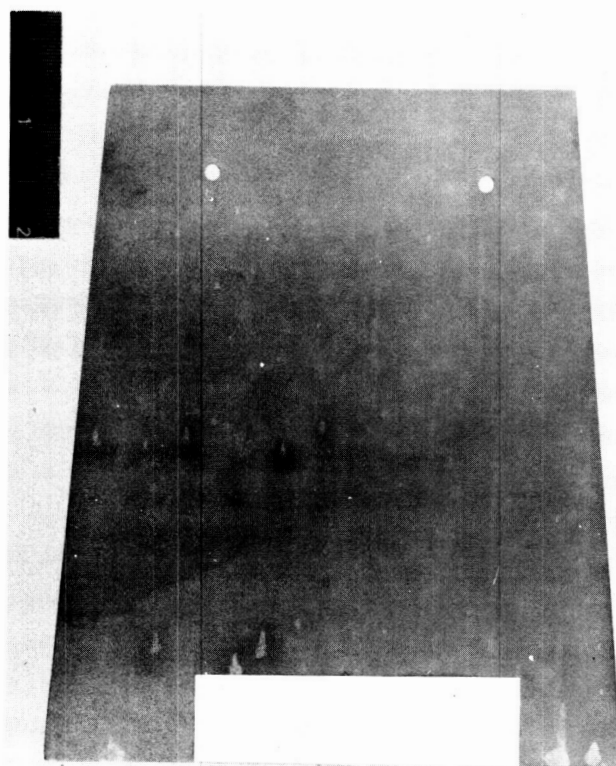
ORIGINAL PAGE IS  
OF POOR QUALITY.

S/N: 50701-2

Mag: 1000X

FD 358199

Figure 2-22. Elemental X-ray Maps of Vac Hyd VH-9 (Sheet 2 of 2)

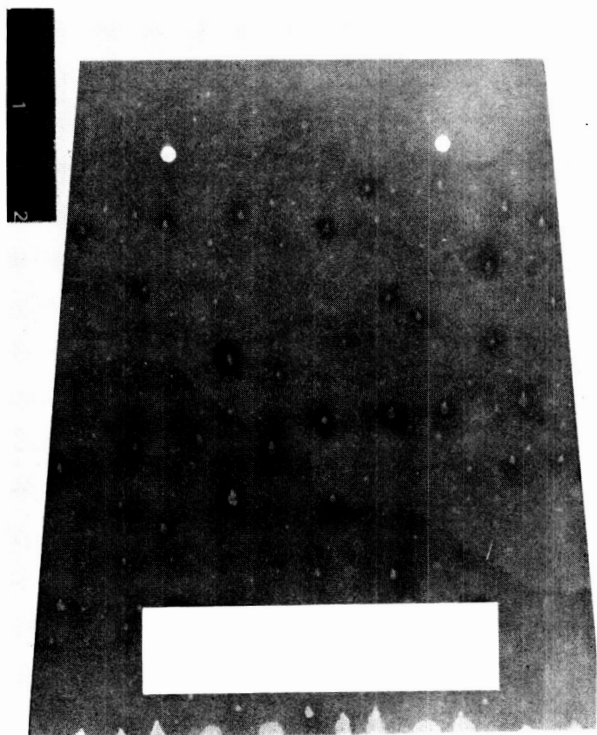


FD 358200

*Figure 2-23. Side 1 of Hitemco R505-F (Flame Side)*

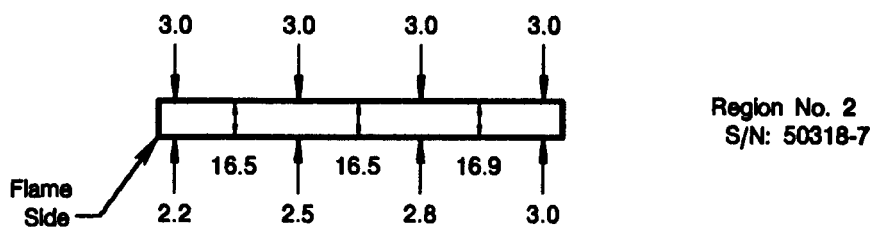
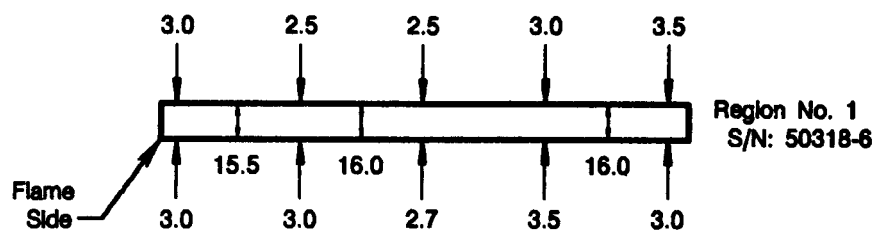
ORIGINAL PAGE IS  
OF POOR QUALITY

ORIGINAL PAGE IS  
OF POOR QUALITY

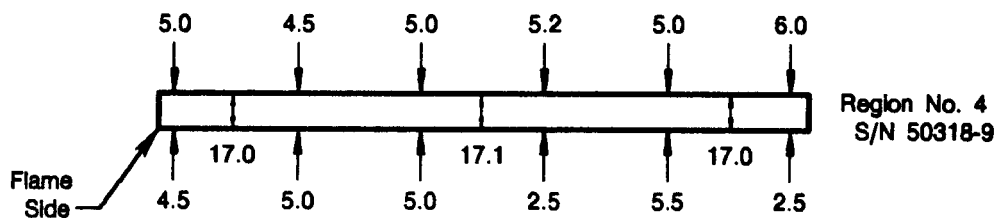
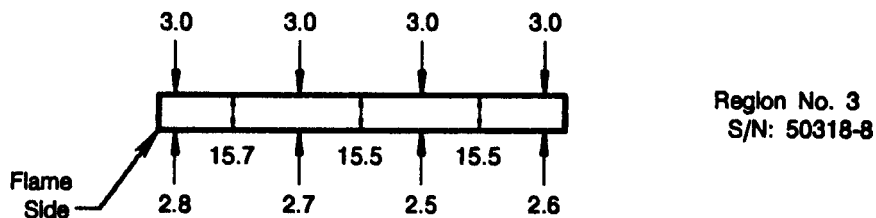


FD 358201

*Figure 2-24. Side 2 of Hitemco R505-F*



All Units Are In Mils

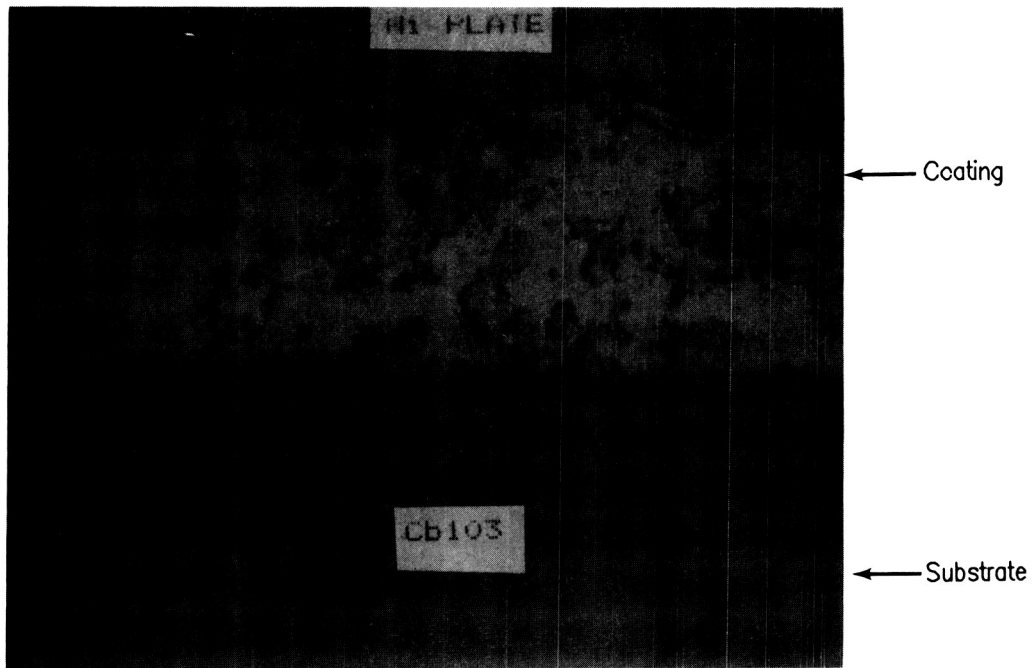


FDA 358202

Figure 2-25. Hitemco R505-F Coating and Substrate Thickness Distributions



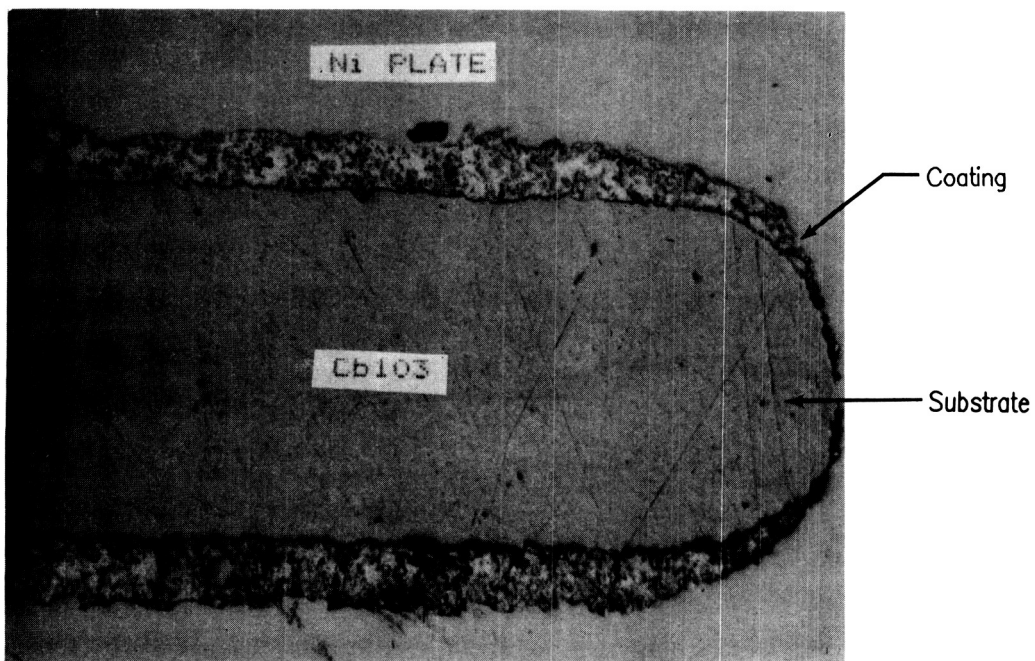
ORIGINAL PAGE IS  
OF POOR QUALITY



M/N 50318-7

Mag: 500X

Side 1: Typical Coating from Region No.2



S/N 50318-9

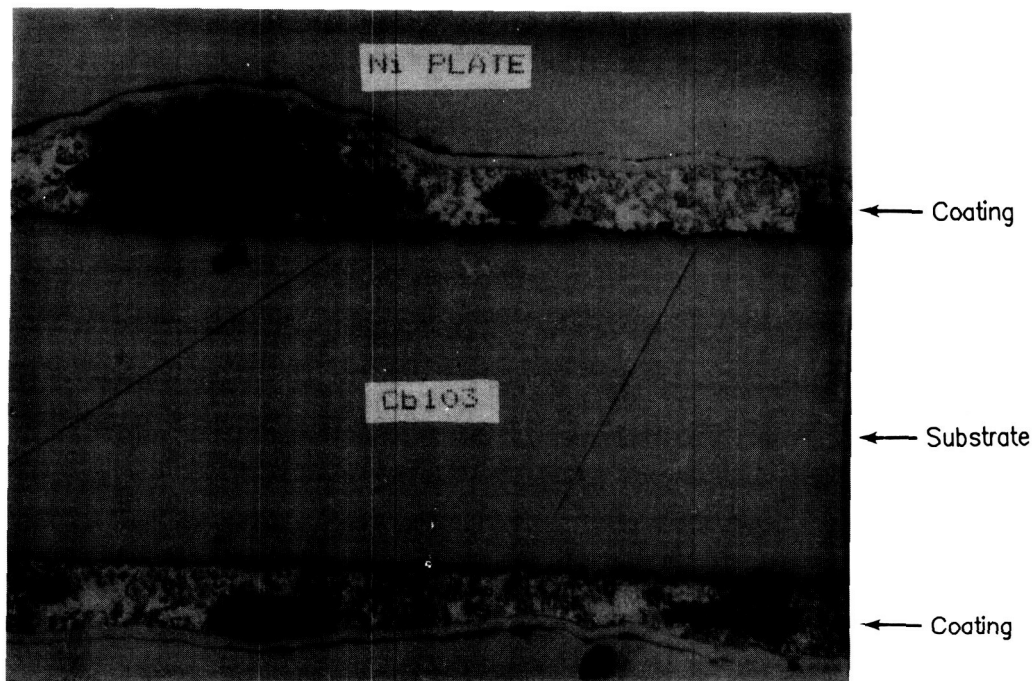
Mag: 100X

Typical Coating Thickness Distributed  
on Panel Edge from Region No.4

FD 358203

Figure 2-26. Hitemco R505-F Microstructure (Etch: 10% HCL; 90% H<sub>2</sub>O; Thickness  $3.4 \pm 1.0$  mils) (Sheet 1 of 2)

ORIGINAL PAGE IS  
OF POOR QUALITY



S/N 50318-6

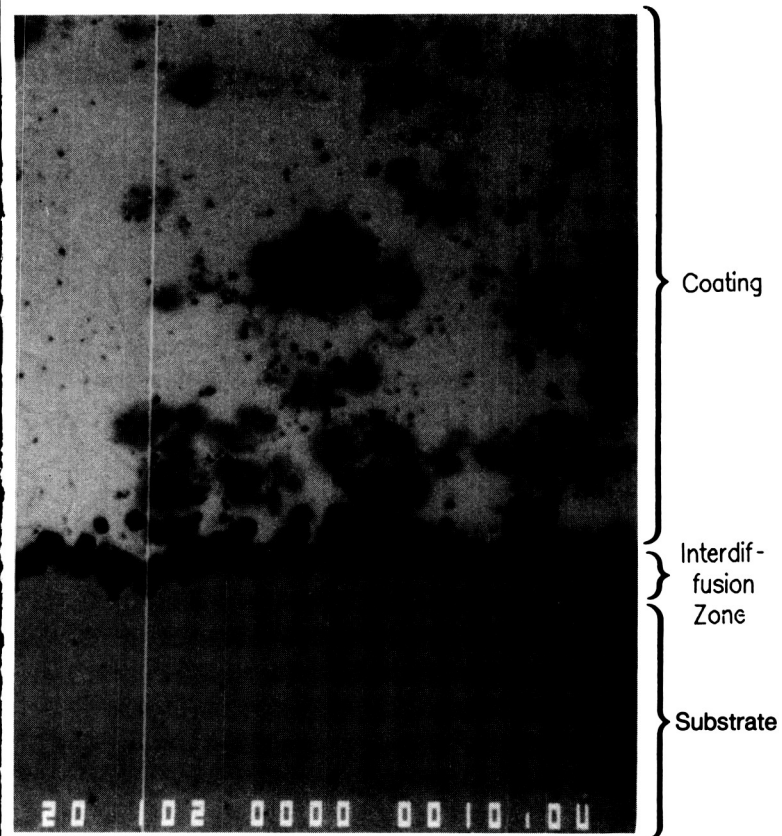
Mag: 100X

Hitemco R505F Coating Microstructure

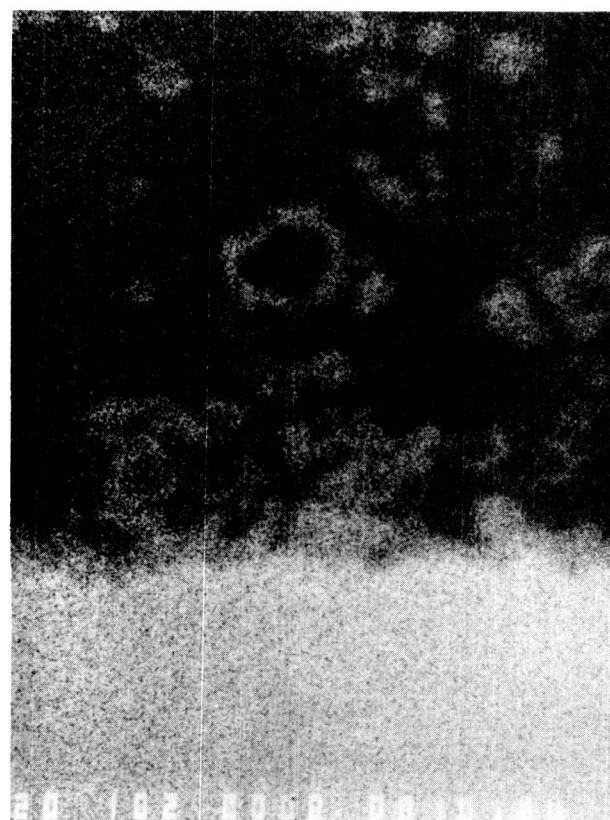
FD 358204

Figure 2-26. Hitemco R505-F Microstructure (Etch: 10% HCL; 90% H<sub>2</sub>O; Thickness  $3.4 \pm 1.0$  mils) (Sheet 2 of 2)

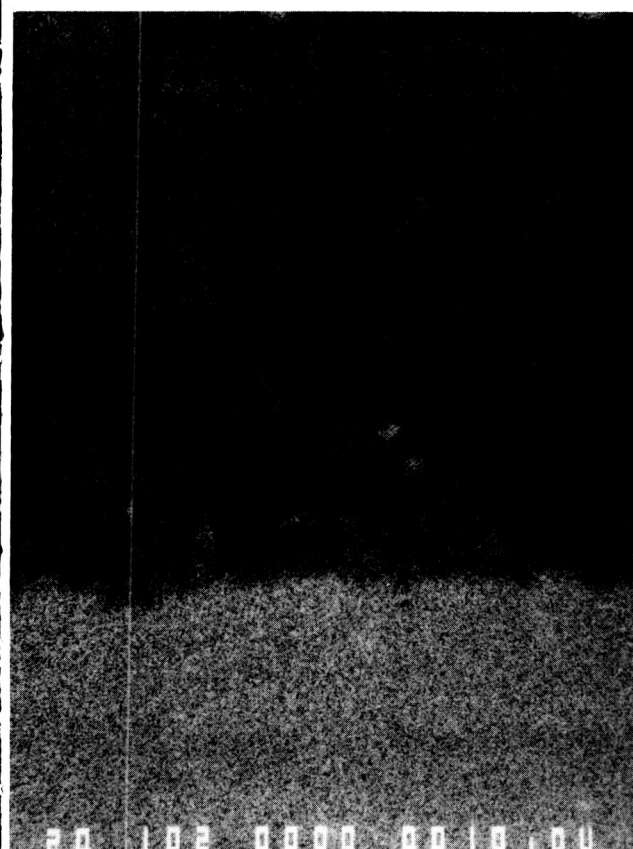




Backscattered Image

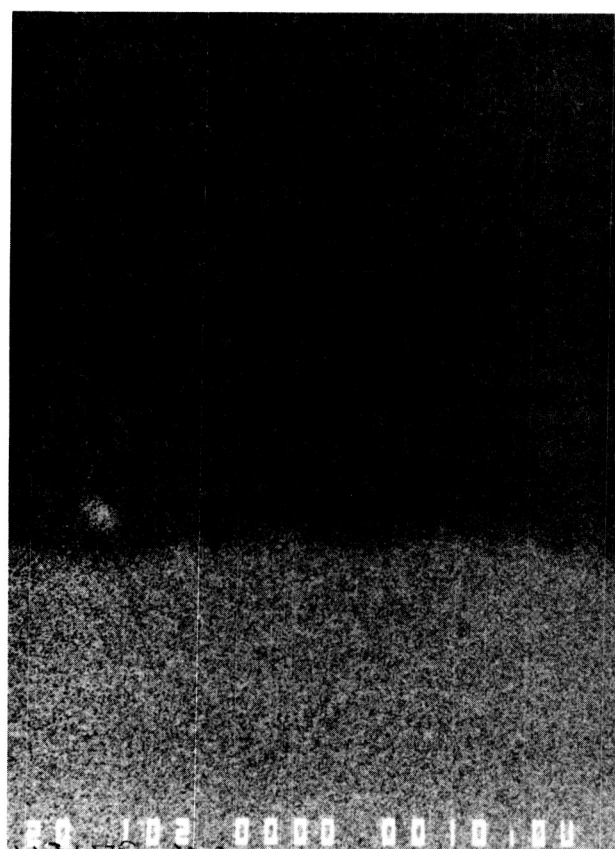


Element - Cb



S/N: 50318-7

Element Hf

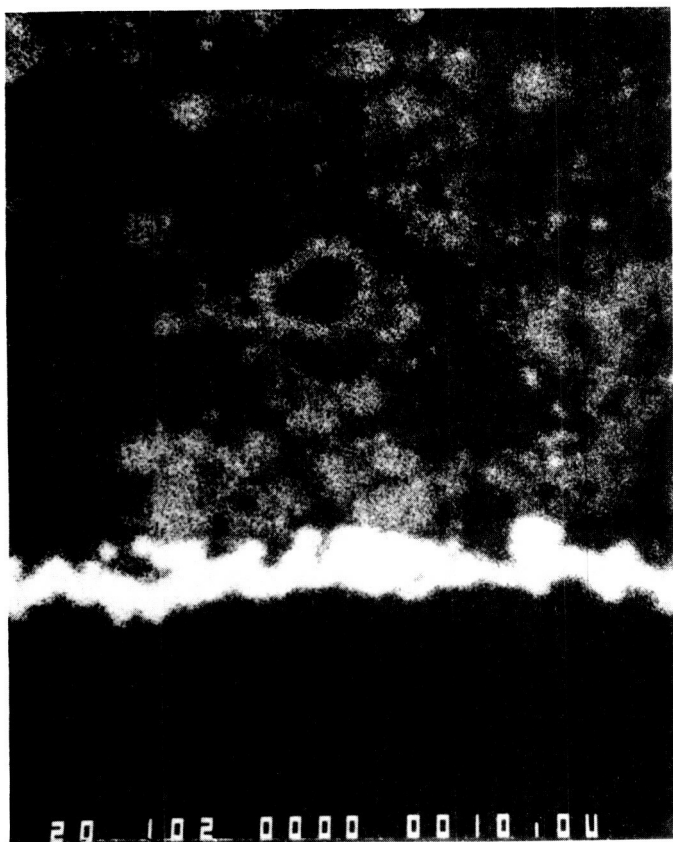


Element - Ti

Mag: 1000X

FD 358205

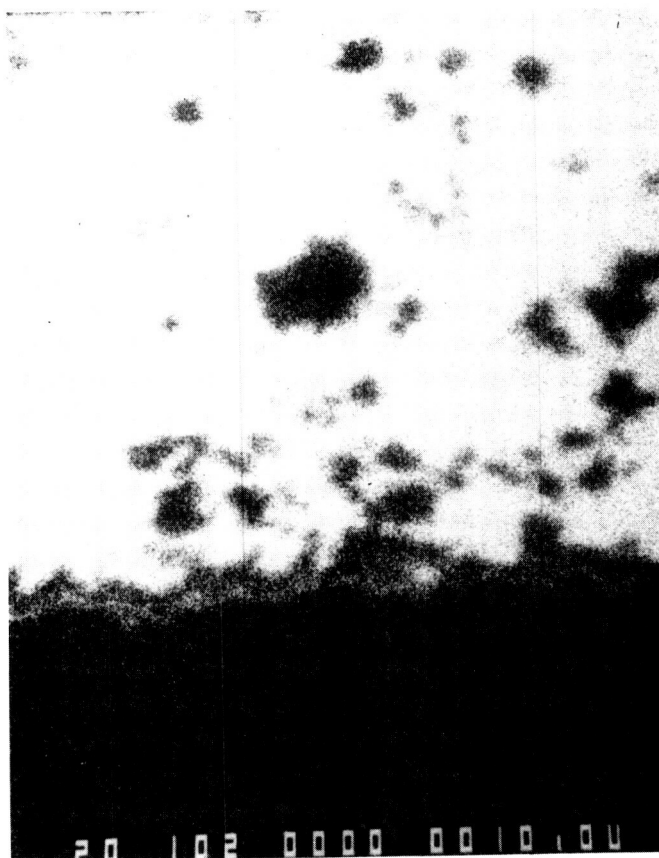
Figure 2-27. Elemental X-ray Maps of Hitemco R505-F (Sheet 1 of 2)



Element - Al



Element - Mo



Element - Sn

S/N: 50318-7

Mag: 1000X

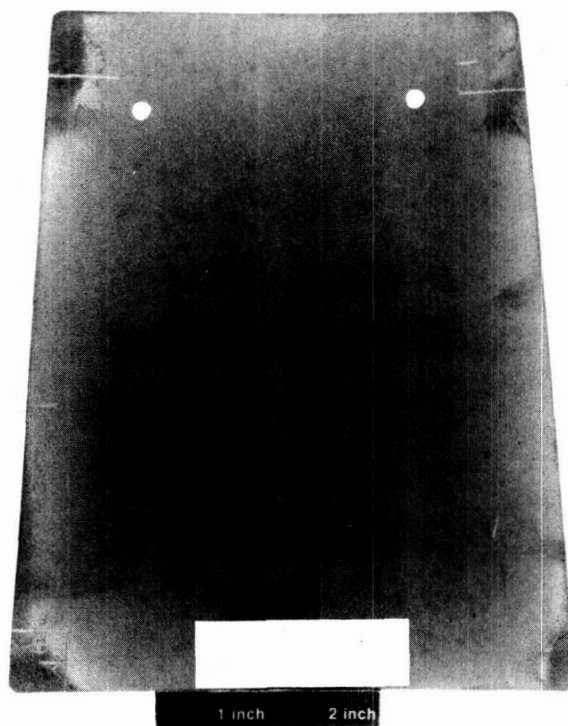
FD 35820

Figure 2-27. Elemental X-ray Maps of Hitemco R505-F (Sheet 2 of 2)

I-44

ORIGINAL PAGE IS  
OF POOR QUALITY

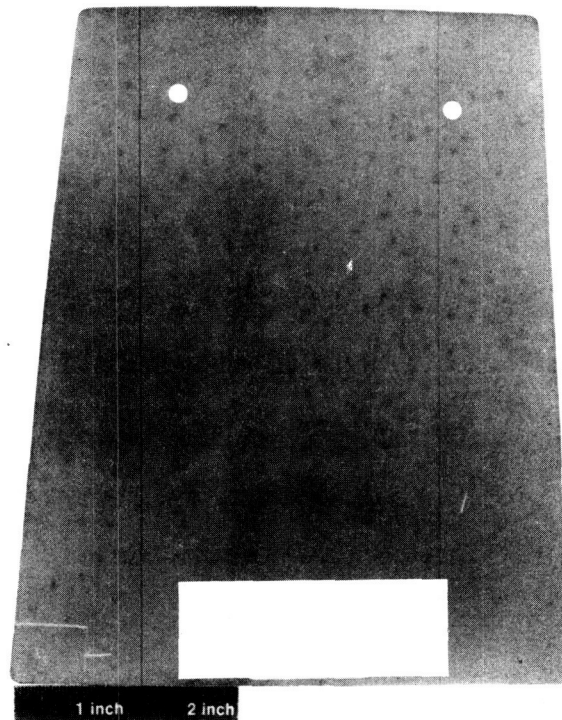
ORIGINAL PAGE IS  
OF POOR QUALITY



FD 358207

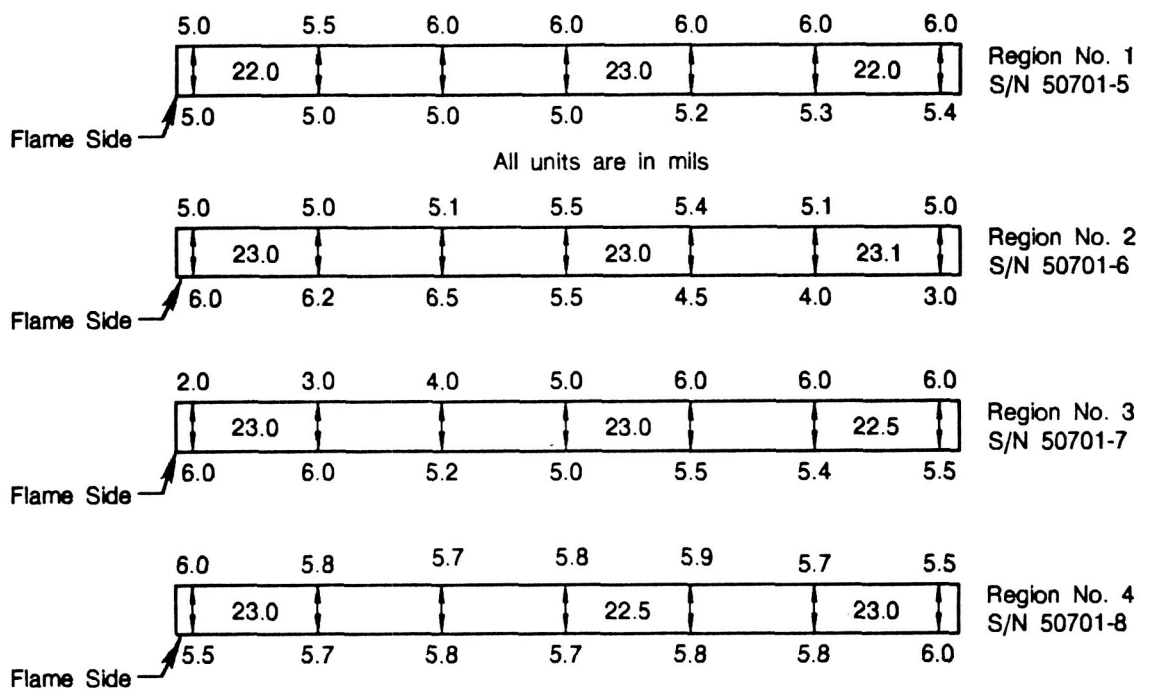
*Figure 2-28. Side 1 of Vac Hyd VH-2 Coating Sample (Flame Side)*

ORIGINAL PAGE IS  
OF POOR QUALITY



FD 358208

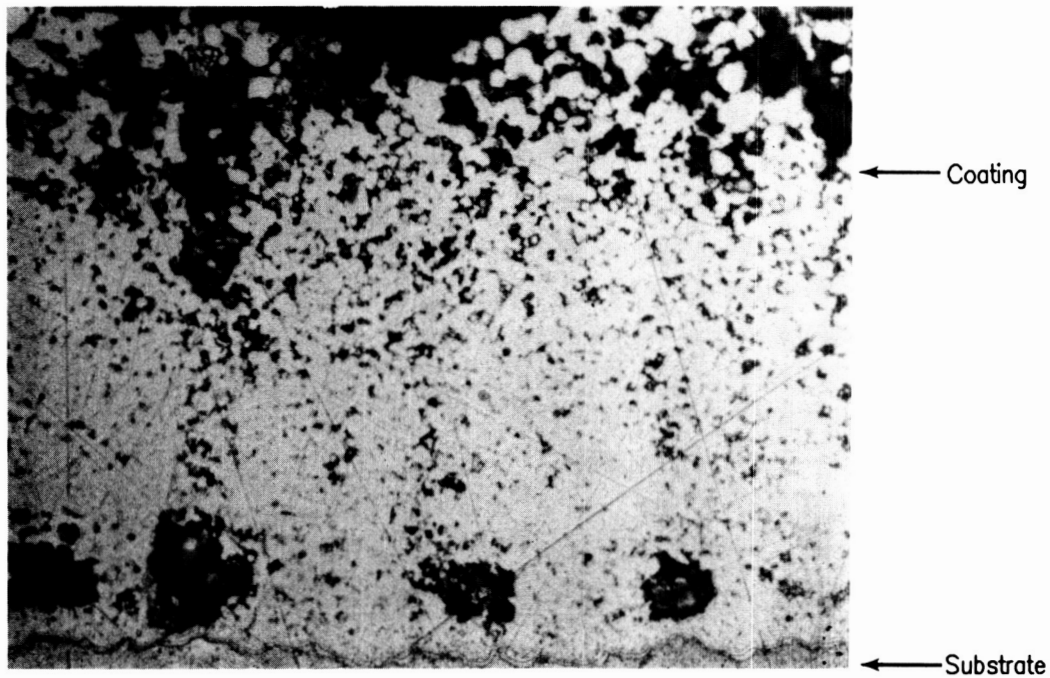
Figure 2-29. Side 2 of Vac Hyd VH-2 Coating Sample



FDA 358209

Figure 2-30. Vac Hyd VH-2 Coating and Substrate Thickness Distributions

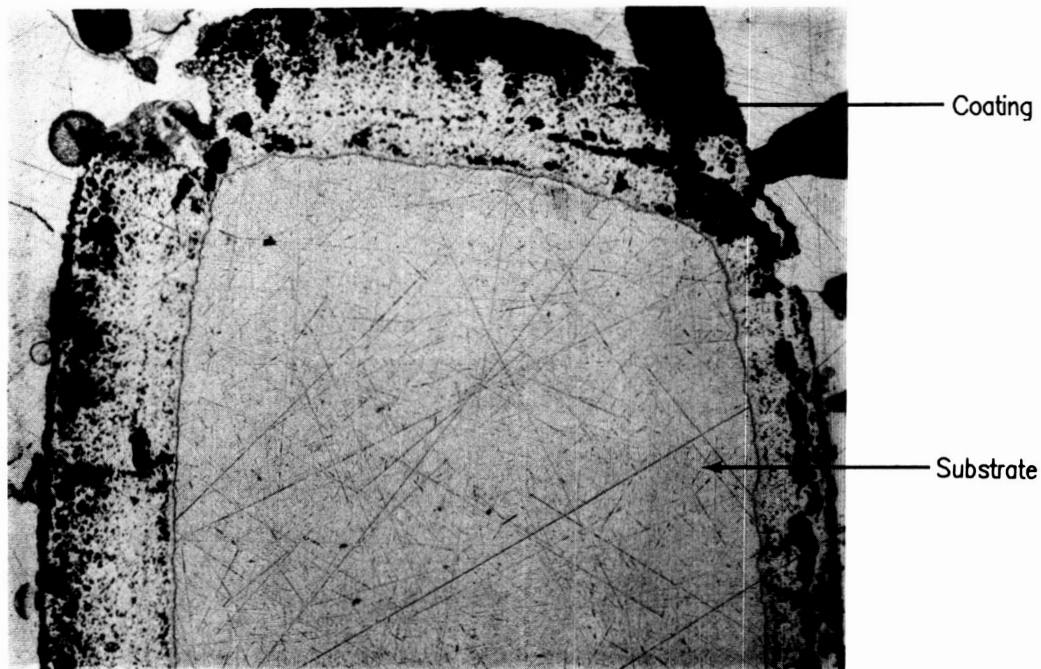
ORIGINAL PAGE IS  
OF POOR QUALITY



S/N 50701-8

Side 1: Typical Coating from Region No.4

Mag: 500X



S/N 50701-6

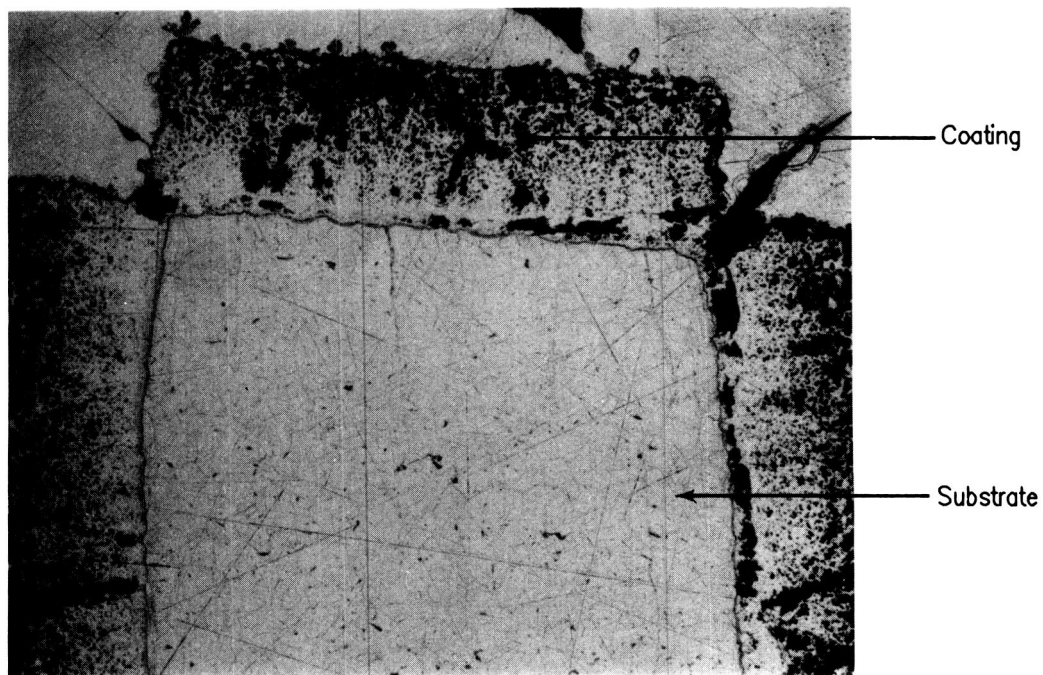
Typical Coating Edge Coverage on  
Lengthwise Panel Edge From Region No.2

Mag: 126X

FD 358210

Figure 2-31. Vac Hyd VH-2 Microstructure (Etch: 60% Lactic; 20%  $\text{HNO}_3$ ; 20%  $\text{Hf}$ ;  
Thickness:  $5.3 \pm 0.8$  mils) (Sheet 1 of 2)

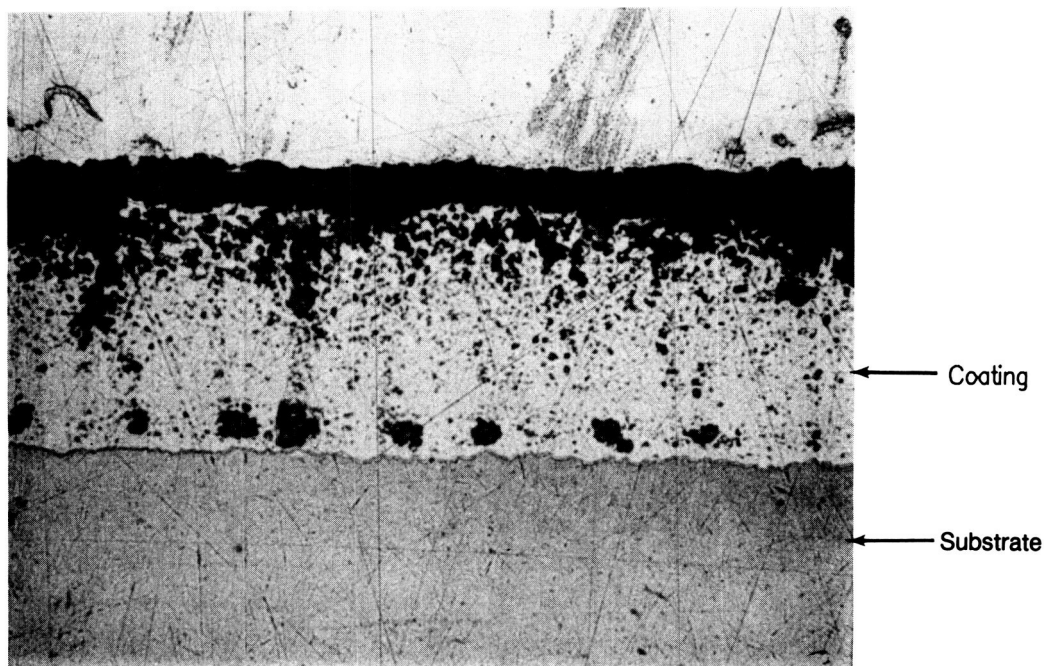




S/N 50701-8

Mag: 126X

Side 1: Panel Corner Coating Showing Non Uniformity



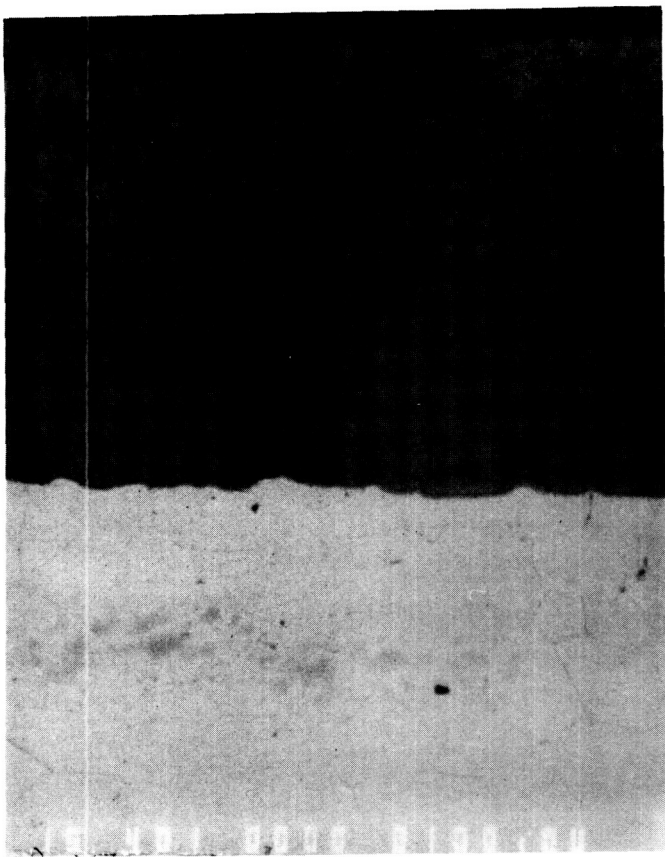
S/N 50701-8

Mag: 200X

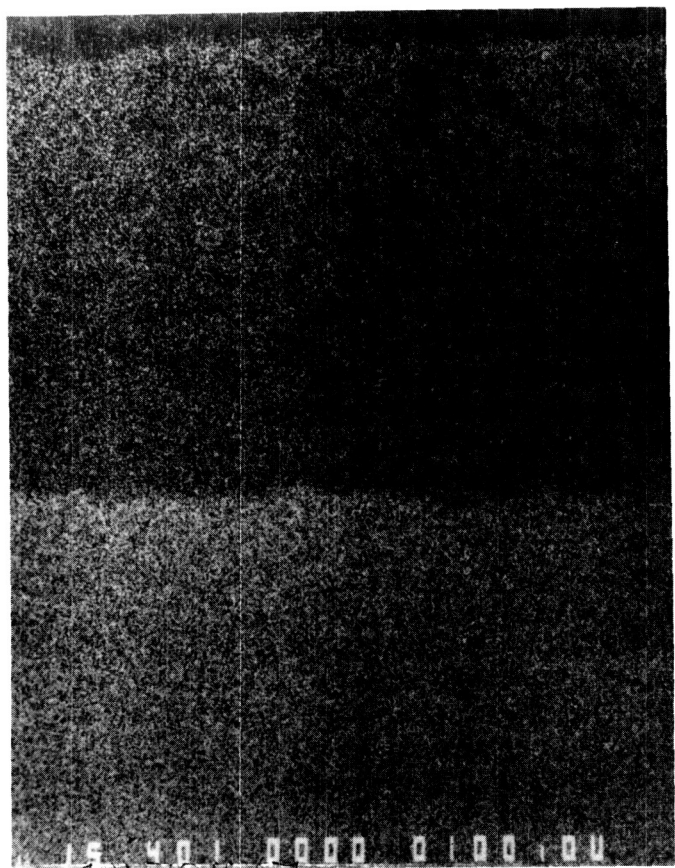
Excess Coating "Pull-Out" During Metallography  
Consistently Occurred 0.6 mils Above the Coating  
Substrate Interface

FD 358211

**Figure 2-31.** *Vac Hyd VH-2 Microstructure (Etch: 60% Lactic; 20% HNO<sub>3</sub>; 20% Hf; Thickness:  $5.3 \pm 0.8$  mils) (Sheet 2 of 2)*



Backscattered Image



Element - Cb



Element - Al

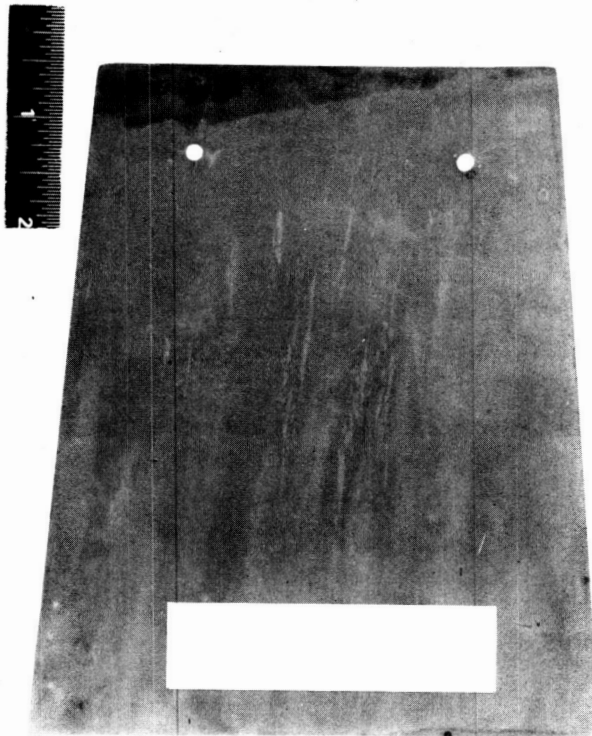
S/N: 50701-8

Mag: 400X

FD 358212

Figure 2-32. Elemental X-ray Maps of Vac Hyd VH-2

ORIGINAL PAGE IS  
OF POOR QUALITY

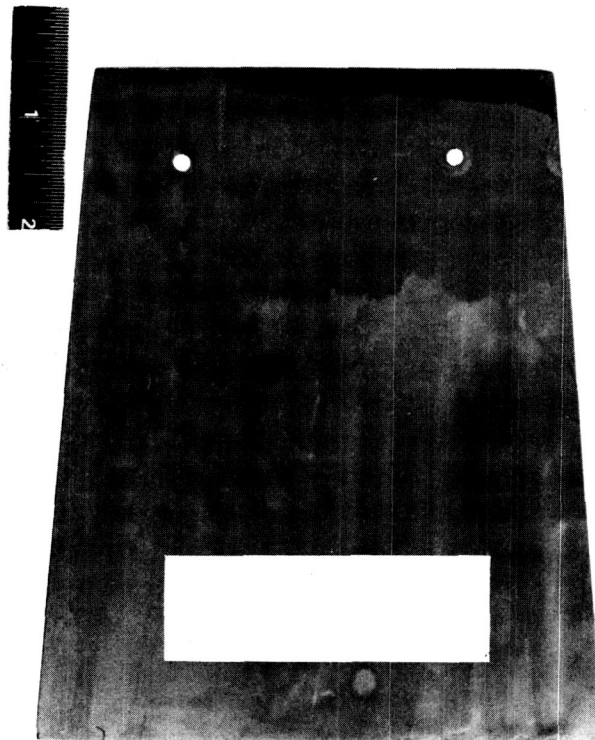


FD 358213

*Figure 2-33. Side 1 of Chromalloy RT-40 (Flame Side)*

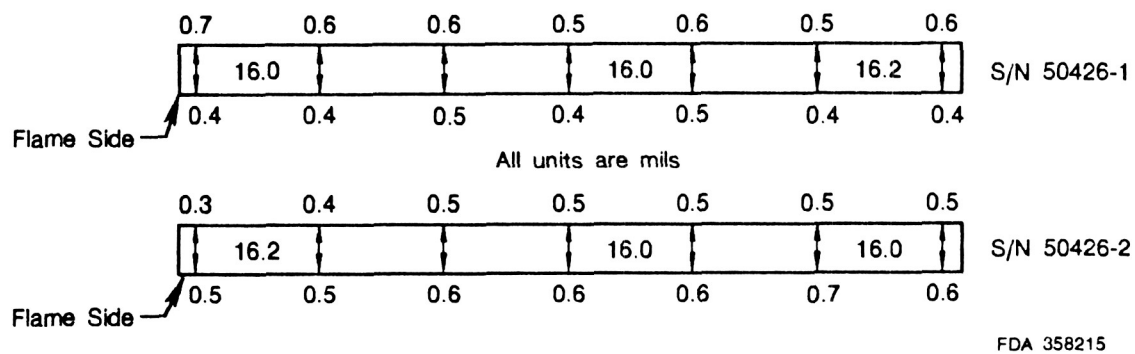


ORIGINAL PAGE IS  
OF POOR QUALITY



FD 358214

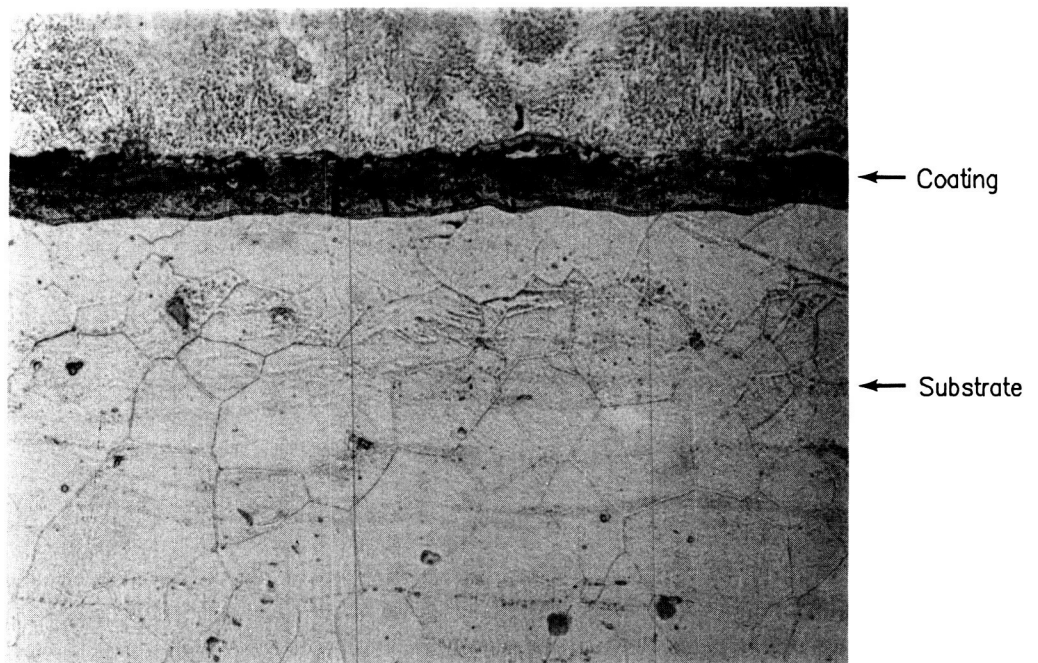
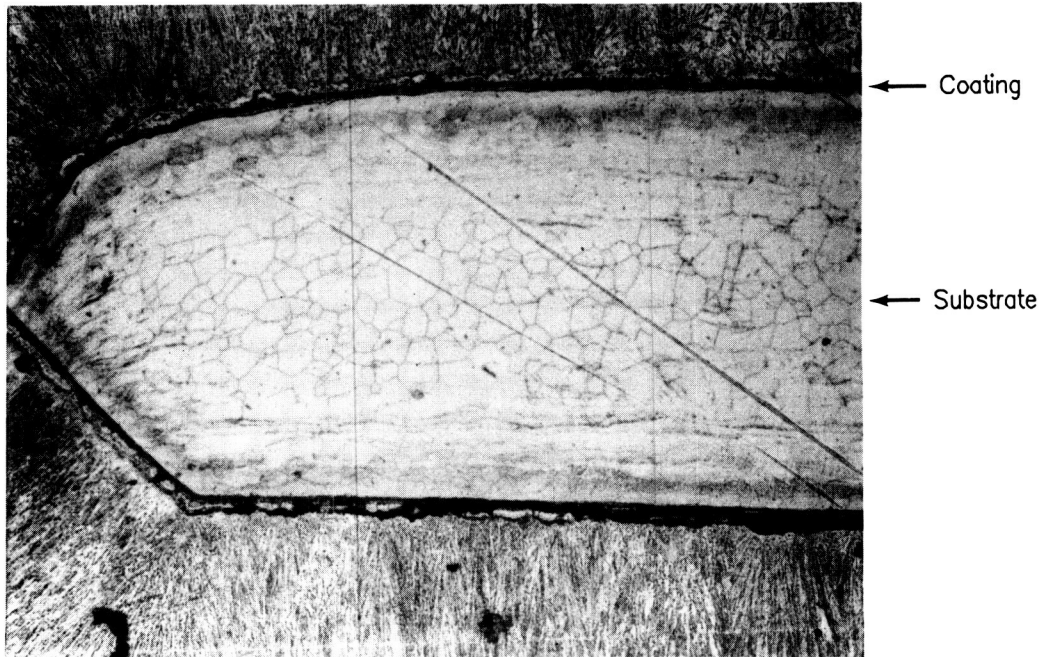
Figure 2-34. Side 2 of Chromalloy RT-40



FDA 358215

Figure 2-35. Chromalloy RT40 Coating and Substrate Thickness Distributions

ORIGINAL PAGE IS  
OF POOR QUALITY

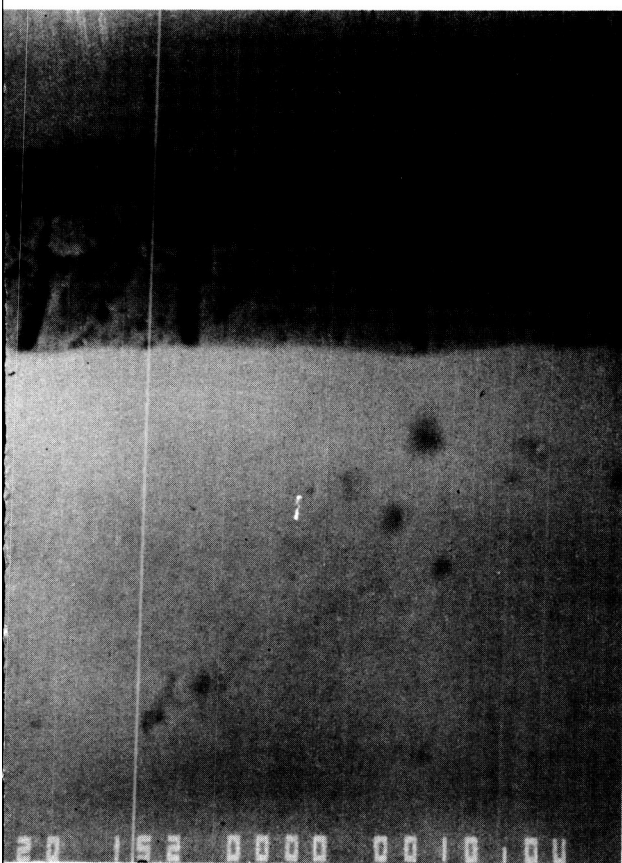


S/N 50426-1

Mag: 500X

FD 358216

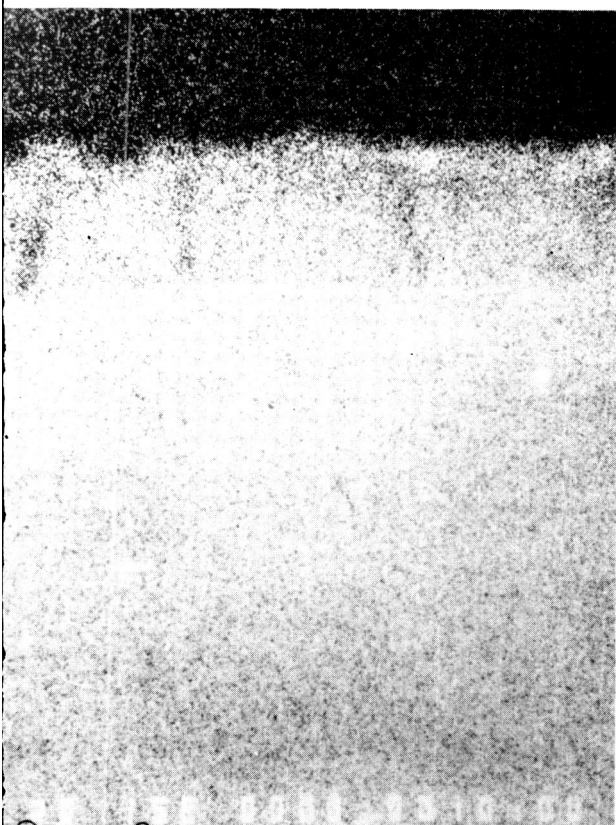
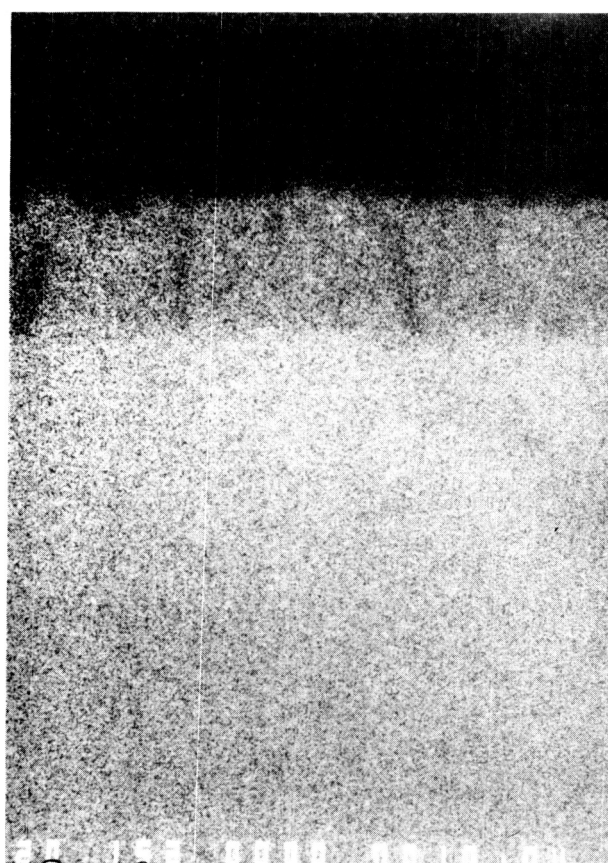
**Figure 2-36.** *Chromalloy RT-40 Microstructure (Etch: 60% Lactic; 20%  $\text{HNO}_3$ ; 20%  $\text{Hf}$ ; Thickness:  $0.5 \pm 0.1$  mil)*



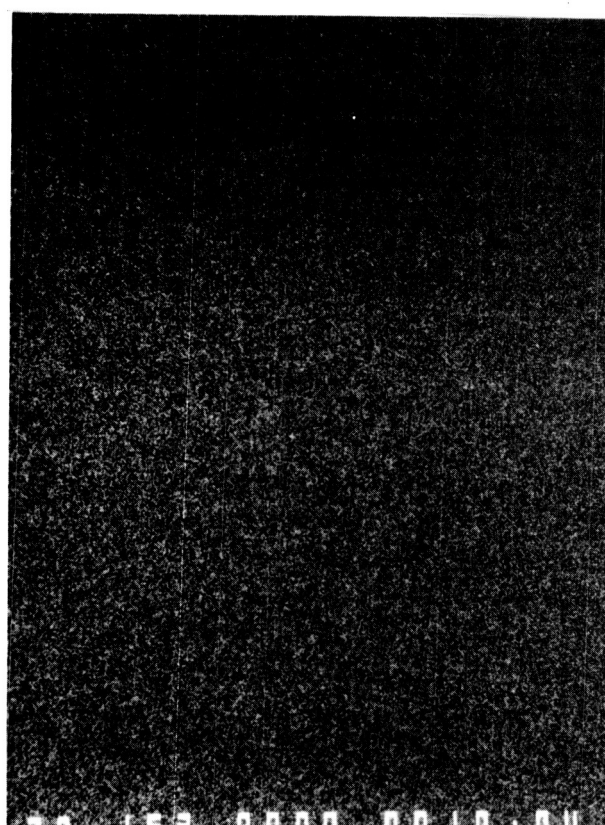
Coating

Interdiffusion Zone

Substrate



Element - Hf



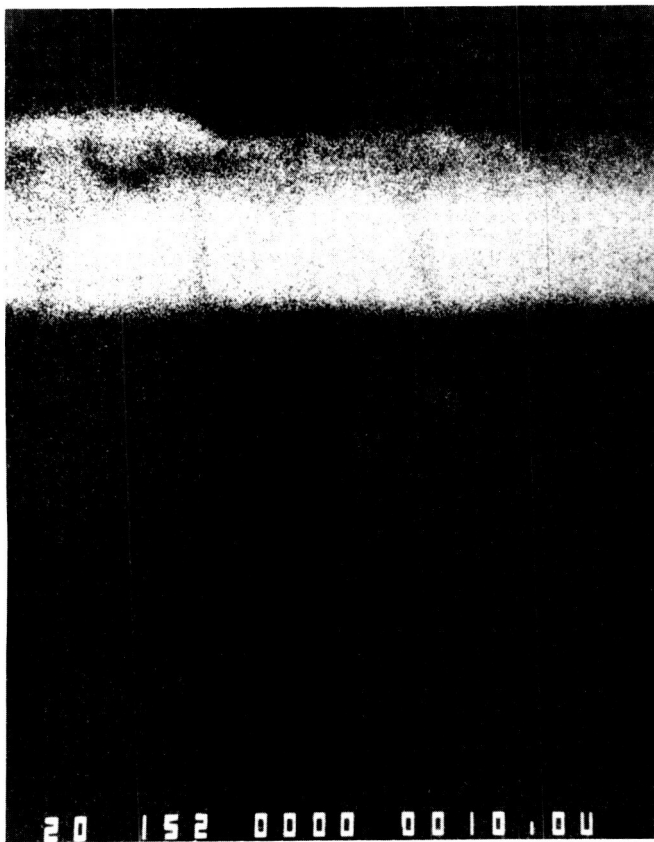
Element - Ti

/N: 50426-2

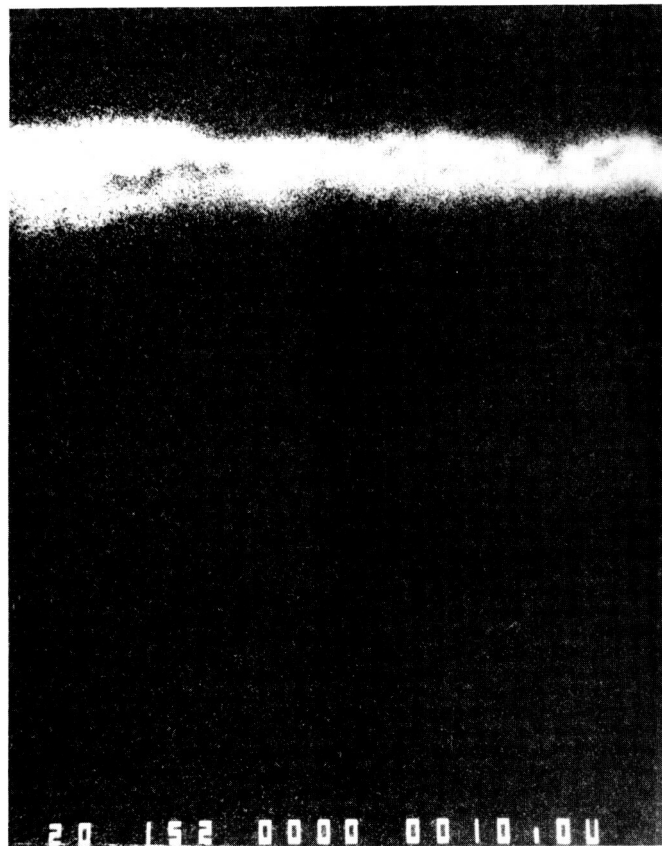
Mag: 1500X

FD 358217

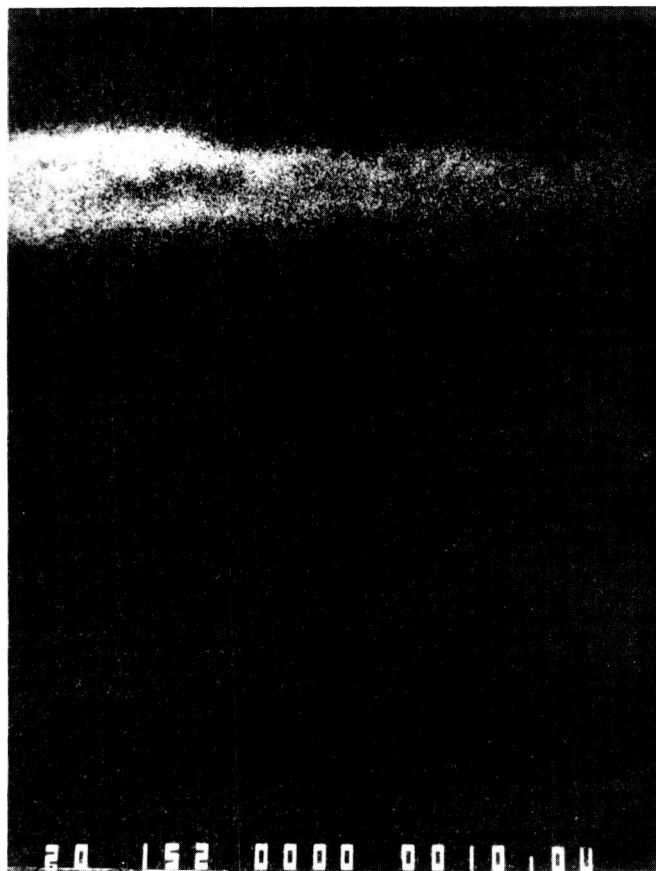
Figure 2-37. Elemental X-ray Maps of Chromalloy RT-40 (Sheet 1 of 2)



Element - Si



Element - Cr



Element - Fe

S/N: 50426-2

Mag: 1500X

FD 358218

Figure 2-37. Elemental X-ray Maps of Chromalloy RT-40 (Sheet 2 of 2)

**PART II**  
**POST ENGINE TEST COATING**  
**EVALUATION**

## CONTENTS

<i>Section</i>	<i>Page</i>
1.0 BACKGROUND .....	II-1
2.0 THEORETICAL CALCULATIONS .....	II-2
3.0 ENGINE TESTED EVALUATION .....	II-5
3.1 Uncoated Columbium (Alloy C-103) .....	II-5
3.1.1 Macrophotographic Documentation .....	II-5
3.1.2 Microstructural Observations .....	II-5
3.1.3 Microhardness Profiles .....	II-5
3.2 VH-109: Vac Hyd .....	II-6
3.2.1 Macrophotographic Documentation .....	II-6
3.2.2 Coating/Substrate Thickness Distributions .....	II-6
3.2.3 Microstructural Observations .....	II-6
3.2.4 Microhardness Profiles .....	II-6
3.3 R512-E: Hitemco .....	II-7
3.3.1 Macrophotographic Documentation .....	II-7
3.3.2 Coating/Substrate Thickness Distributions .....	II-7
3.3.3 Microstructural Observations .....	II-7
3.3.4 Microhardness Profiles .....	II-7
4.0 COMPARATIVE ANALYSIS .....	II-8
4.1 H <sub>2</sub> and O <sub>2</sub> Gas Absorption .....	II-8
4.2 Microstructural .....	II-9
4.3 Compositional .....	II-11
5.0 SUMMARY .....	II-12
6.0 CONCLUSIONS .....	II-13
7.0 REFERENCES .....	II-14

PRECEDING PAGE BLANK NOT FILMED

## ILLUSTRATIONS

<i>Figure</i>		<i>Page</i>
1-1	As-Coated Microstructures of VH-109 and R512E from Part I .....	II-15
1-2	Typical Test Panel Attachment to RL10 Exhaust Nozzle .....	II-16
3-1	Gas-Path Environment Side of Uncoated C-103 Test Panel with Sectioning Pattern — Run Time: 1203 seconds — Start/Stop Cycles: 6 .....	II-17
3-2	Chamber Environment Side of Uncoated C-103 Test Panel with Sectioning Pattern — Run Time: 1203 seconds — Start/Stop Cycles: 6 .....	II-18
3-3	Uncoated C-103 Microstructure at Region A (S/N 60210-3) — Run Time: 1203 seconds — Start/Stop Cycles: 6 .....	II-19
3-4	Uncoated C-103 Microstructure at Region B (S/N 60210-4) — Run Time: 1203 seconds — Start/Stop Cycles: 6 .....	II-20
3-5	Uncoated C-103 Microstructure at Region C (S/N 60210-5) — Run Time: 1203 seconds — Start/Stop Cycles: 6 .....	II-21
3-6	Uncoated C-103 Microstructure at Region D (S/N 60210-6) — Run Time: 1203 seconds — Start/Stop Cycles: 6 .....	II-22
3-7	Uncoated C-103 Microstructure at Region E (S/N 60210-7) — Run Time: 1203 seconds — Start/Stop Cycles: 6 (Sheet 2 of 2) .....	II-23
3-8	Oxygen X-ray Line Scan vs Intensity .....	II-24
3-9	Microstructure Measurement Through the Thickness of Virgin C-103 — 50X — Unetched — S/N 60701-1 .....	II-25
3-10	Microhardness Measurements Through the Thickness of the Uncoated C-103 Panel — Run Time: 1203 seconds — Start/Stop Cycles: 6 — Unetched — S/N 60210-3,4,5,6,7 .....	II-26
3-11	Gas Path Environment Side of VH-109 Coated C-103 Test Panel — Run Time: 4451 seconds — Start/Stop Cycles: 23 .....	II-27
3-12	Warping of VH-109 Panel (Arrow Indicates Crack Location) .....	II-28
3-13	Gas-Path View of Crack in VH-109 Panel .....	II-29
3-14	Chamber Environment Side of VH-109 Coated C-103 Test Panel (Note: Arrow Points to Pinhole Oxidation Which Correlates to Surface Blemish on Gas-Path Side of Panel) — Run Time: 4451 seconds — Start/Stop Cycles: 23 .....	II-30
3-15	Macrograph of Pinhole Oxidation .....	II-31



## ILLUSTRATIONS (Continued)

<i>Figure</i>		<i>Page</i>
3-16	Sectioning Pattern of Flame-Side VH-109 Coated C-103 Test Panel — Run Time: 4451 seconds — Start/Stop Cycles: 23 .....	II-32
3-17	Coating Thickness Distribution Diagrams of VH-109 Coated C-103 Test Panel — Run Time: 4451 seconds — Start/Stop Cycles: 23 .....	II-33
3-18	VH-109 Coating Microstructure at Region 1 (S/N 60321-1) — Run Time: 4451 seconds — Start/Stop Cycles: 23 .....	II-34
3-19	VH-109 Coating Microstructure at Region 3 (S/N 60321-3) — Run Time: 4451 seconds — Start/Stop Cycles: 23 .....	II-35
3-20	VH-109 Coating Microstructure at Region 4 (S/N 60321-4) — Run Time: 4451 seconds — Start/Stop Cycles: 23 .....	II-36
3-21	VH-109 Coating Microstructure at Region 5 (S/N 60321-5) — Run Time: 4451 seconds — Start/Stop Cycles: 23 .....	II-37
3-22	VH-109 Coating Microstructure at Region 7 (S/N 60321-7) — Run Time: 4451 seconds — Start/Stop Cycles: 23 .....	II-38
3-23	Cross Section of Crack on VH-109 Coated C-103 Test Panel — Run Time: 4451 seconds — Start/Stop Cycles: 23 .....	II-39
3-24	Cross Section of Pinhole Coating Failure Illustrating the Mechanical Damage That Led to C-103 Oxidation .....	II-40
3-25	Microhardness Measurements Through the Thickness of VH-109 Coated C-103 Test Panel — Run Time: 4451 seconds — Start/Stop Cycles: 23 .....	II-41
3-26	Gas-Path Environment Side of R512-E Coated C-103 Test Panel — Run Time: 4451 seconds — Start/Stop Cycles: 23 .....	II-42
3-27	Downstream View of R512-E Coated C-103 Test Panel (Note the Cooling Tube Spacing Pattern Shown by the Surface Scale of the Panel) .....	II-43
3-28	Bracket Crack (Arrow Shows Crack in Support Bracket Which May Have Reduced Constraining Stresses, Thus Minimizing Warping) .....	II-44
3-29	Chamber Environment Side of R512-E Coated C-103 Test Panel (Arrow Locates a Coating Chip at Exit Plane) — Run Time: 4451 seconds — Start/Stop Cycles: 23 .....	II-45
3-30	Close-Up View of Coating Chip on Figure 3-29 .....	II-46
3-31	As-Coated R512-E Thickness Distribution of $5.0 \pm 1.0$ mil Coating .....	II-47



## ILLUSTRATIONS (Continued)

<i>Figure</i>	<i>Page</i>
3-32      Sectioning Pattern of Gas Path (Flame) Side of R512-E Coated C-103 Test Panel — Run Time: 4451 seconds — Start/Stop Cycles: 23 .....	II-48
3-33      Coating Thickness Distribution Diagram of R512-E Coated C-103 Test Panel — Run Time: 4451 seconds — Start/Stop Cycles: 23 .....	II-49
3-34      R512-E Coating Microstructure at Region 1 (S/N 60317-1) — Run Time: 4451 seconds — Start/Stop Cycles: 23 .....	II-50
3-35      R512-E Coating Microstructure at Region 3 (S/N 60317-3) — Run Time: 4451 seconds — Start/Stop Cycles: 23 .....	II-51
3-36      R512-E Coating Microstructure at Region 4 (S/N 60317-4) — Run Time: 4451 seconds — Start/Stop Cycles: 23 .....	II-52
3-37      R512-E Coating Microstructure at Region 5 (S/N 60317-5) — Run Time: 4451 seconds — Start/Stop Cycles: 23 .....	II-53
3-38      R512-E Coating Microstructure at Region 6 (S/N 60317-6) — Run Time: 4451 seconds — Start/Stop Cycles: 23 .....	II-54
3-39      Microhardness Measurements Through the Thickness of R512-E Coated C-103 Test Panel — Run Time: 4451 seconds — Start/Stop Cycles: 23 .....	II-55
4-1      Cross Sections After Grit Blasting to Remove Surface Oxides and Coating .....	II-56
4-2      Schematic of Gas Analysis Locations .....	II-57
4-3      Hydrogen/Columbium Data .....	II-58
4-4      The Effect of Hydrogen Content on the Ductile-to-Brittle Transition Temperature of Columbium .....	II-59
4-5      Equivalent Flame-Side Microstructures of R512-E and VH-109 After Engine Exposure — Run Time: 4451 seconds — Start/Stop Cycles: 23 .....	II-60
4-6      Pretest and Post Test Flame-Side Microstructures of R512-E .....	II-61
4-7      Pretest and Post Test Flame-Side Microstructures of VH-109 .....	II-62
4-8      As-Coated R512-E Composition Profile .....	II-63
4-9      Engine Tested R512-E Composition Profile of Region 5 — Run Time: 4451 seconds — Start/Stop Cycles: 23 .....	II-64
4-10      As-Coated VH-109 Composition Profile .....	II-65

## ILLUSTRATIONS (Continued)

<i>Figure</i>		<i>Page</i>
4-11	Engine Tested VH-109 Composition Profile of Region 5 — Run Time: 4451 seconds — Start/Stop Cycles: 23 .....	II-66
5-1	Coating Thickness Reproducibility Assessment for VH-109 and R512-E	II-67

## SECTION 1.0 BACKGROUND

To increase the specific impulse of the RL10 liquid hydrogen/liquid oxygen rocket engine, a nozzle extension has been proposed. The extension will translate between stowed and deployed positions. When stowed, the extension will be nested with the regeneratively cooled RL10 nozzle. Two versions of the extension are planned for different models of the RL10. One version will be designed for the RL10A-3-3A and be 20 inches long, while the other version will be for the RL10-IIB, 55 inches long.

A commercially available columbium (niobium) alloy, C-103, has been chosen as the structural material for the nozzle extension. This alloy has the necessary high-temperature strength properties that are estimated to be required for the longer version of the nozzle. However, C-103 is susceptible to both hydrogen and oxygen embrittlement as well as high-temperature oxidation. Therefore, a coating must be applied to C-103 to protect the alloy from the deleterious effects of the  $H_2O/H_2/O_2$  environment created by the RL10.

Part I of this report analyzed and ranked seven different coatings in the as-received condition from three vendors. The resultant rankings were based on the integrity and consistency of the coating. The most highly ranked coatings were R512-E from Hitemco and VH-109 from Vac Hyd (Figure 1-1). C-103 panels coated with R512-E and VH-109, and an uncoated C-103 panel, were fixtured to an RL10 to simulate an operating environment for this analysis (Figure 1-2). The following consolidates theoretical calculations and experimental results to identify the best coating candidate for the columbium nozzle extension.

## SECTION 2.0 THEORETICAL CALCULATIONS

To assist in understanding the role that oxygen takes in the RL10 environment, thermodynamic data has been used to calculate the partial pressure of oxygen in the exhaust products and the partial pressure of oxygen required for the formation of oxides of columbium (Cb) and silicon (Si). The calculations were performed at three temperatures of operation; 298K (536R), 1144K (2059R), and 1450K (2610R). The maximum temperature was obtained from thermocouple measurements taken from a nickel-based alloy that was tested in a manner similar to the C-103 panels.

To calculate oxygen partial pressures ( $p_{O_2}$ ), free energy data must be related to the reactants and products involved. Free energy data as a function of temperature can be obtained from published tables in the literature<sup>1</sup>. These tables provided this information in the form of:

$$\Delta G_T = A + BT \log T + CT \quad (1)$$

where A, B, and C are constants whose values are given below and  $\Delta G_T$  and T are free energy and temperature respectively; with A in cal/mole; B in cal/mole °T; T in degrees Kelvin; C in cal/mole °T, Delta G in cal/mole, R in cal/mole °T.

For the equilibrium between steam ( $H_2O$ ), hydrogen ( $H_2$ ), and oxygen ( $O_2$ ) the relationship is:

$$H_2 + 1/2 O_2 = H_2O \quad \begin{array}{ccc} \underline{A} & \underline{B} & \underline{C} \\ -57,250 & 4.48 & -2.21 \end{array} \quad (2)$$

Therefore,

$$\begin{aligned} \Delta G_{1144} &= -57,250 + 4.48(1144) \log 1144 + (-2.21)(1144) \\ &= -44,103 \text{ cal/mole.} \end{aligned}$$

$G_T$  is related to the partial pressures of the gases involved by:

$$\Delta G_T = -RT \ln \frac{P_{H_2O}}{P_{H_2}(P_{O_2})^{1/2}} \quad (3)$$

Thus,

$$\begin{aligned} -44,103 &= -(1.987)(1144) \ln \frac{P_{H_2O}}{P_{H_2}(P_{O_2})^{1/2}} \\ 2.67 \times 10^8 &= \frac{P_{H_2O}}{P_{H_2}(P_{O_2})^{1/2}} \end{aligned}$$

Since  $p_A = X_A p_T$  where  $p_A$  is the partial pressure of species A,  $X_A$  is the mole fraction of species A, and  $p_T$  is the total pressure, the above equation can be rewritten as:

$$2.67 \times 10^8 = \frac{X_{H_2O} p_T}{X_{H_2} p_T (p_{O_2})^{1/2}}$$

and

$$2.67 \times 10^8 = \frac{X_{H_2O}}{X_{H_2} (p_{O_2})^{1/2}}$$

From theoretical equilibrium calculation of the exhaust gases of the RL10 at the exit plane<sup>2</sup>:

$$\begin{aligned} X_{H_2O} &= 0.76 \\ X_{H_2} &= 0.24. \end{aligned}$$

Therefore,

$$2.67 \times 10^8 = \frac{0.76}{0.24 (p_{O_2})^{1/2}}$$

$$p_{O_2} = 1.41 \times 10^{-16} \text{ atm.}$$

This value is the partial pressure of oxygen in equilibrium with hydrogen and steam in the exhaust gases of the RL10.

Similar calculations can be performed for Cb and Si:

$$\Delta G_T = A + BT \log T + CT$$

	<u>A</u>	<u>B</u>	<u>C</u>
$Cb_2 O_5 = 2CbO_2 + 1/2 O_2$	74,850	5.75	-34.5
$2CbO_2 = 2CbO + O_2$	185,100	11.5	-79.5
$2CbO = 2Cb + O_2$	198,700	11.5	-77.0
$Cb_2 O_5 = 2Cb + 5/2 O_2$	458,650	28.75	-191

(4)

Thus,

$$\begin{aligned} \Delta G_T &= 458,650 + 28.75(1144) \log 1144 + (-191)(1144) \\ &= 340,737 \text{ cal/mole.} \end{aligned}$$

and

$$\Delta G_T = -RT \ln \frac{p_{Cb} (p_{O_2})^{5/2}}{p_{Cb_2O_5}} \quad (5)$$

In this case, the partial pressures of the solids, Cb and  $Cb_2O_5$ , can be assumed to be unity. Therefore;

$$\begin{aligned} \Delta G_T &= -RT \ln (p_{O_2})^{5/2} \\ 340,737 &= -(1.987) (1144) \ln (p_{O_2})^{5/2} \\ -150 &= \ln (p_{O_2})^{5/2} \\ p_{O_2} &= 9.12 \times 10^{-27} \text{ atm.} \end{aligned}$$

This value is the partial pressure of oxygen in equilibrium with columbium and columbium pentoxide at 1144K. If the partial pressure of oxygen in the environment exceeds this value, columbium pentoxide formation is thermodynamically permitted. Therefore, the partial pressure of oxygen in the RL10 exhaust ( $1.41 \times 10^{-16}$  atm) is great enough to cause  $\text{Cb}_2\text{O}_5$  formation.

Although the formation of  $\text{Cb}_2\text{O}_5$  is not desired, the formation of an  $\text{SiO}_2$  scale on the coating is desired. This scale creates a barrier to oxygen and hydrogen which should retard the diffusion of these gases into the C-103 substrate. The partial pressure of oxygen required to create this scale was calculated as follows:

$$\Delta G_T = A + BT \log T + CT \quad (\text{Ref. 2})$$

$$\text{SiO}_2 = \text{Si} + \text{O}_2 \quad \begin{array}{ccc} \underline{A} & \underline{B} & \underline{C} \\ 215,600 & - & -41.5 \end{array}$$

Thus,

$$\begin{aligned} \Delta G_T &= 215,600 + (-41.5) (1144) \\ &= 168,124 \text{ cal/mole.} \end{aligned}$$

and

$$\Delta G_T = -RT \ln \frac{P_{\text{Si}} P_{\text{O}_2}}{P_{\text{SiO}_2}} \quad (7)$$

Again, the solids have a partial pressure of unity. Thus,

$$\begin{aligned} \Delta G_T &= -RT \ln p_{\text{O}_2} \\ 168,124 &= -(1.987) (1144) \ln p_{\text{O}_2} \\ -74 &= \ln p_{\text{O}_2} \\ p_{\text{O}_2} &= 7.57 \times 10^{-33} \text{ atm.} \end{aligned}$$

This value is lower than the value needed to oxidize columbium. Therefore, the formation of an  $\text{SiO}_2$  scale on the silicide coatings is thermodynamically allowable.

This theoretical analysis has determined that the RL10 exhaust environment will favor  $\text{Cb}_2\text{O}_5$  and  $\text{SiO}_2$  formation at 1144K. Table 2-1 compiles similar  $p_{\text{O}_2}$  calculations at 298K and 1450K in addition to 1144K. Although the RL10 produces a hydrogen-rich exhaust, there is enough oxygen in equilibrium with the exhaust products to allow the formation of the aforementioned oxides at all predicted operating temperatures.

TABLE 2-1. — PARTIAL PRESSURE OF OXYGEN IN EQUILIBRIUM WITH WATER, COLUMBIUM PENTOXIDE, AND SILICON DIOXIDE AT 298K, 1144K, AND 1450K

Temperature		Partial Pressures		
		$\text{H}_2/\text{H}_2\text{O}$	$\text{Cb}_2\text{O}_5$	$\text{SiO}_2$
(K)	(F)	$P_{\text{O}_2}$	$P_{\text{O}_2}$	$P_{\text{O}_2}$
298	77	$7.9 \times 10^{-80}$	$< 1 \times 10^{-100}$	$< 1 \times 10^{-100}$
1144	1600	$1.4 \times 10^{-16}$	$9.1 \times 10^{-27}$	$7.6 \times 10^{-33}$
1450	2150	$9.2 \times 10^{-12}$	$1.3 \times 10^{-19}$	$3.7 \times 10^{-24}$

R20482/4

## **SECTION 3.0**

### **ENGINE TESTED EVALUATION**

Three samples were attached to the exit plane of the RL10 regeneratively cooled nozzle. The samples were located equidistant from each other for symmetry. The test started with an uncoated C-103 panel, an R512-E coated C-103 panel, and a VH-109 coated C-103 panel. The uncoated panel experienced excessive warping, cracking, and oxidation at 1203 seconds and six start/stop cycles into the testing sequence. It was removed and replaced by a nickel-based superalloy sample. The coated samples were tested through the entire testing sequence for 4451 seconds and 23 stop/start cycles.

#### **3.1 UNCOATED COLUMBIUM (ALLOY C-103)**

Run Time: 1203 seconds  
Start/Stop Cycles: 6 cycles.

##### **3.1.1 Macrophotographic Documentation**

Visual inspection of the uncoated C-103 panel (Figures 3-1 and 3-2) showed excessive warping near the center of the panel, a large circumferentially oriented crack associated with the warping, and white oxidation products. More oxidation was associated with the chamber (capsule) side of the panel than the gas-path (flame) side of the panel. A corner of the panel was chipped during removal from the engine indicating the brittle nature of the tested C-103 panel.

##### **3.1.2 Microstructural Observations**

The panel was sectioned in the pattern shown in Figures 3-1 and 3-2. Metallographic examination concurs with the visual observations. Figures 3-3 through 3-7 document typical microstructures of the gas-path side, the chamber side, and the panel core. A line-scan of oxygen x-rays vs intensity (Figure 3-8) illustrates the presence of oxygen in the surface scale and in grain boundary precipitates. In general, the oxide on the chamber side was thicker than the oxide on the gas-path side. An obvious change in microstructural features was noted in most sections near the midpoint of the panel thickness. The ductile characteristics of the polished core (excessive scratches) resembled the ductile characteristics of polished, virgin C-103. The polished surrounding material displayed signs of brittleness which is characteristic of oxygen embrittled C-103.

##### **3.1.3 Microhardness Profiles**

For comparative purposes, a baseline (uncoated and untested) sheet sample, from the same lot of material that all test panels were fabricated, was sectioned, mounted, and polished. A line of microhardness measurements was made through the sample thickness to provide a reference for the microhardness of the other panels (Figure 3-9). The microhardness was consistent through the panel thickness with a VHN of 160.

All microhardness measurements for the uncoated panel are documented in Figure 3-10. Region A was located near the inlet plane of the nozzle extension. No significant change in microhardness was noted for Region A. Region B appeared to be below a hot streak as the oxidation pattern on Figure 3-1 indicates. Microhardness measurements reflected this observation. The hardness profile varied from about 170 VHN in the center to about 700 VHN near both surfaces. Region C, which visually showed the most oxidation, had a hard central core (440 VHN) as well as a hard perimeter (600 VHN). Regions D and E were similar to region B with a ductile core (VHN 170) and a hard perimeter (700 VHN and 800 VHN respectively).

### **3.2 VH-109: VAC HYD**

Run Time: 4451 seconds

Start/Stop Cycles: 23 cycles.

#### **3.2.1 Macrophotographic Documentation**

During the engine test, the gas-path surface of the VH-109 panel maintained a relatively consistent grey color (Figure 3-11). A large, light grey central flame pattern seemed to indicate a hot streak. Constraint of the panel by the C-103 support bracket caused significant warping of the panel. A crack was located about 1.5 inches downstream from the inlet plane of the exhaust extension along one side of the panel. Figures 3-12 and 3-13 illustrate the warp and the crack. After the panel was removed from the support bracket, a small pinhole coating flaw was observed (Figures 3-14 and 3-15). Closer inspection revealed that the flaw was located directly opposite a coating blemish on the gas-path side. In general, the panel gas-path surface color resembled the as-received condition. The chamber side had a scale that had a slightly whiter tone than the original grey color.

#### **3.2.2 Coating/Substrate Thickness Distributions**

From Part I of this report, the initial coating and substrate thicknesses were 4.1 and 10.5 mils respectively. Figure 3-16 displays the sectioning pattern used to document the thicknesses shown in Figure 3-17. More coating thickness variation was noted after the engine test. The post-test thickness averaged 4.8 mils with a standard deviation of 0.7 mil. Prior to the test, the thickness was documented at 4.1 mils with a standard deviation of 0.4 mil<sup>3</sup>.

#### **3.2.3 Microstructural Observations**

Review of the microstructures, progressing from the inlet plane of the extension to the exit plane of the extension, revealed only small microstructural changes (Figures 3-18 through 3-22). Two differences, noted from the as-received microstructure, were the distribution of secondary phases and an increase of porosity in the first one-to-two mils of coating. The second phase distribution transformed from large intermittent precipitates to a continuous population of fine particles. Porosity in the first one-to-two mils of coating was more predominant after the engine test. No logical pattern was evident to explain the occurrences of increased porosity .

Two anomalies were associated with this panel, a crack caused by warping and a pinhole flaw. The cross section of the crack in this panel was typical of exposed C-103 (Figure 3-23). An oxygen embrittled zone with grain boundary oxides were associated with the crack. The pinhole flaw was initiated by mechanical damage prior to the engine test, not engine operation. The cross section of the flaw indicates that the C-103 substrate was locally bent (Figure 3-24). The damage caused a break in the coating which exposed the substrate to the oxidizing environment.

#### **3.2.4 Microhardness Profiles**

The C-103 substrate appears to have been protected from the embrittling effects of H<sub>2</sub> and O<sub>2</sub> gases. No significant change in microhardness from virgin C-103 was detected (Figure 3-25). The virgin material had a microhardness of about 160 VHN while the tested VH-109 coated C-103 microhardness ranged from about 150 VHN to 190 VHN. Region 1 had measurements that were significantly above the virgin C-103 values. This minor variation may be due to solid solution strengthening caused by the inward diffusion of coating elements.



### **3.3 R512-E: HITEMCO**

Run Time: 4451 seconds

Start/Stop Cycles: 23 cycles.

#### **3.3.1 Macrophotographic Documentation**

Unlike the VH-109 panel, the R512-E panel had various rainbow color patterns on both the gas-path and chamber side environments (Figures 3-26 through 3-29). The colors varied from blue to gold. A region near the inlet plane of the nozzle extension appeared to be unaffected by engine operation and remained grey. When the panel was rotated to examine the downstream view of the exhaust gases, a pattern that matched the cooling tube spacing was observed (Figure 3-27). Warping of the panel was minimal. However, a crack was noted in one of the support bracket legs (Figure 3-28). This crack may have relieved stresses which minimized the amount of warping on this panel. Examination of the exit plane edge of the panel revealed a small chip in the coating on the chamber side (Figures 3-29 and 3-30). No significant evidence for Cb oxidation was associated with the chip.

#### **3.3.2 Coating/Substrate Thickness Distributions**

The first test of R512-E was conducted with a panel processed to a coating thickness of 3.1 mils as documented in Part I of this report. The bracket used for that test did not provide sufficient downstream support, and the panel experienced a low cycle fatigue failure. No additional panels with three mils of coating were available, therefore, a panel with five mils was used for this engine test evaluation. Previous analysis documents the coating/substrate thickness distribution for this panel in Figure 3-31. The initial coating thickness for R512-E averaged 4.5 mils with a standard deviation of 1.0 mil. Figures 3-32 and 3-33 display the sectioning pattern and the coating thickness distribution after engine testing respectively. The average coating thickness in Figure 3-33 was 4.4 mils with a standard deviation of 0.4 mil.

#### **3.3.3 Microstructural Observations**

Review of the microstructures, progressing from the inlet plane of the extension to the exit plane of the extension, revealed no significant deleterious features (Figures 3-34 through 3-38). Changes in the original coating microstructure did occur. Thermal exposure allowed additional elemental partitioning. Thus, the composition of coating phases may have been slightly altered during engine exposure.

#### **3.3.4 Microhardness Profiles**

The C-103 substrate appears to have been protected from the embrittling effects of  $H_2$  and  $O_2$  gases. No significant change in microhardness from virgin C-103 was detected (Figure 3-39). The values ranged from 155 VHN to 170 VHN as compared with the 160 VHN for virgin C-103. One location in Region 3 (260VHN) and one location in Region 5 (unlabeled) were higher than expected; but, again, the measurements appear to have been affected by coating/substrate alloy effects.

## SECTION 4.0 COMPARATIVE ANALYSIS

### 4.1 H<sub>2</sub> AND O<sub>2</sub> GAS ABSORPTION

Isolation of the C-103 from the embrittling effects of hydrogen and oxygen was the goal of this coating evaluation. Since the coatings create protective oxide scales, a gas analysis of a bulk sample would detect oxygen from the scale as well as from the C-103 substrate. Therefore, removal of the coating (and oxide scale of the uncoated panel) prior to a gas absorption analysis would provide a fair comparison of the effectiveness of each coating.

A lengthwise narrow strip of material was removed from the center of the flame pattern of each panel. The strips were grit blasted to remove all coating and surface oxides. This procedure produced a sample that was essentially substrate with no coating (Figure 4-1). Five equally spaced locations were then removed from each panel (Figure 4-2) and tested by a Leco Gas Analyzer.

The gas analysis determined the amount of oxygen, hydrogen, and nitrogen remaining in the tested C-103 in the uncoated, VH-109 coated, and R512-E coated conditions. Table 4-1 summarizes these results. From the uncoated panel, it is clear that the RL10 environment can cause C-103 to absorb substantial amounts of oxygen, hydrogen, and nitrogen and the amount of gases absorbed was dependent on the location of the panel analyzed. From the warps and hot spots observed from Figures 3-1 and 3-2, it is obvious that the thermal exposure of the panel was not uniform. Thus, it would be expected that significant variations in the amount of gases absorbed would be detected.

TABLE 4-1. — ABSORBED GAS (O, H, AND N) ANALYSIS OF GRIT BLASTED UNCOATED C-103, VH-109 COATED C-103, AND R512-E COATED C-103

Location	Atomic Percent					
	O	H	N	*Ti	*Hf	*Cb
<i>Uncoated (1203 sec)</i>						
1	18.532	1.153	0.361	1.609	4.327	74.017
3	0.461	1.570	0.020	1.987	5.302	90.662
4	2.062	0.996	0.040	1.962	5.244	89.696
5	0.313	1.955	0.034	1.973	5.288	90.437
6	1.335	1.920	0.067	1.955	5.232	89.492
<i>VH-109 (4451 sec)</i>						
1	0.848	1.689	0.094	1.968	5.270	90.130
3	0.977	1.079	0.095	1.978	5.297	90.575
4	0.804	1.386	0.081	1.975	5.289	90.465
5	0.911	1.872	0.054	1.964	5.259	89.940
6	0.602	2.632	0.053	1.954	5.238	89.520
<i>R512-E (4451 sec)</i>						
1	0.592	1.527	0.061	1.976	5.292	90.553
3	0.451	1.372	0.061	1.981	5.312	90.823
4	0.848	1.034	0.061	1.981	5.308	90.769
5	0.800	1.183	0.074	1.979	5.300	90.664
6	0.197	1.171	0.014	1.991	5.342	91.287
<i>PWA 1095 (C-103)</i>						
	0.151	0.143	0.069	2.011	5.396	92.230

\*Denotes compositions determined by difference.

R20482/4

Both coatings significantly reduced the amount of oxygen absorbed by the C-103 substrate, especially when noted that the coated panels were exposed to four times the duration of the uncoated panel. Although the deleterious effects of oxygen were not reflected in the microhardness profiles, the coatings could not provide a totally impervious barrier to oxygen absorption. Thus, oxygen levels exceeded the PWA 1095 specification limit of 0.151 percent by substantial amounts.

The effect of the coatings on preventing base alloy hydrogen absorption was minimal. The amount of hydrogen absorbed by the uncoated sample was almost equivalent to the amount absorbed by the coated samples. Published solubility data from Figure 4-3(a)<sup>4</sup> indicates that the absorption of hydrogen decreases with increasing temperature. The amount of hydrogen absorbed at 1144K (2059R) can be expected to be on the order of a few atomic percent. This value corresponds well with the measured values in Table 4-1.

Additionally, hydrogen is very mobile in b.c.c materials, and Cb has been documented to transport hydrogen at very rapid rates. Figure 4-3(b)<sup>5</sup> predicts a diffusion coefficient of near  $10^{-4}$  cm<sup>2</sup>/sec at the temperature range of interest. The magnitude of this coefficient is large enough for classification as liquid diffusion. Transport of hydrogen to all locations of the panel will be rapid; therefore, the amount of hydrogen absorbed should be uniformly distributed about the panel. The variation in hydrogen content in Table 4-1 is relatively small. Thus, the observed results correspond well with the above prediction.

Figure 4-4<sup>6</sup> illustrates the effect hydrogen concentration has on the ductile-to-brittle transition temperature. At concentrations of a few atomic percent hydrogen, the transition temperature is near or below room temperature. Hence, changes in ductility due to hydrogen absorption may or may not be detectable via microhardness measurements.

In summary, there is good agreement between the observed hydrogen phenomenon and earlier work regarding hydrogen and columbium. The panels absorbed one to two atomic percent hydrogen with a relatively uniform distribution of hydrogen about the panel. Microhardness measurements did not detect significant ductility changes in regions not embrittled by oxygen. Although the coating protected the substrates from oxygen embrittlement, hydrogen did penetrate the coatings and was absorbed by the C-103 panels. The effect of hydrogen on the ductility of these panels was undetected by microhardness measurements. Considering the 4X difference in exposure time, the data appears to indicate that the coatings retarded hydrogen absorption into the panels. However, this is not absolutely conclusive evidence. Hydrogen concentrations may have equilibrated before the uncoated panel was removed at 1203 seconds.

## 4.2 MICROSTRUCTURAL

From the data presented in paragraph 3.1 (Uncoated Columbium) and 4.1 (H<sub>2</sub> and O<sub>2</sub> Gas Absorption), it is clear that the RL10 environment is oxidizing with respect to C-103. Oxides were found on the panel surface on grain boundaries (Figure 3-8). With the occurrence of oxides, embrittlement by interstitial oxygen was expected and detected in microhardness profiles (Figure 3-10). Both coating systems protected the C-103 from significant oxygen embrittlement; their microhardness profiles were essentially unaffected by engine exposure.

The embrittling role of hydrogen was not clear. No obvious hydride phases were detected. Interstitial hydrogen absorption occurred, even in the coated panels, but a clear effect of hydrogen on mechanical properties was not observed. The neutral effect that hydrogen had on the mechanical properties may be related to the hydrogen solubility at the temperature range studied. At two at% hydrogen the ductile-to-brittle transition temperature is near room temperature for Cb.

Figure 4-5 compares typical microstructures of engine tested R512-E and VH-109. Figures 4-6 and 4-7 compare the as-received and engine tested coatings of R512-E and VH-109 respectively. Microstructural degradation of either coating was minimal. Subtle microstructural changes were more prevalent in the VH-109 coating (second phase instability and increased near surface porosity) than the R512-E coating (elemental partitioning). The protective nature of each coating is illustrated by microhardness measurements (Table 4-2). Aside from coating affected data points, no locations were significantly embrittled by engine exposure.

TABLE 4-2. — MICROHARDNESS MEASUREMENTS FROM RL10 ENGINE  
TESTED R512-E AND  
VH-109 COATED C-103 PANELS

		<i>Through-Thickness Distance From Gas Path (Flame) Side</i>					
<i>(Ref. Figure 3-32)</i>		<i>0.020 in. **</i>	<i>0.040 in.</i>	<i>0.060 in.</i>	<i>0.080 in.</i>	<i>0.100 in.</i>	<i>0.120 in.</i>
R512E Loc.	1	165.0	162.3	153.2	160.9	159.6	162.3
	2	162.3	151.2	153.2	157.1	152.1	148.3
	3	*259.5	150.7	151.9	162.3	151.9	176.7
	4	163.6	159.6	155.7	165.0	162.3	161.9
	5	*242.3	165.0	157.0	157.0	158.3	166.4
	6	169.3	162.3	157.0	164.1	166.4	167.2
	7	169.1	167.8	154.4	162.3	167.8	165.0
	8	167.8	153.2	149.5	158.3	157.0	163.6

<i>(Ref. Figure 3-16)</i>							
VH-109	1	188.1	162.3	160.9	159.6	163.1	175.2
	2	179.9	169.3	173.7	172.2	173.7	169.8
	3	153.2	151.2	152.3	151.2	150.7	153.2
	4	***	173.7	175.2	173.1	174.3	174.7
	5	***	163.1	162.3	151.9	160.9	169.1
	6	153.2	150.7	145.3	148.7	147.6	147.6
	7	166.4	160.9	151.9	153.2	157.0	***
	8	179.9	161.0	159.6	160.9	160.9	***
	9	163.6	155.7	158.3	155.8	158.3	***

\*Data points were closer to the gas path surface than 0.020 inch. The hardness readings are exhibiting the effects of some interdiffusion between the coating and the substrate.

\*\*The distance from the gas path side original reading varied from 0.020 inch but the spacing between the data points was precisely 0.020 inch.

\*\*\*The thickness of the substrate thinned and prohibited the placement of a sixth hardness test at the same spacing.

R20482/4

Table 4-3 summarizes the coating and substrate thicknesses after the engine test. The R512-E system thickness was essentially unaffected. The VH-109 system thickness thinned in the central region of the panel. Both coating and substrate thicknesses were reduced.

TABLE 4-3. — AVERAGE COATING AND PANEL THICKNESS AT VARIOUS LOCATIONS OF THE R512-E AND VH-109 COATED PANELS

		Average Panel Thickness	Average Chamber Side Coating	Average Gas Path Side Coating
R512E Loc.	1	14.4	4.6	4.4
	3	13.3	4.6	4.2
	4	13.2	4.3	4.1
	5	13.4	4.5	4.4
	6	13.2	4.6	4.5
VH109 Loc.	1	13.5	6.0	5.0
	3	11.5	5.1	4.3
	4	10.1	4.7	4.0
	5	10.1	4.4	4.0
	6	13.5	6.0	5.6

R20482/4

### 4.3 COMPOSITIONAL

Figures 4-8 and 4-9, and 4-10 and 4-11 illustrate the composition profiles of R512-E and VH-109 before and after testing, respectively. The R512-E microstructural features shown in the backscattered electron images indicate no change due to the engine exposure. The concentration profiles show activity at the coating surface. Initially, high concentrations of Cb and Si were present at the coating surface. After engine testing, depletion of Cb and Si and an enrichment of Cr and Fe occurs in the near-surface coating. This type of compositional change would be expected due to the formation of Cb/Si oxide scales. Examination of the VH-109 coating showed significant change in the microstructural distribution of secondary phases. The presence of large intermittent Cr/Hf phases was altered to form a continuous population of fine precipitates. Figure 4-10 shows the trace of the profile as it passes through a large second-phase region and the associated Cr and Hf enrichment. Figure 4-11 shows the trace initially encountering a zone of similar compositional characteristics, but the zone is short-lived as it breaks down into the compositional peaks of smaller, finely dispersed precipitates. Near-surface elemental depletion/enrichment associated with oxide formation, occurred in a manner similar to the R512-E coating.

All composition profiles detected Fe and Cr past the inward diffusion limit of Si. This may explain the slight microhardness increase near the coating/substrate interface. Solid solution strengthening by Fe and Cr, in advance of the Si diffusion front, may have increased the local hardness of the C-103 alloy.

## SECTION 5.0

### SUMMARY

Reduced substrate cross-sectional thickness was the primary difference between the performance of the coatings (Table 4-3). The observation that additional substrate may have been consumed by the VH-109 coating and the redistribution of secondary phases indicates that VH-109 may not be totally stable in this temperature range. The panel thickness varied from 13.5 mils at the inlet and exit planes to 10.1 mils at the panel center. The R512-E panel thickness was relatively constant at 13.3 mils. Data presented by Battelle, Columbus as part of this nozzle study concurred with the greater thickness predictability of the R512-E over the VH-109 (Figure 5-1<sup>6</sup>). The predictability of the coating/substrate system interaction is critical. An unexpected deviation in the load-bearing cross-sectional area of the nozzle could result in an overload condition.

Therefore, based on the above results, R512-E is the best coating candidate for the RL10 columbium nozzle extension. It protected the substrate from significant O<sub>2</sub> and H<sub>2</sub> embrittlement. It retained its original thickness and did not consume additional substrate material during the thermal exposure. It has a history of being applied to prescribed thickness consistently.

Although no deleterious effects of hydrogen were detected by this investigation, an important aspect of reusable operation was not considered. Upon shutdown in low earth orbit, the nozzle would be expected to cool to cryogenic temperatures. With the hydrogen absorbed during the firing to orbit, and the subsequent low temperature exposure, the C-103 alloy may transform from a ductile to brittle material. This may compromise mechanical properties of the substrate that are required for succeeding firings. Incorporation of a low temperature exposure should be included into the flight weight nozzle testing.

## **SECTION 6.0**

### **CONCLUSIONS**

1. Theoretical calculations indicated that Cb will oxidize in the RL10 exhaust environment.
2. Uncoated C-103 oxidized and absorbed significant amounts of  $H_2$  and  $O_2$  when exposed to the RL10 exhaust. Substantial loss of cross-sectional area and loss of ductile properties were the result of this exposure.
3. Both silicide type coatings formed protective  $SiO_2$  scales and inhibited oxygen gas absorption for the duration of this test. Microhardness profiles showed no significant change in the Vicker's Hardness Number (VHN) after engine testing.
4. Neither coating prevented hydrogen absorption by the substrate. Evidence suggests that the coatings may have retarded the rate of hydrogen by the substrate.
5. The Hitemco R512-E coating was more stable than the Vac Hyd VH-109 coating. R512-E showed no significant change in microstructural features after the engine test. VH-109 showed thickness variability, secondary-phase instability and porosity in the coating after engine exposure.
6. The effect of absorbed hydrogen on refiring after a low temperature exposure should be considered.

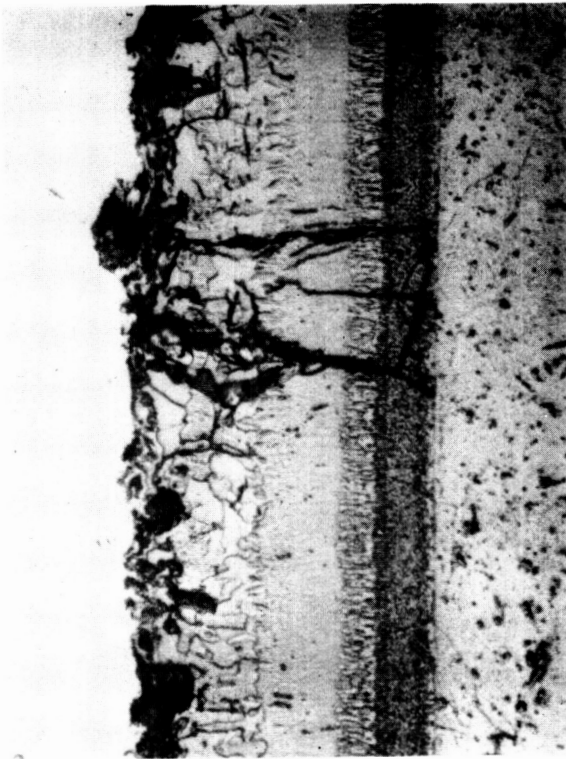
## **SECTION 7.0**

### **REFERENCES**

1. Kubaschewski, O. and Alcock, C.B., "Metallurgical Thermochemistry", 5th Edition, Pergamon Press, 1979.
2. Svehla, R. A. and McBride, B. J., "Fortran IV Computer Program for Calculation of Thermodynamic and Transport Properties of Complex Chemical Systems", NASA TN D-7056, Lewis Research Center, January 1973.
3. Murphy, K. S., "RL10 Radiantly Cooled Columbium Nozzles Extension Coating Screening Effort", P&W GPD Lab Report 27272, October 18, 1985.
4. Shunk, F.A., "Constitution of Binary Alloys, Second Supplement", McGraw-Hill, 1969.
5. Volkl, J. and Alefeld, G., "Diffusion of Hydrogen in Metals", "Topics in Applied Physics", Springer-Verlag, 1978.
6. Bartlett, E. S., Brockway C., Foster, E., and Weller, B., "RL10 Rocket Nozzle Study", Contract No. NAS3-3595, Battelle Columbus Division, December 12, 1985.



ORIGINAL PAGE IS  
OF POOR QUALITY



Mag: 500X

FD 358219

R512E



Mag: 500X S/N 50701-14

VH109

S/N 50701-10

*Figure 1-1. As-Coated Microstructures of VH-109 and R512-E from Part I*

ORIGINAL PAGE IS  
OF POOR QUALITY

FD 358171

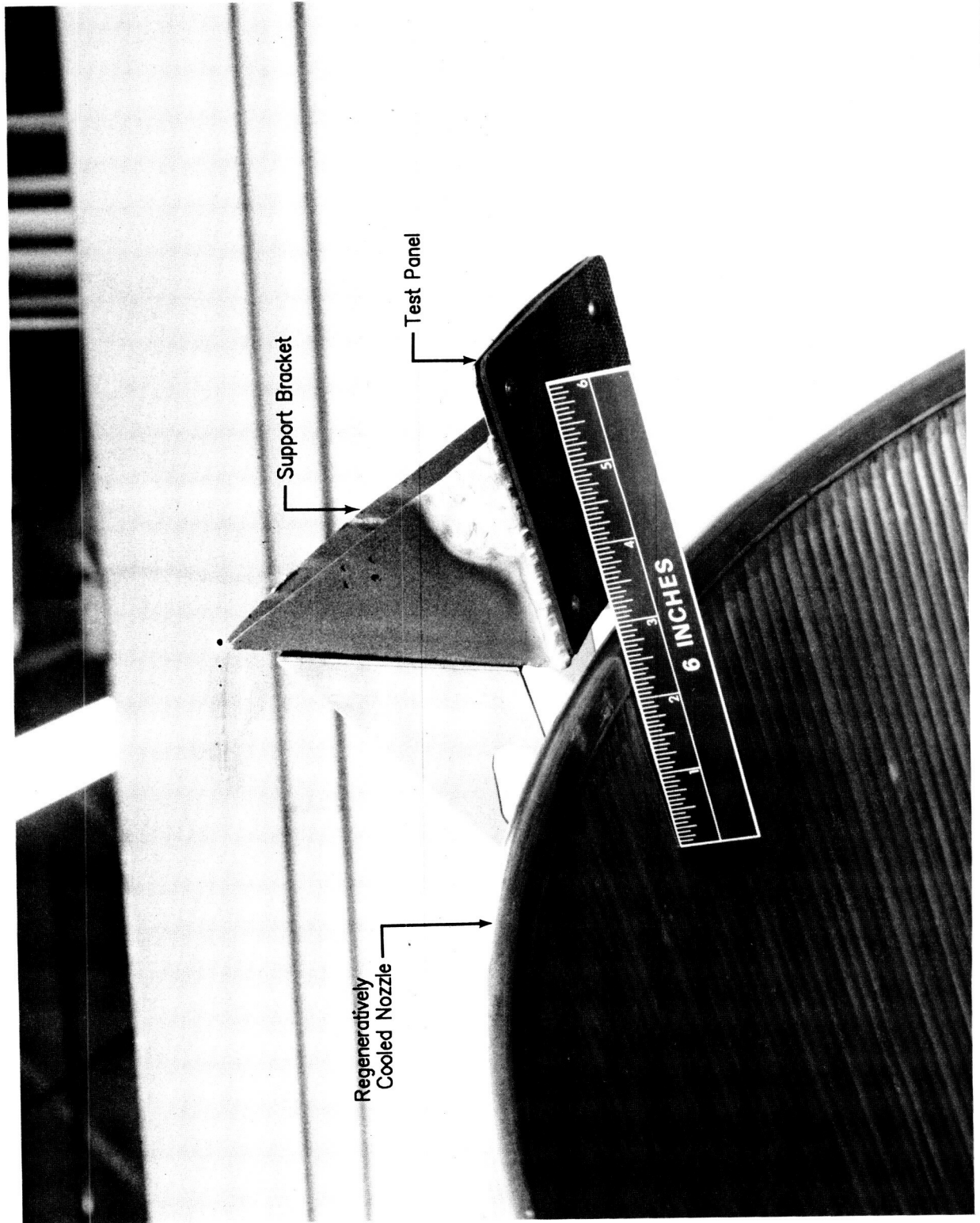
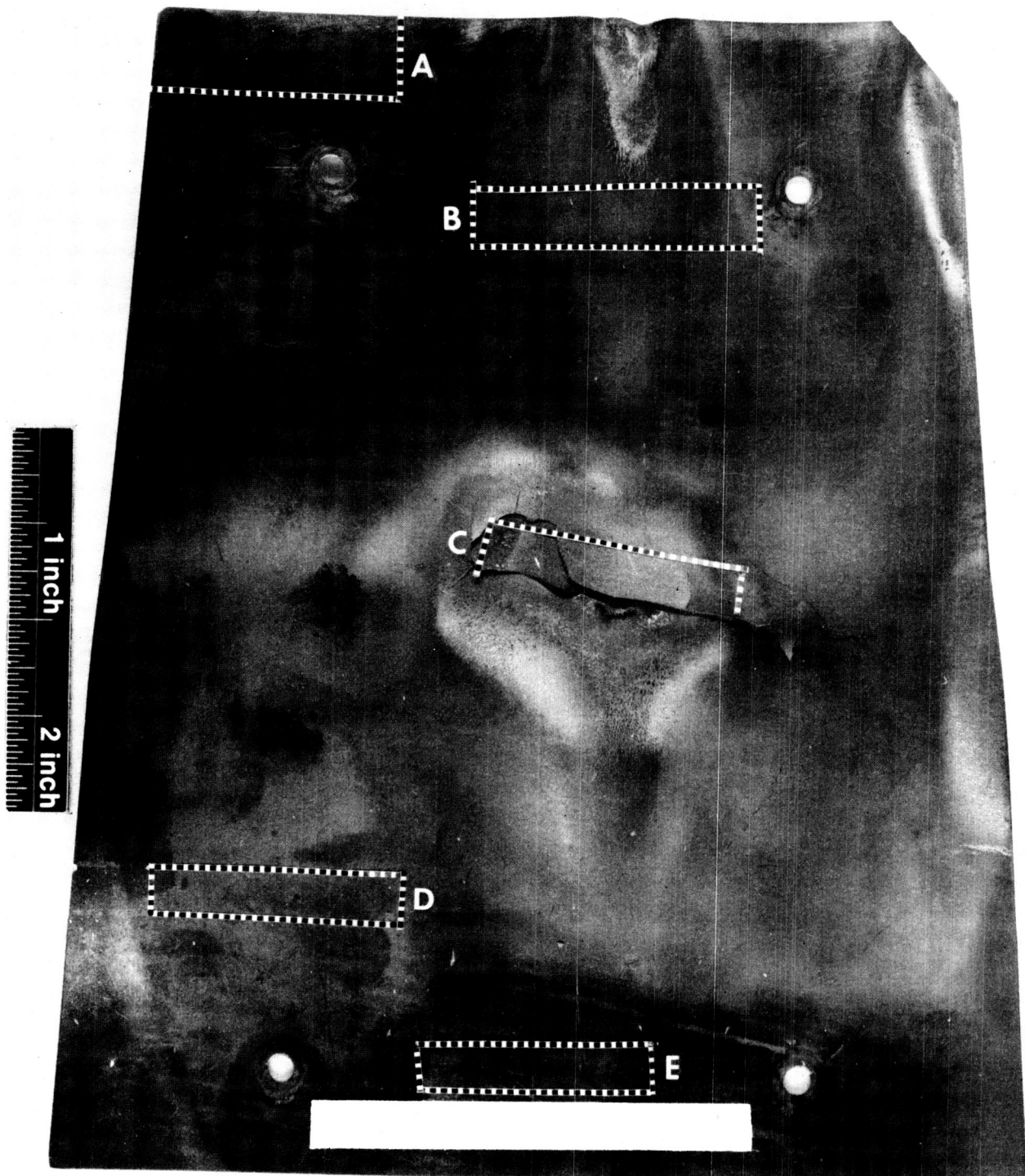


Figure 1-2. Typical Test Panel Attachment to RL10 Exhaust Nozzle

ORIGINAL PAGE IS  
OF POOR QUALITY

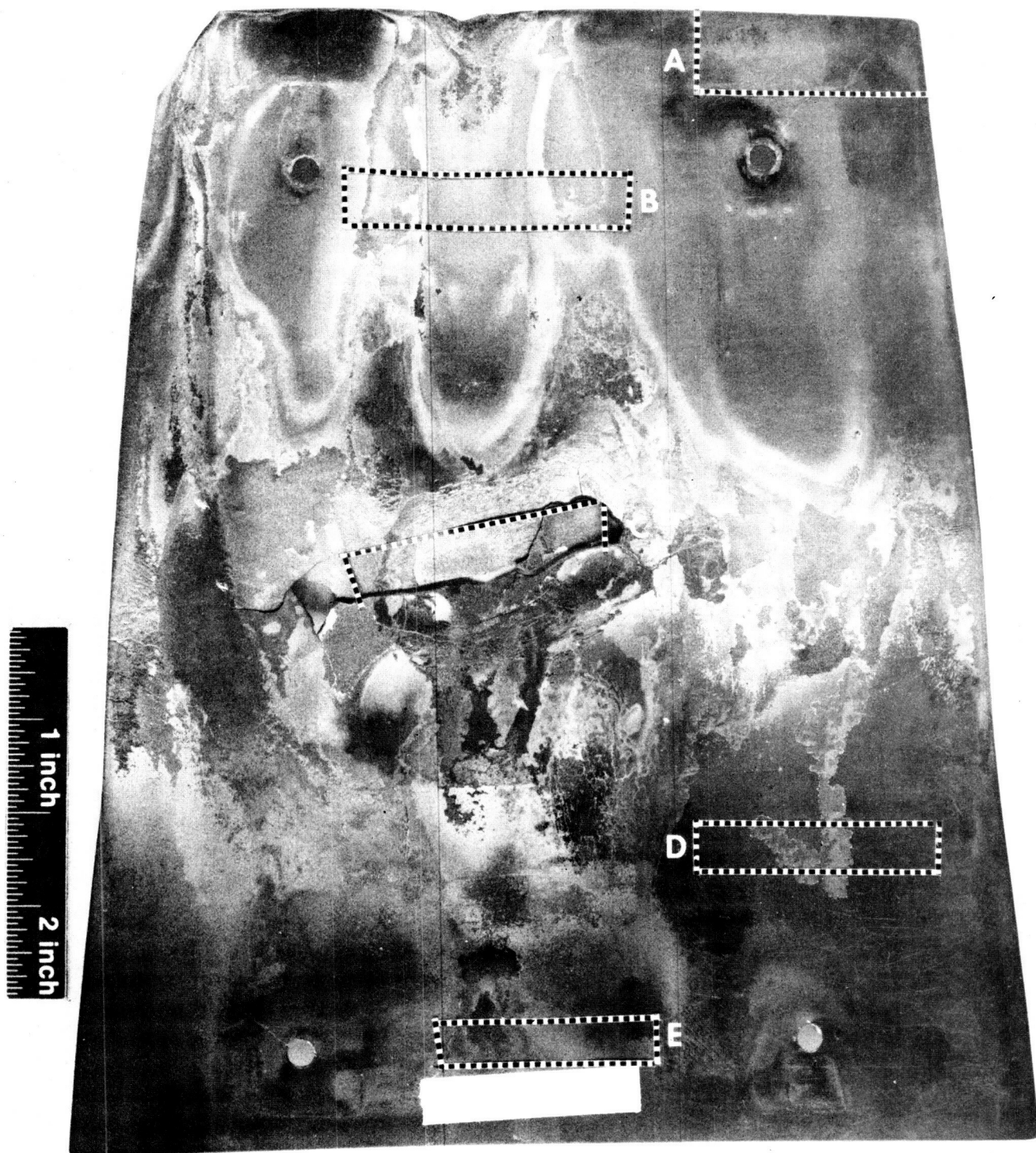


Run Time: 1203 sec  
Start/Stop Cycles: 6

FD 358221

*Figure 3-1. Gas-Path Environment Side of Uncoated C-103 Test Panel with Sectioning Pattern — Run Time: 1203 seconds — Start/Stop Cycles: 6*

ORIGINAL PAGE IS  
OF POOR QUALITY



Run Time: 1203 sec  
Start/Stop Cycles: 6

FD 358222

*Figure 3-2. Chamber Environment Side of Uncoated C-103 Test Panel with Sectioning Pattern — Run Time: 1203 seconds — Start/Stop Cycles: 6*

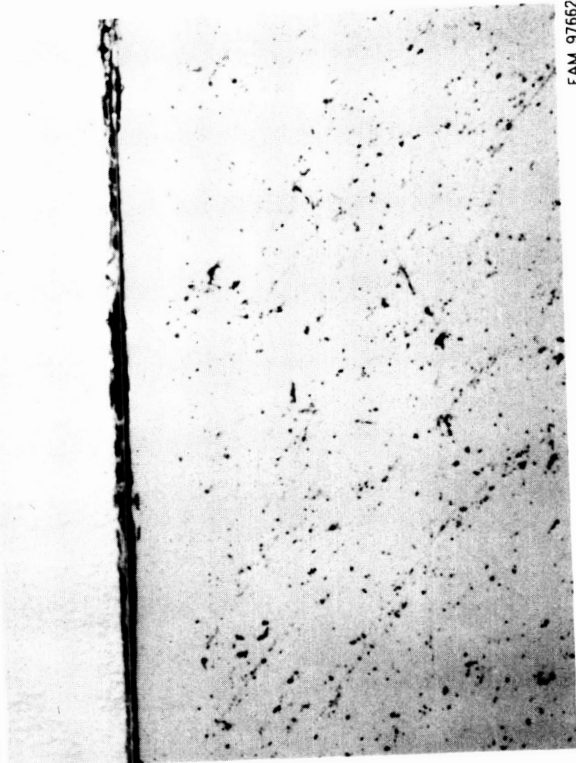


ORIGINAL PAGE IS  
OF POOR QUALITY



FAM 97663  
Mag: 500X

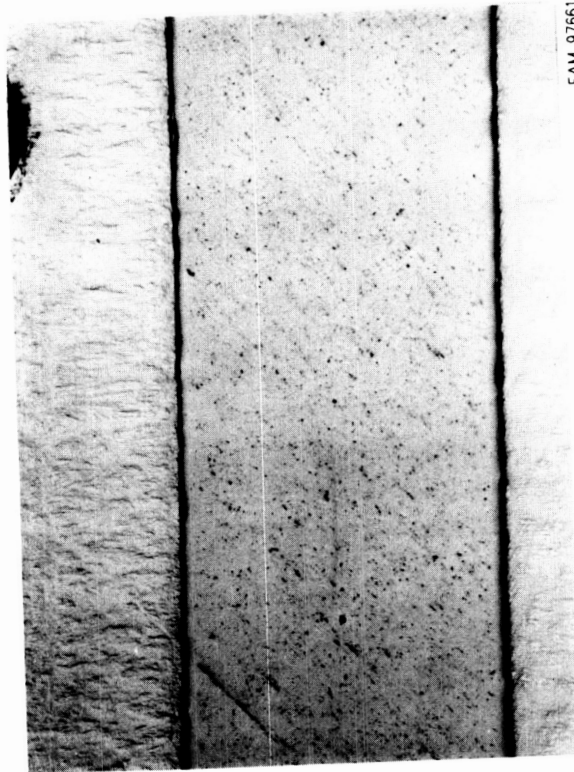
Gas Path Side



FAM 97662  
Mag: 500X

Chamber Side

Gas Path Side



FAM 97661  
Mag: 100X

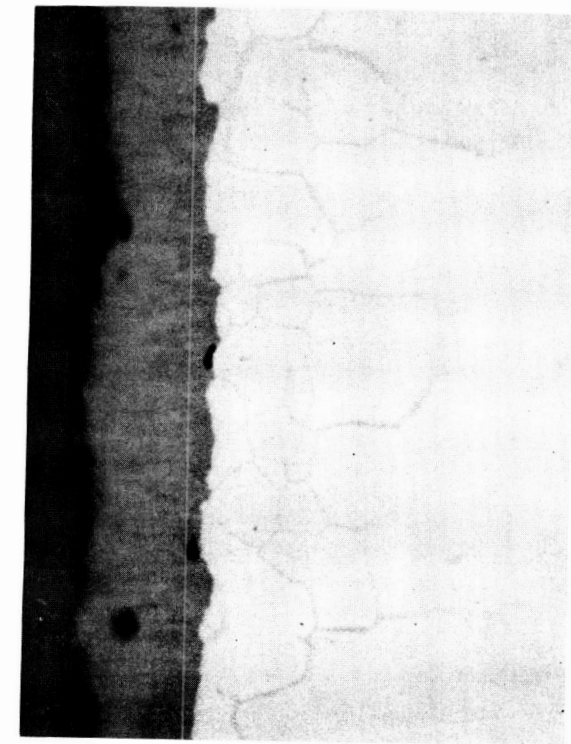
Chamber Side

FD 358223

Run Time: 1203 sec  
Start/Stop Cycles: 6

Figure 3-3. Uncoated C-103 Microstructure at Region A (S/N 60210-3) — Run Time:  
1203 seconds — Start/Stop Cycles: 6

ORIGINAL PAGE IS  
OF POOR QUALITY



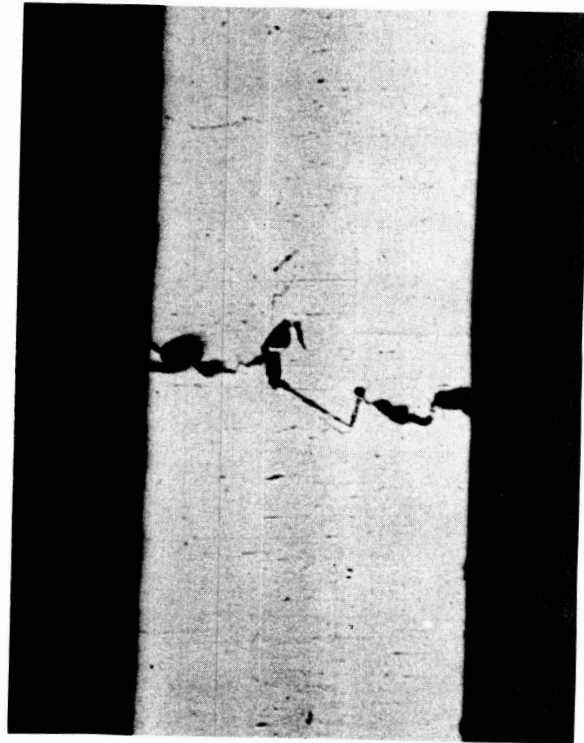
FAM 97674  
Mag: 500X

Chamber Side  
Gas Path Side



FAM 97675  
Mag: 500X

Gas Path Side  
Chamber Side



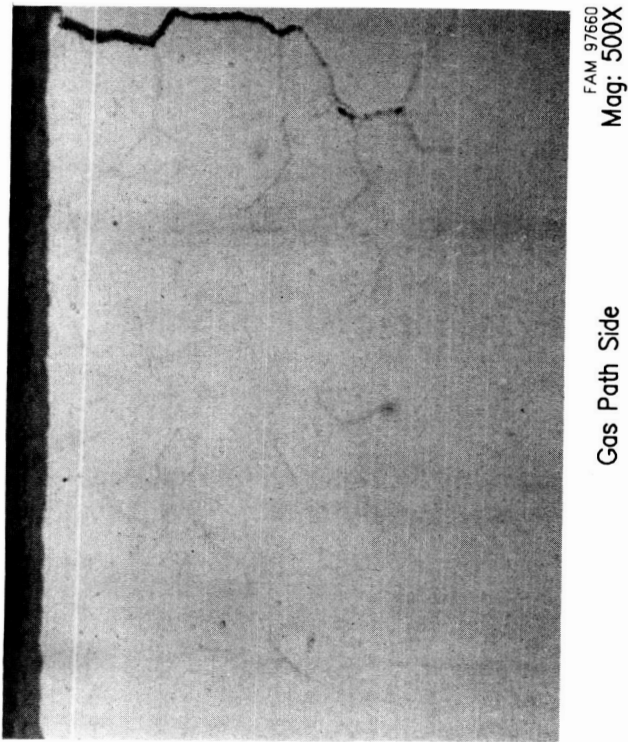
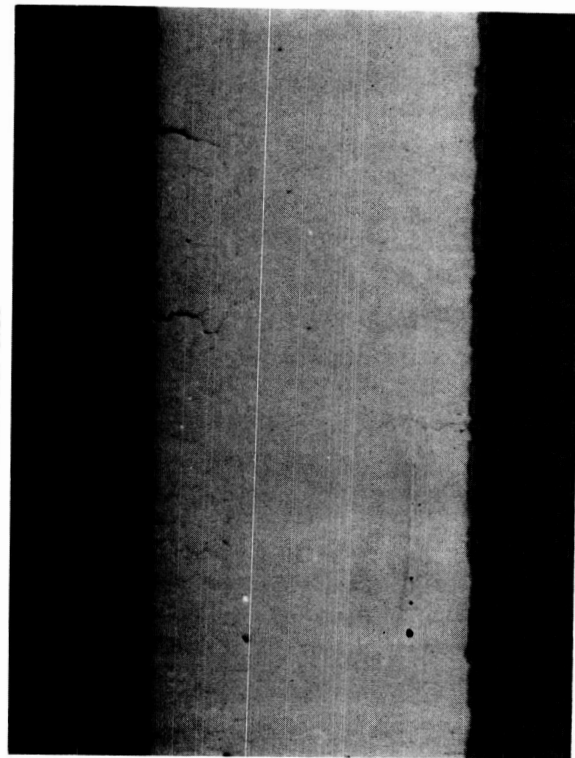
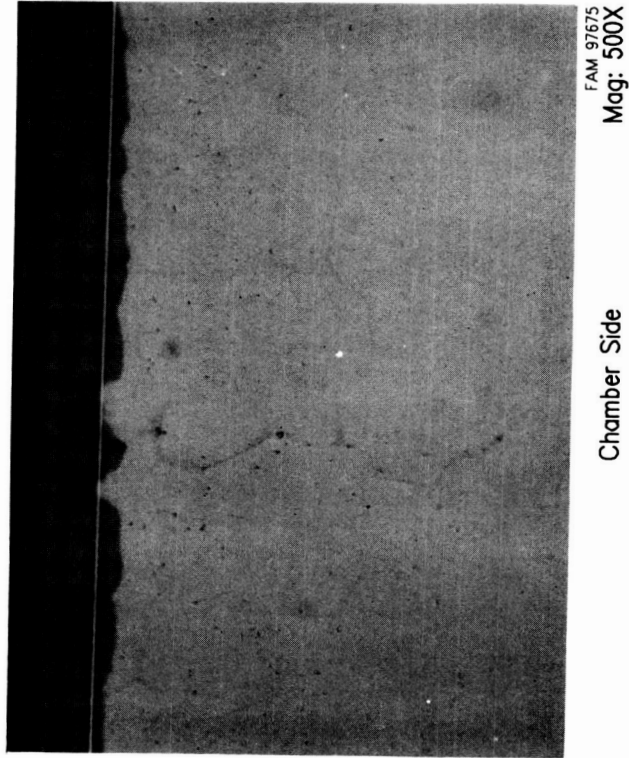
FAM 97673  
Mag: 100X

Chamber Side  
Gas Path Side

Run Time: 1203 sec  
Start/Stop Cycles: 6

Figure 3-4. Uncoated C-103 Microstructure at Region B (S/N 60210-4) — Run Time:  
1203 seconds — Start/Stop Cycles: 6

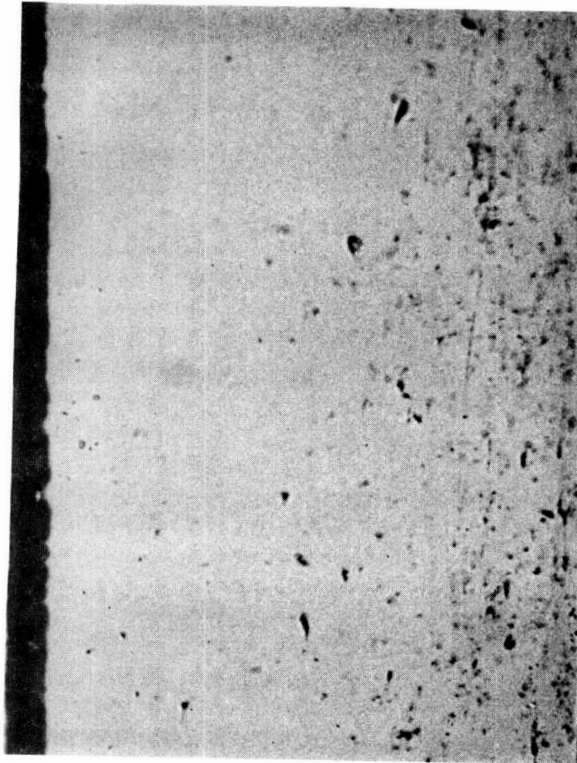
ORIGINAL PAGE IS  
OF POOR QUALITY



Run Time: 1203 sec  
Start/Stop Cycles: 6

Figure 3-5. Uncoated C-103 Microstructure at Region C (S/N 60210-5) — Run Time:  
1203 seconds — Start/Stop Cycles: 6

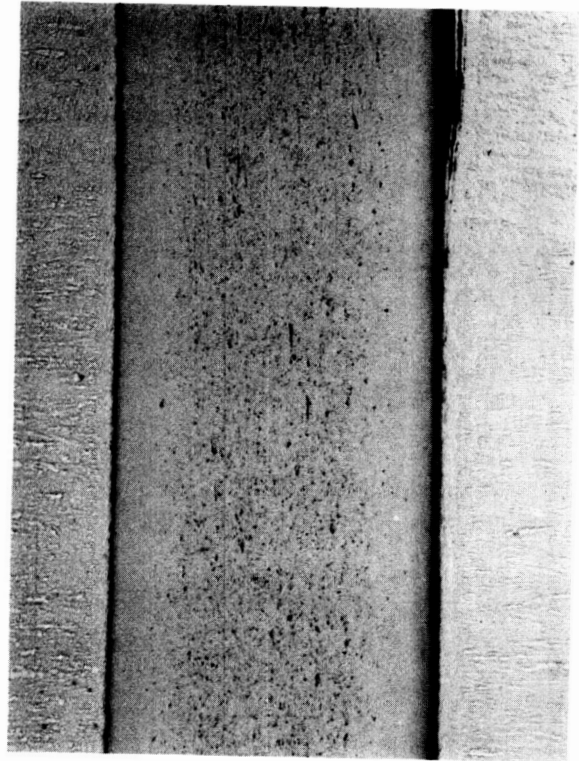
ORIGINAL PAGE IS  
OF POOR QUALITY



FAM 97672  
Mag: 500X

Chamber Side

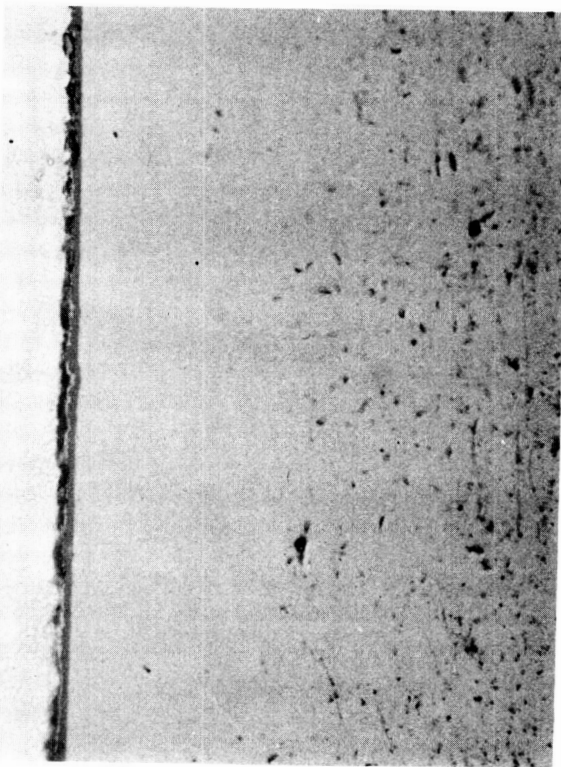
Gas Path Side



FAM 97670  
Mag: 100X

Chamber Side

FD 358226



FAM 97671  
Mag: 500X

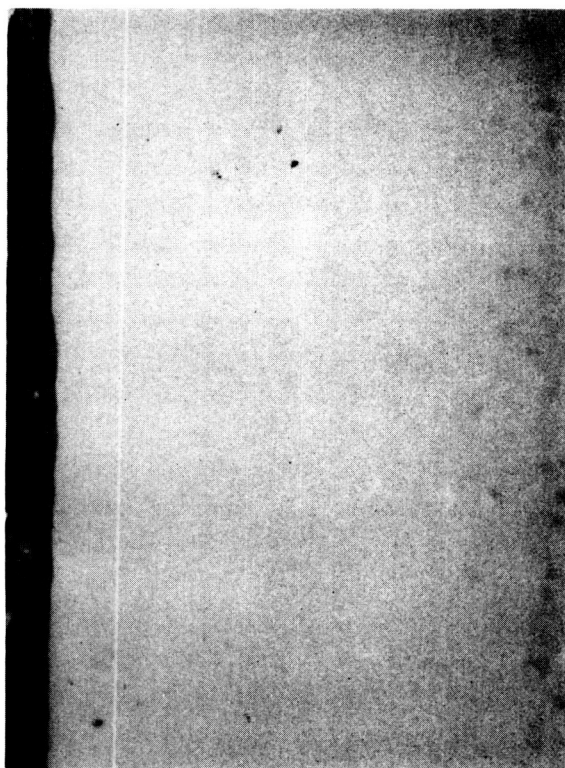
Gas Path Side

Run Time: 1203 sec  
Start/Stop Cycles: 6

Figure 3-6. Uncoated C-103 Microstructure at Region D (S/N 60210-6) — Run Time:  
1203 seconds — Start/Stop Cycles: 6



ORIGINAL PAGE IS  
OF POOR QUALITY.



FAM 97669  
Mag: 500X

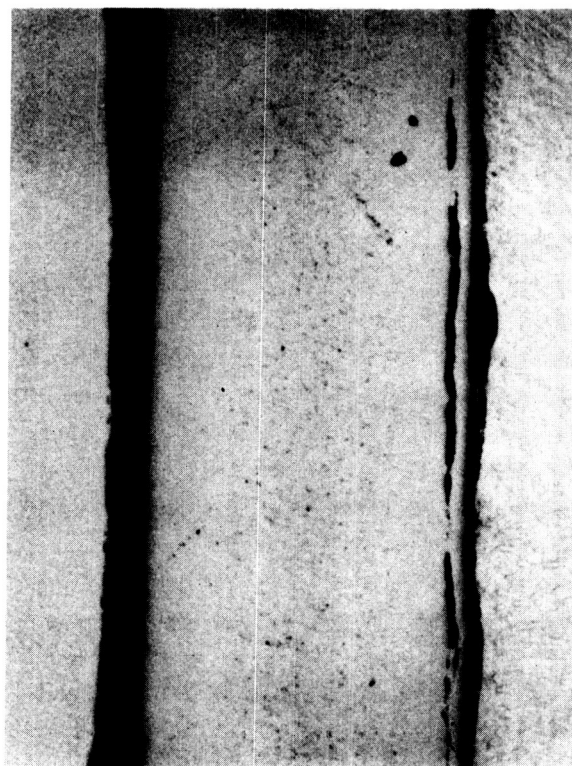
Chamber Side

Gas Path Side



FAM 97668  
Mag: 500X

Gas Path Side



FAM 97667  
Mag: 100X

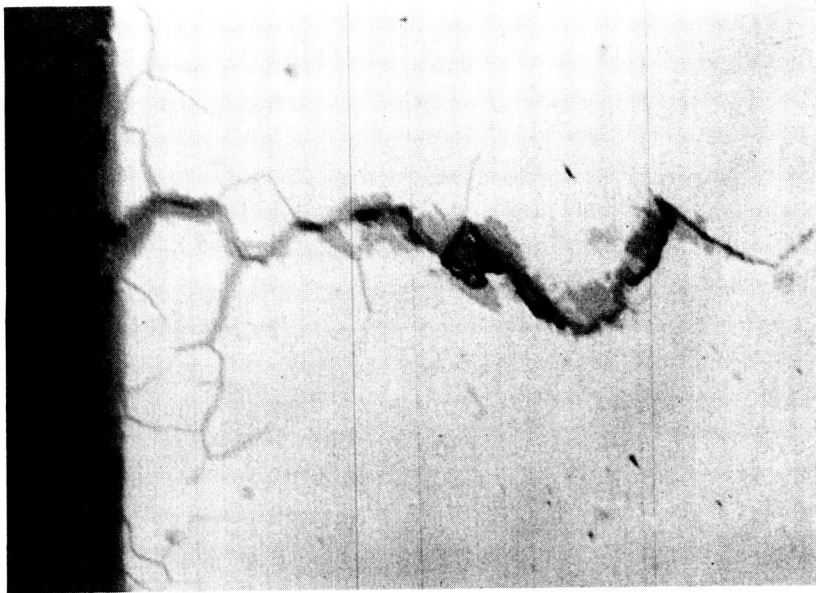
Chamber Side

FD 358228

Run Time: 1203 sec  
Start/Stop Cycles: 6

Figure 3-7. Uncoated C-103 Microstructure at Region E (S/N 60210-7) — Run Time:  
1203 seconds — Start/Stop Cycles: 6 (Sheet 2 of 2)

ORIGINAL PAGE IS  
OF POOR QUALITY



(a)  
General Location Showing Oxide  
Scale and Intergranular Cracking



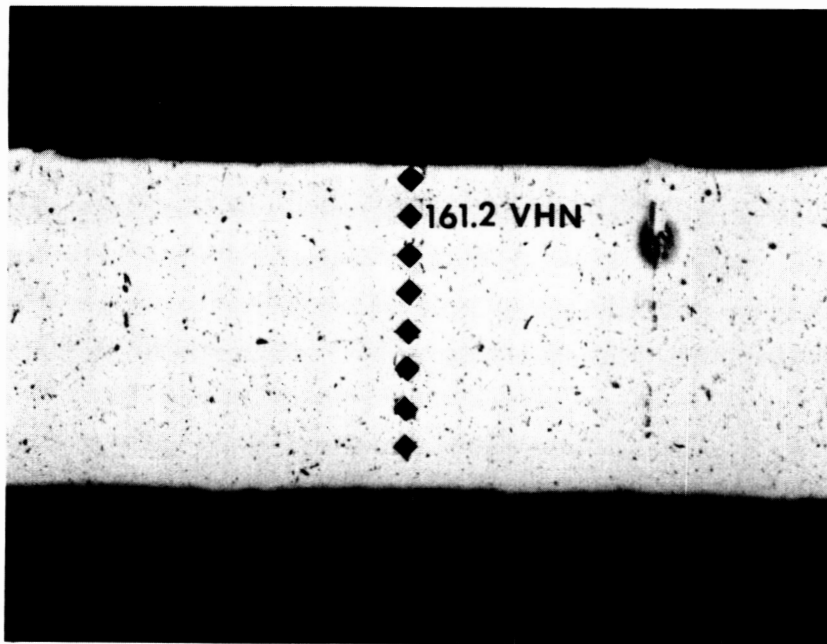
Line Trace  
Across Sample

(b)  
Line Scan Showing Oxygen Peaks at  
Sample Surface and Grain Boundaries

FD 358229

*Figure 3-8. Oxygen X-ray Line Scan vs Intensity*

ORIGINAL PAGE IS  
OF POOR QUALITY



S/N 60701-1

Unetched

Mag: 50X

FD 358230

*Figure 3-9. Microstructure Measurement Through the Thickness of Virgin C-103 — 50X  
— Unetched — S/N 60701-1*

ORIGINAL PAGE IS  
OF POOR QUALITY

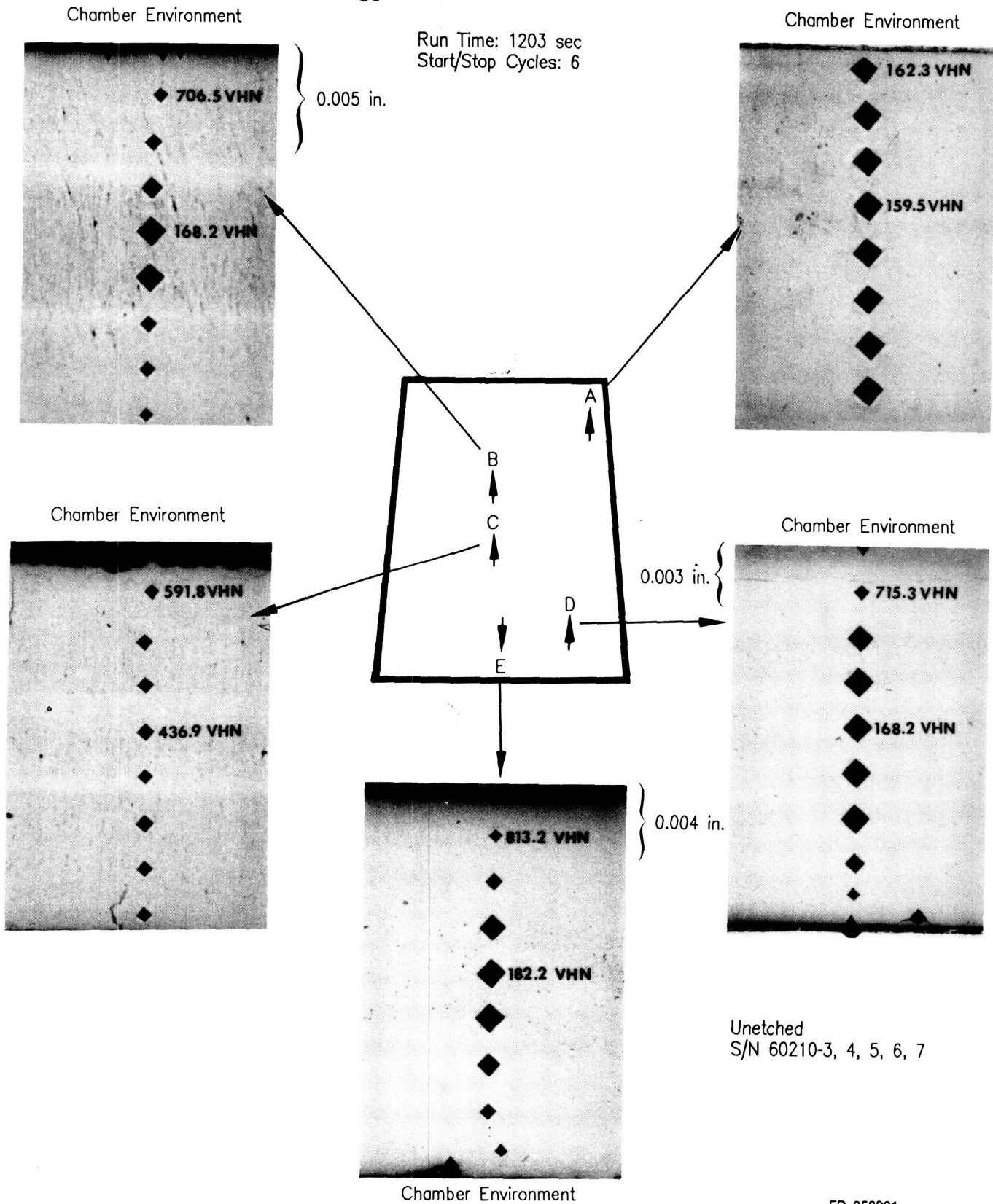
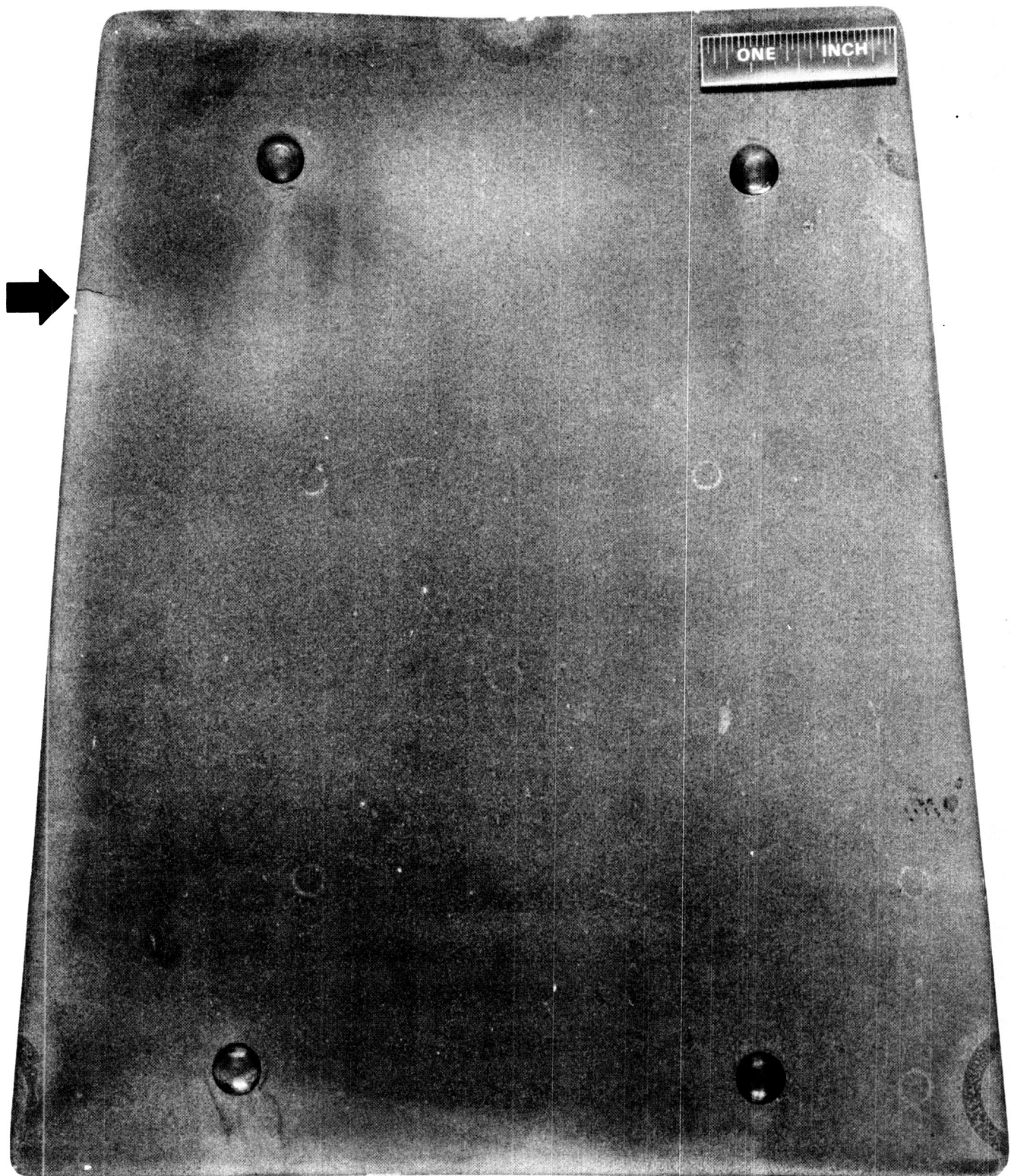


Figure 3-10. Microhardness Measurements Through the Thickness of the Uncoated C-103 Panel — Run Time: 1203 seconds — Start/Stop Cycles: 6 — Unetched — S/N 60210-3,4,5,6,7



ORIGINAL PAGE IS  
OF POOR QUALITY

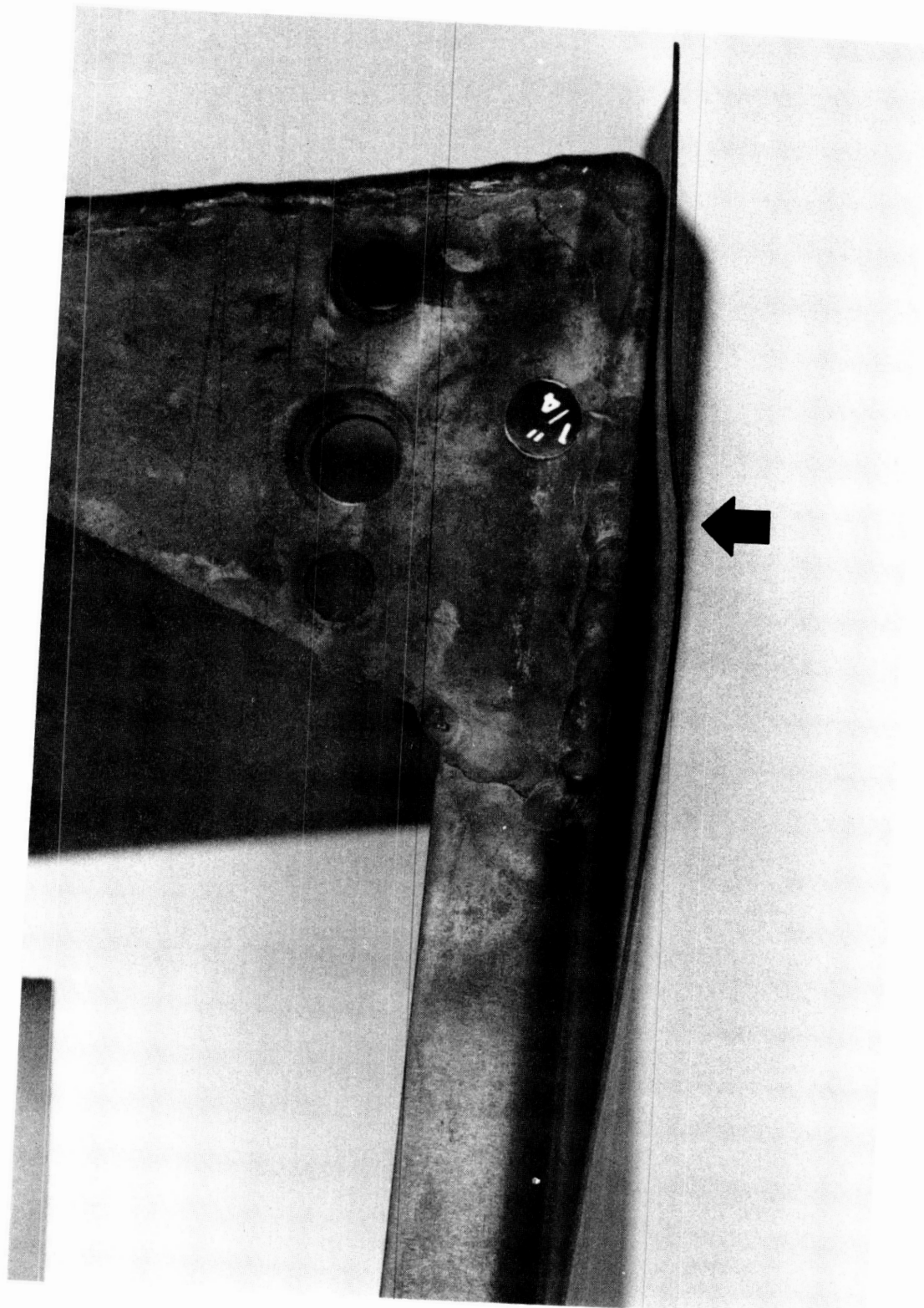


Run Time: 4451 sec  
Start/Stop Cycles: 23

FD 358232

*Figure 3-11. Gas Path Environment Side of VH-109 Coated C-103 Test Panel — Run Time: 4451 seconds — Start/Stop Cycles: 23*

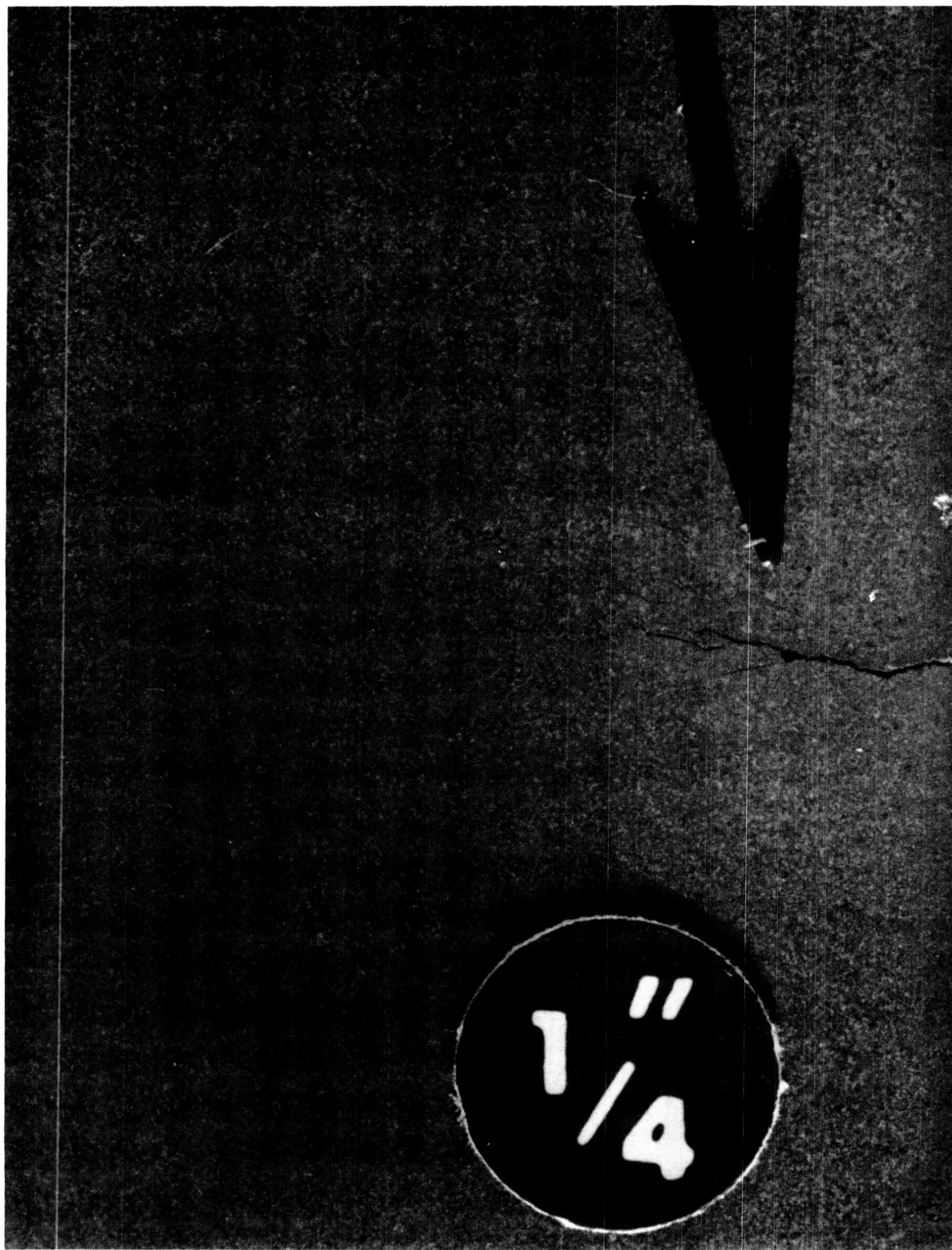
ORIGINAL PAGE IS  
OF POOR QUALITY



FD 358233

*Figure 3-12. Warping of VH-109 Panel (Arrow Indicates Crack Location)*

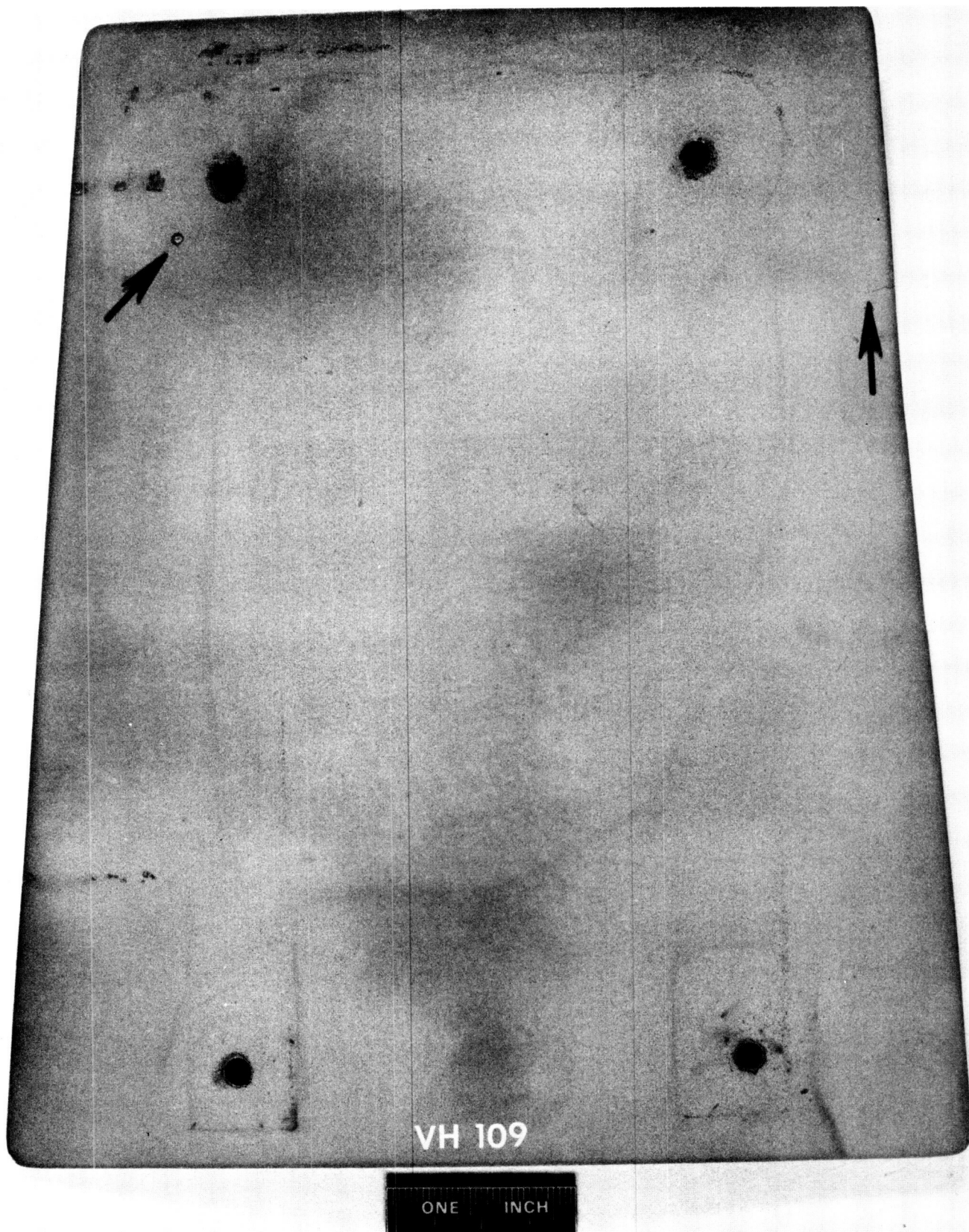
ORIGINAL PAGE IS  
OF POOR QUALITY



FD 358234

*Figure 3-13. Gas-Path View of Crack in VH-109 Panel*





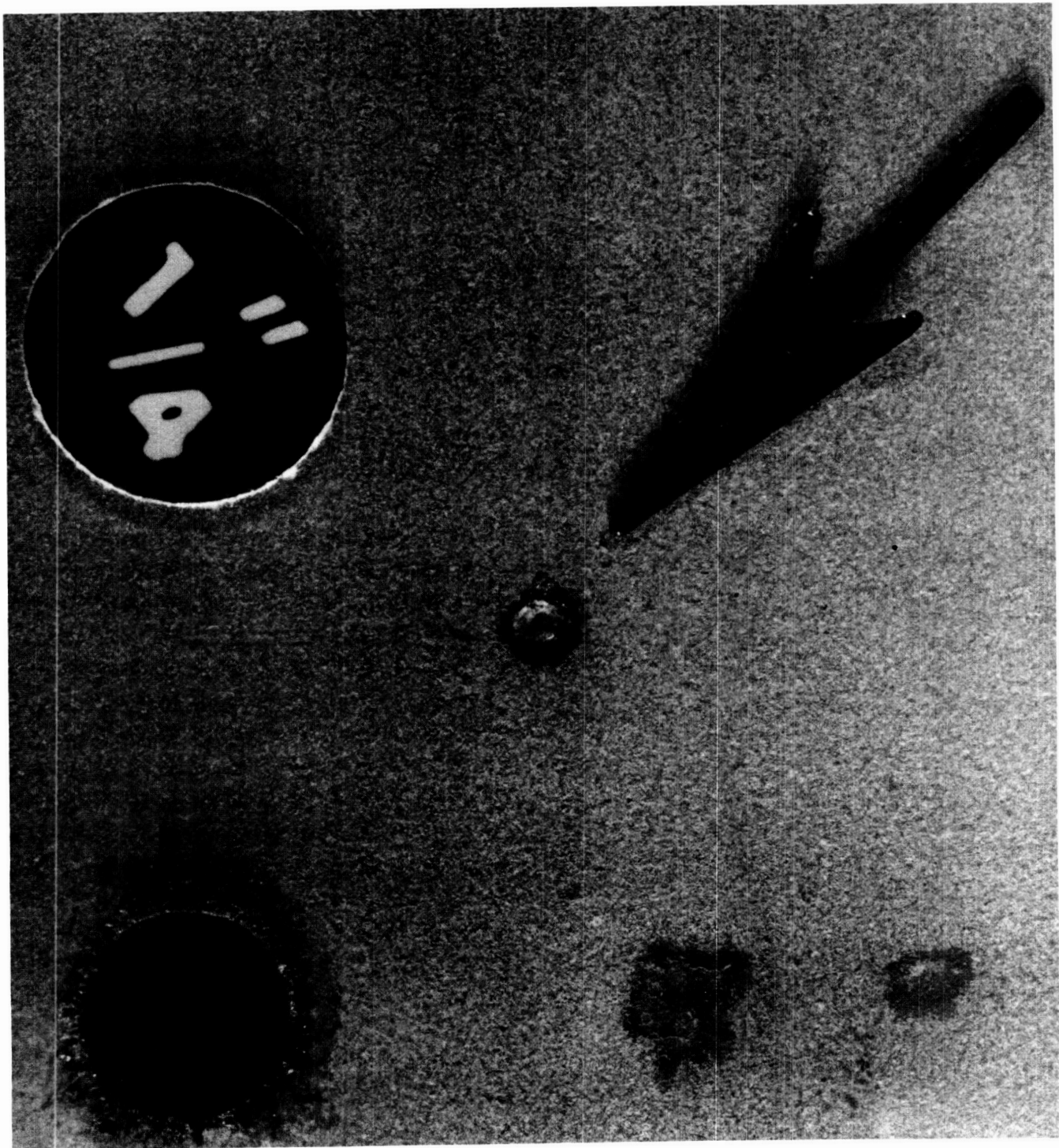
Run Time: 4451 sec  
Start/Stop Cycles: 23

FD 358235

*Figure 3-14. Chamber Environment Side of VH-109 Coated C-103 Test Panel (Note: Arrow Points to Pinhole Oxidation Which Correlates to Surface Blemish on Gas-Path Side of Panel) — Run Time: 4451 seconds — Start/Stop Cycles: 23*

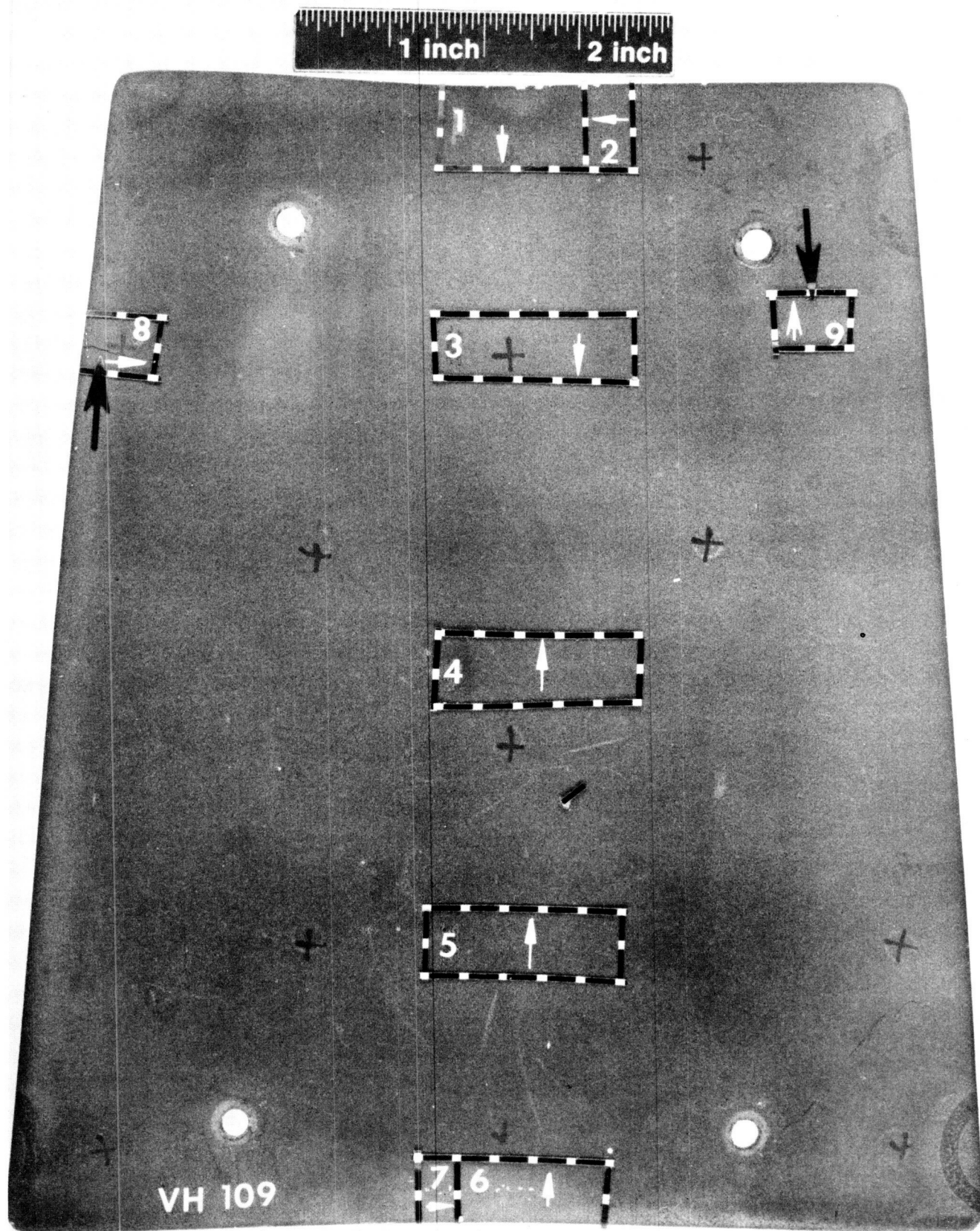


ORIGINAL PAGE IS  
OF POOR QUALITY



FD 358236

*Figure 3-15. Macro photograph of Pinhole Oxidation*

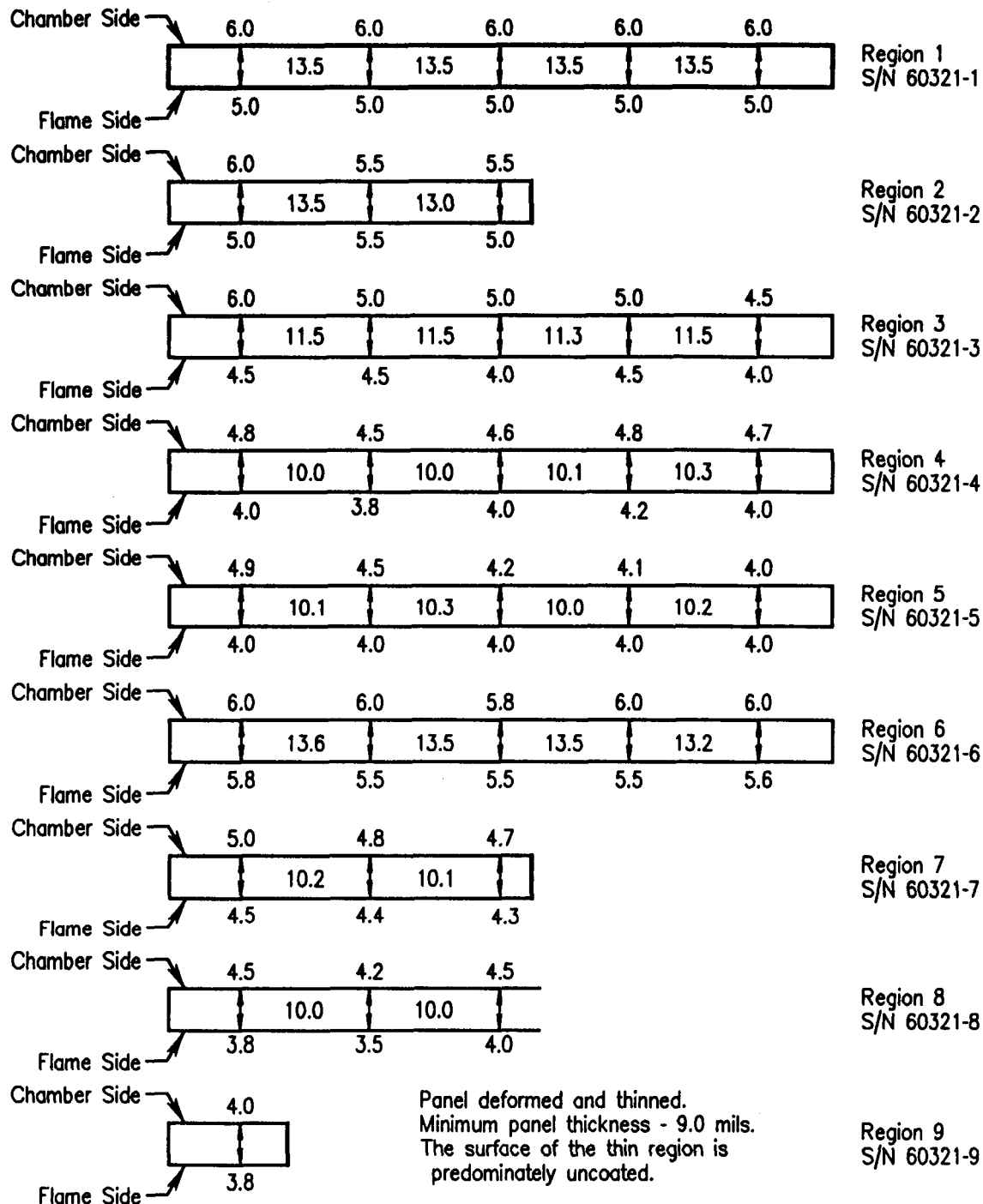


Run Time: 4451 sec  
Start/Stop Cycles: 23

FD 358237

*Figure 3-16. Sectioning Pattern of Flame-Side VH-109 Coated C-103 Test Panel — Run Time: 4451 seconds — Start/Stop Cycles: 23*

Run Time: 4451 sec  
Start/Stop Cycles: 23



FD 358238

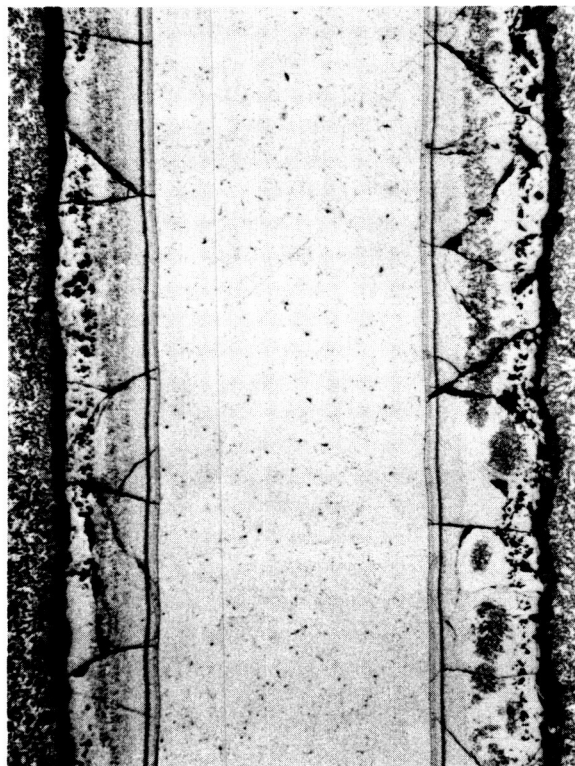
Figure 3-17. Coating Thickness Distribution Diagrams of VH-109 Coated C-103 Test Panel  
— Run Time: 4451 seconds — Start/Stop Cycles: 23

ORIGINAL PAGE IS  
OF POOR QUALITY



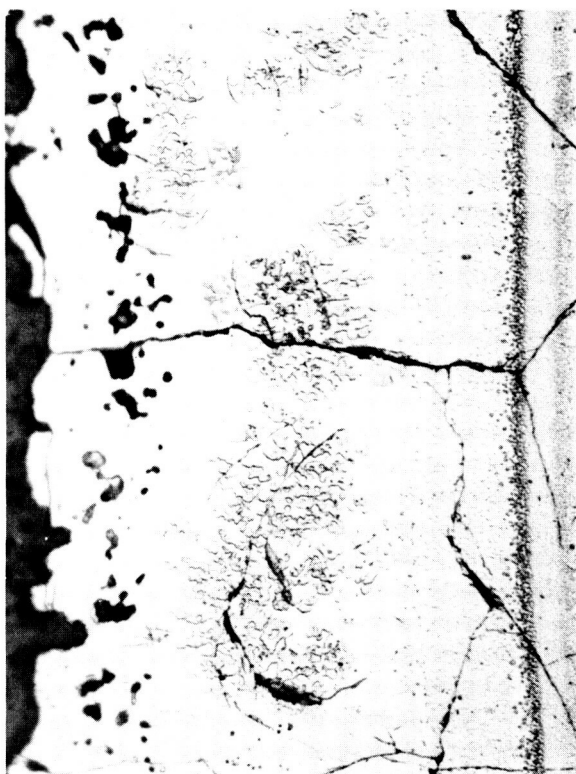
FAM 97551  
Mag: 500X

Gas Path Side



FAM 97649  
Mag: 100X

Chamber Side



FAM 97550  
Mag: 500X

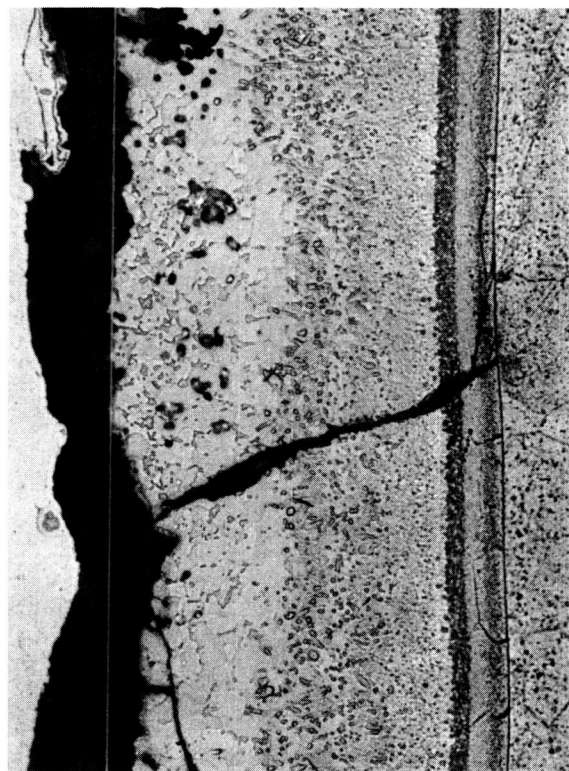
Chamber Side

Run Time: 4451 sec  
Start/Stop Cycles: 23

Figure 3-18. VH-109 Coating Microstructure at Region 1 (S/N 60321-1) — Run Time: 4451 seconds — Start/Stop Cycles: 23



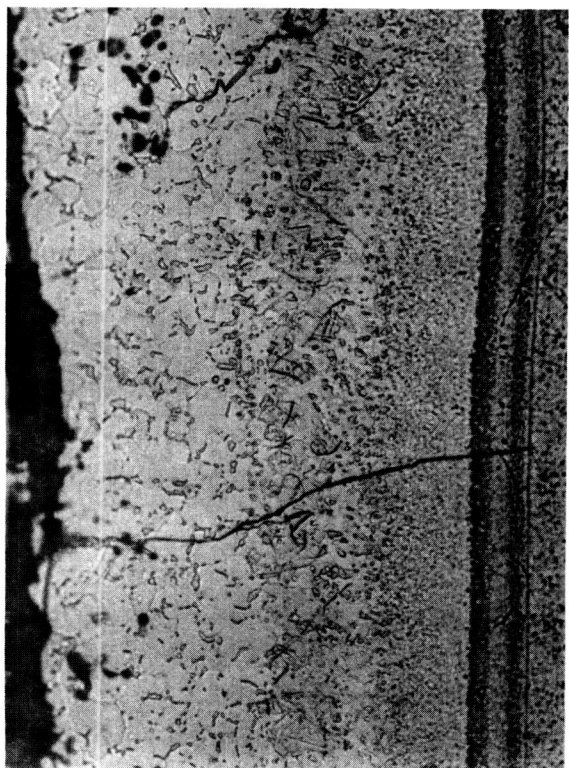
ORIGINAL PAGE IS  
OF POOR QUALITY



Mag: 500X

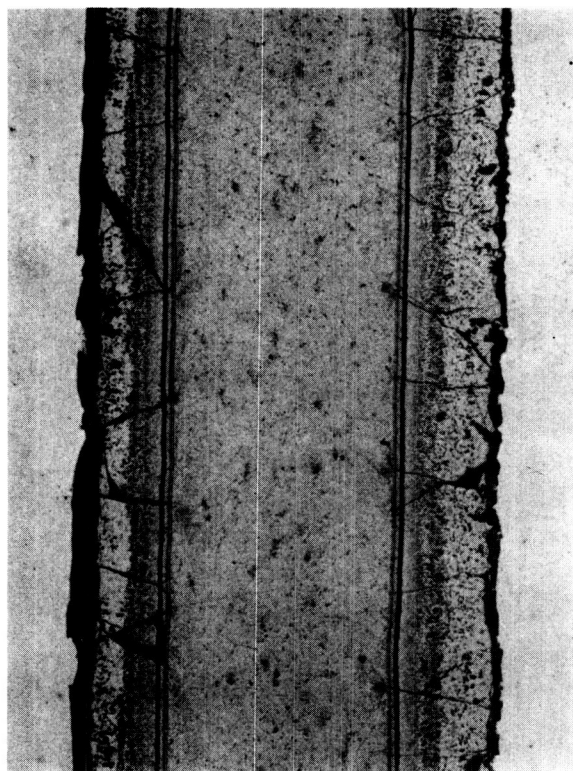
Gas Path Side

Gas Path Side



Mag: 500X

Chamber Side



Mag: 100X

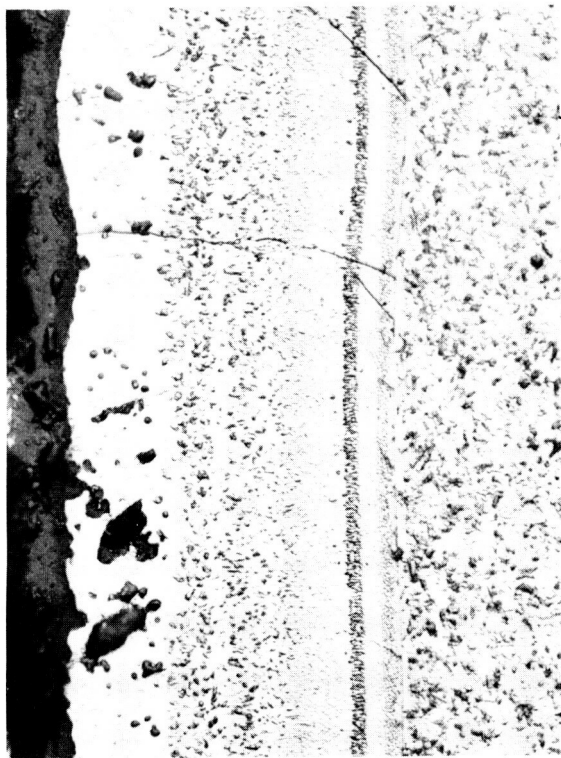
Chamber Side

FD 358240

Run Time: 4451 sec  
Start/Stop Cycles: 23

Figure 3-19. VH-109 Coating Microstructure at Region 3 (S/N 60321-3) — Run Time:  
4451 seconds — Start/Stop Cycles: 23

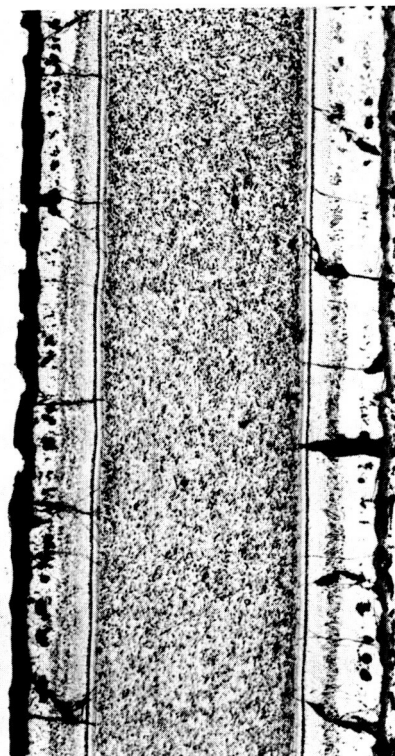
ORIGINAL PAGE IS  
OF POOR QUALITY



FAM 97645  
Mag: 500X

Gas Path Side

Gas Path Side



FAM 97643  
Mag: 100X

Chamber Side

FD 358241



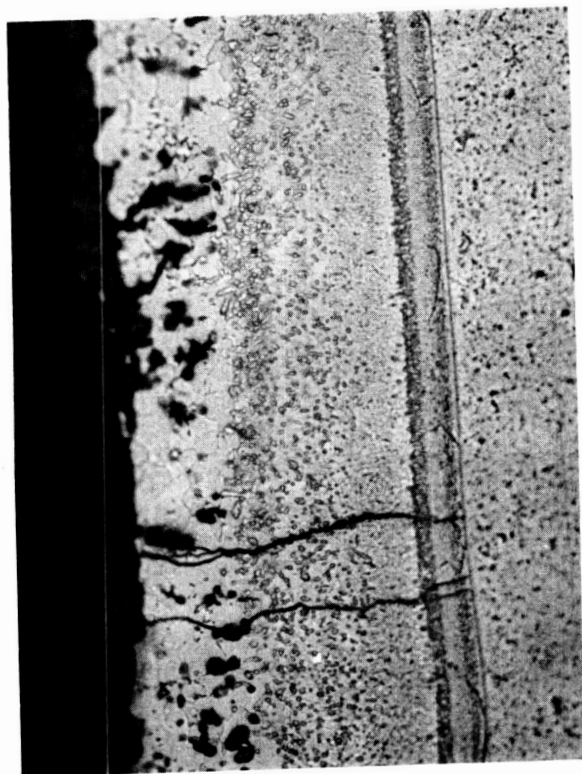
FAM 97664  
Mag: 500X

Chamber Side

Run Time: 4451 sec  
Start/Stop Cycles: 23

Figure 3-20. VH-109 Coating Microstructure at Region 4 (S/N 60321-4) — Run Time:  
4451 seconds — Start/Stop Cycles: 23

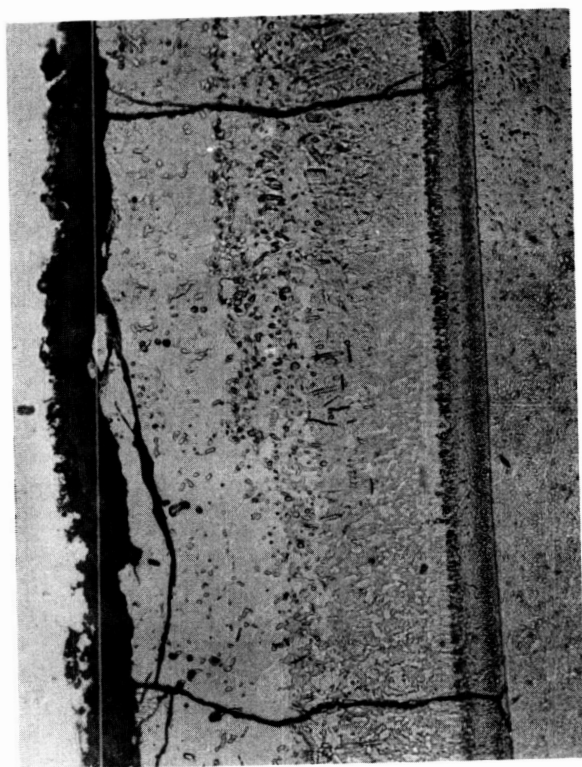
ORIGINAL PAGE IS  
OF POOR QUALITY



Mag: 500X

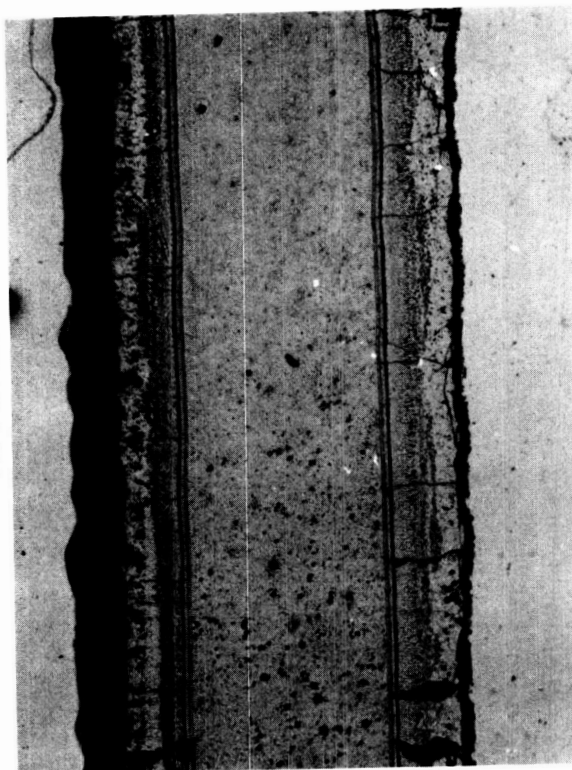
Gas Path Side

Gas Path Side



Mag: 500X

Chamber Side



Mag: 100X

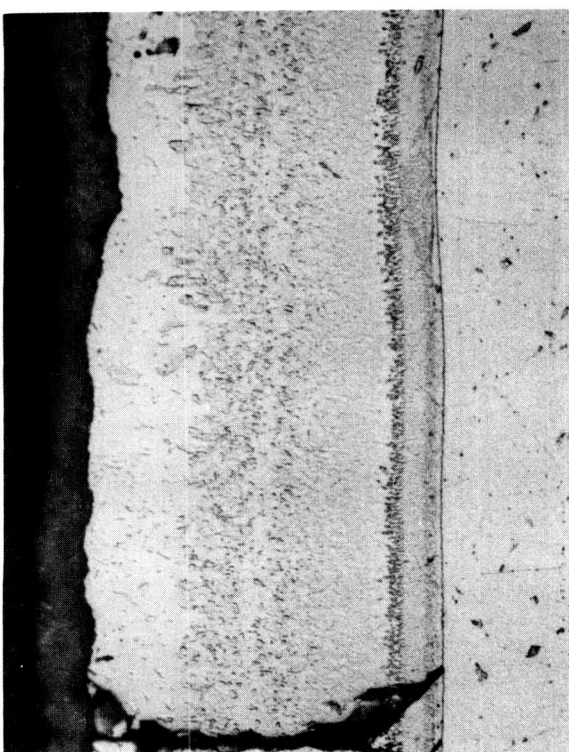
Chamber Side

FD 358242

Run Time: 4451 sec  
Start/Stop Cycles: 23

Figure 3-21. VH-109 Coating Microstructure at Region 5 (S/N 60321-5) — Run Time: 4451 seconds — Start/Stop Cycles: 23

ORIGINAL PAGE IS  
OF POOR QUALITY



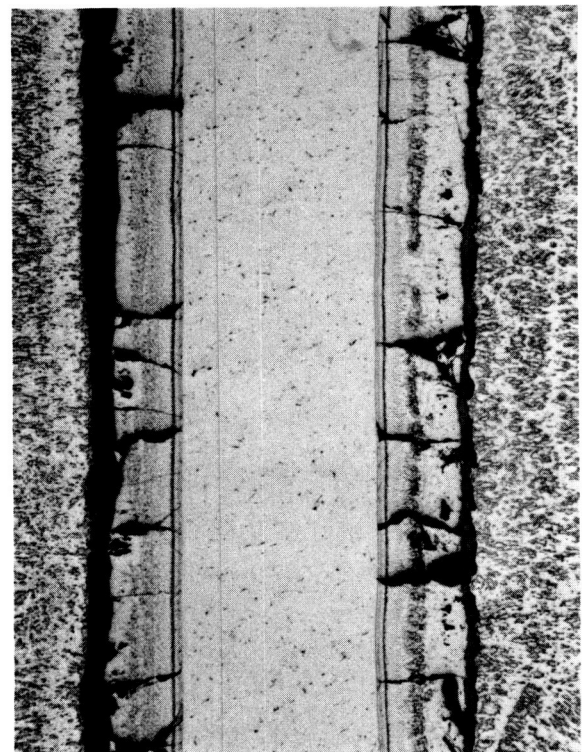
FAM 97647  
Mag: 500X

Gas Path Side



FAM 97648  
Mag: 500X

Chamber Side



FAM 97646  
Mag: 100X

Chamber Side

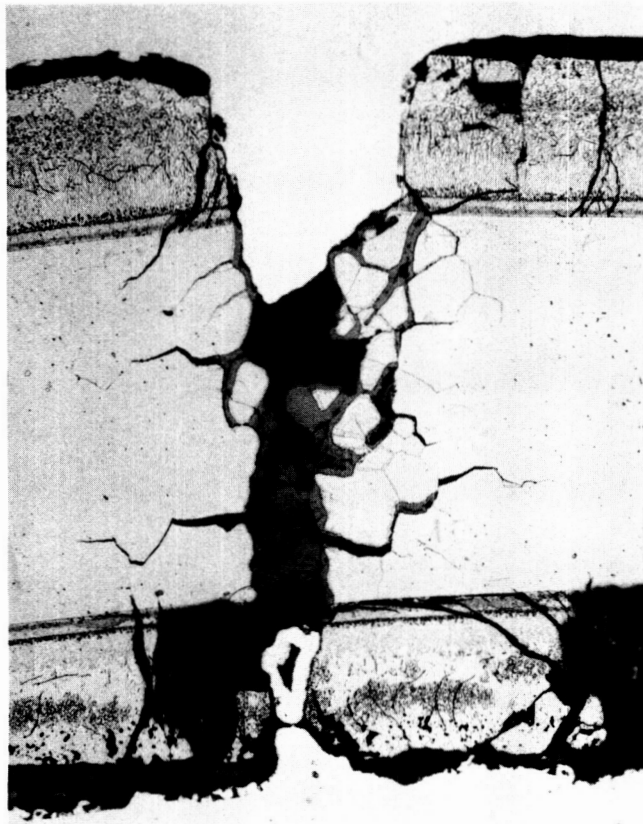
Run Time: 4451 sec  
Start/Stop Cycles: 23

Figure 3-22. VH-109 Coating Microstructure at Region 7 (S/N 60321-7) — Run Time:

FD 358243



ORIGINAL PAGE IS  
OF POOR QUALITY



S/N 60321-8

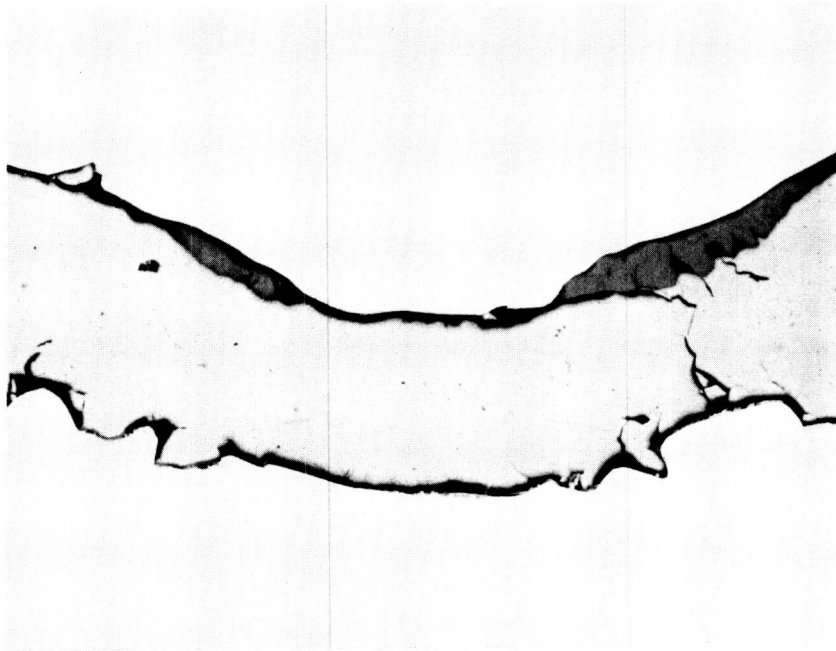
Run Time: 4451 sec  
Start/Stop Cycles: 23

Mag: 200X

FD 358244

*Figure 3-23. Cross Section of Crack on VH-109 Coated C-103 Test Panel — Run Time: 4451 seconds — Start/Stop Cycles: 23*

ORIGINAL PAGE IS  
OF POOR QUALITY



S/N 60321-9

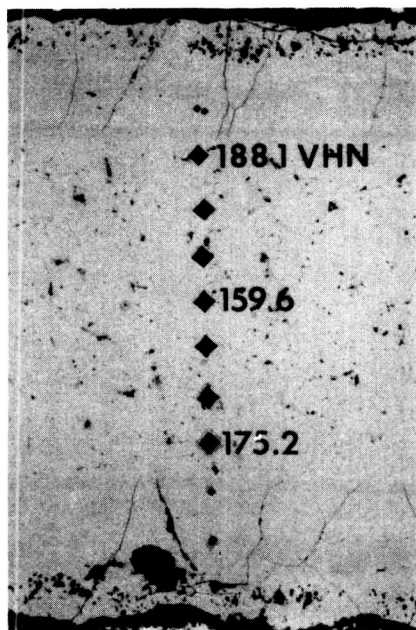
Mag: 100X

FD 358245

*Figure 3-24. Cross Section of Pinhole Coating Failure Illustrating the Mechanical Damage That Led to C-103 Oxidation*

Run Time: 4451 sec  
Start/Stop Cycles: 23

Chamber Environment

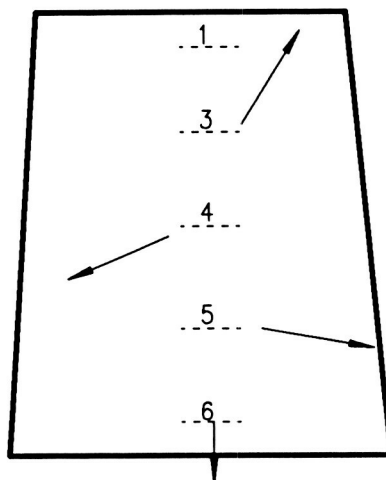
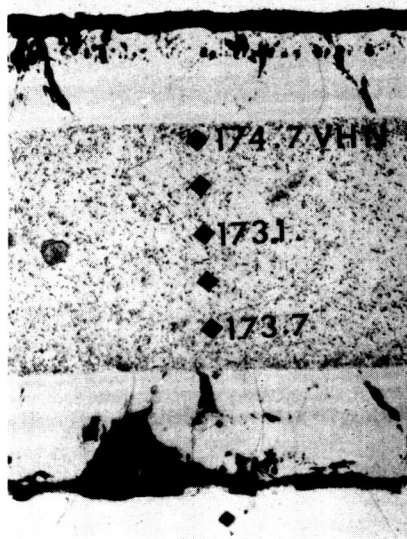


ORIGINAL PAGE IS  
OF POOR QUALITY

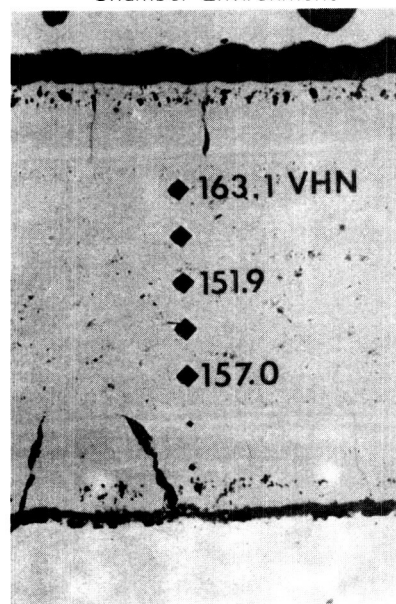
Chamber Environment



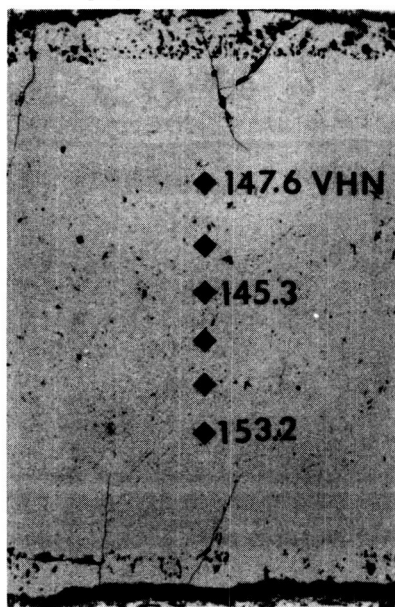
Chamber Environment



Chamber Environment

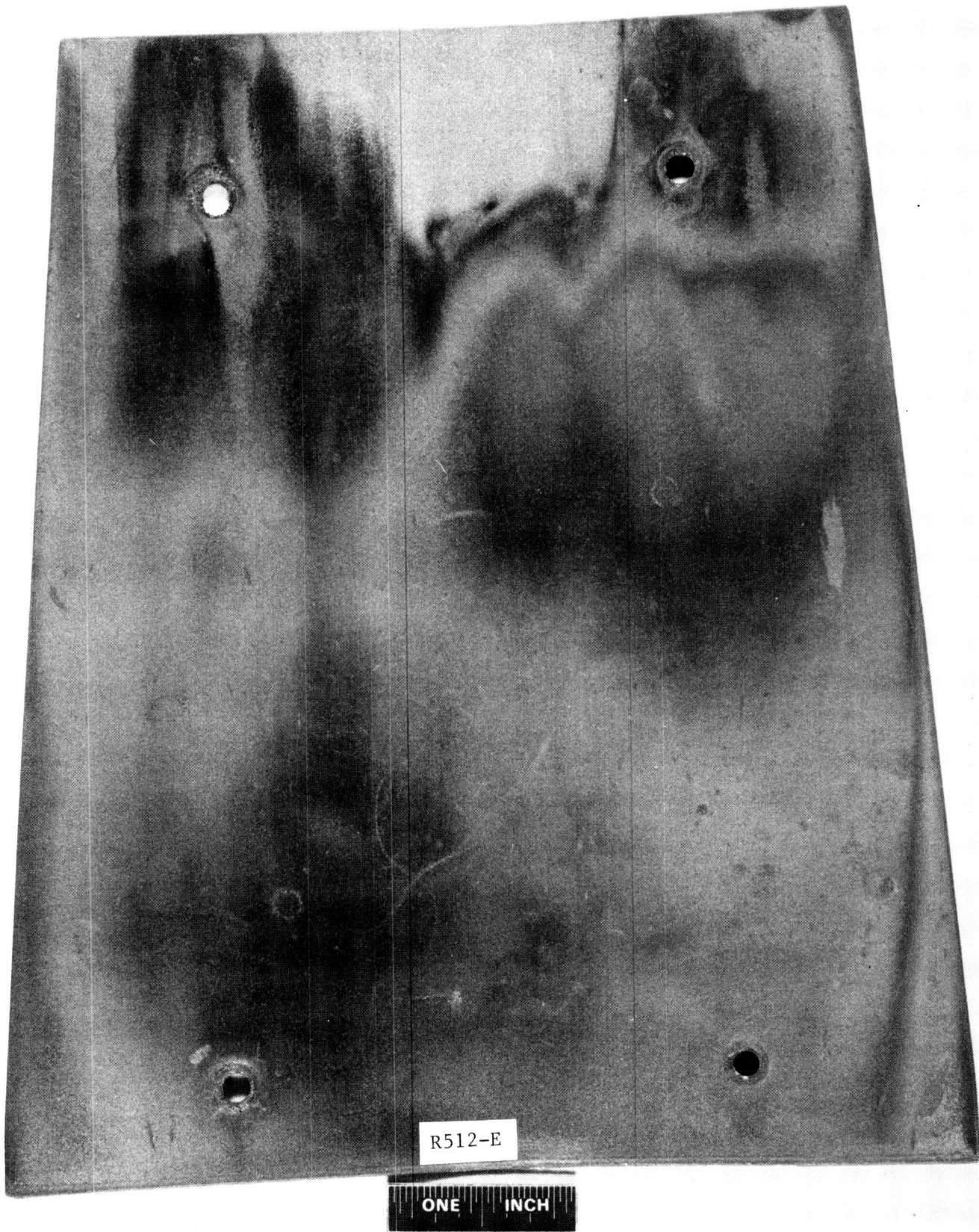


Chamber Environment



FD 358246

Figure 3-25. Microhardness Measurements Through the Thickness of VH-109 Coated C-103 Test Panel — Run Time: 4451 seconds — Start/Stop Cycles: 23

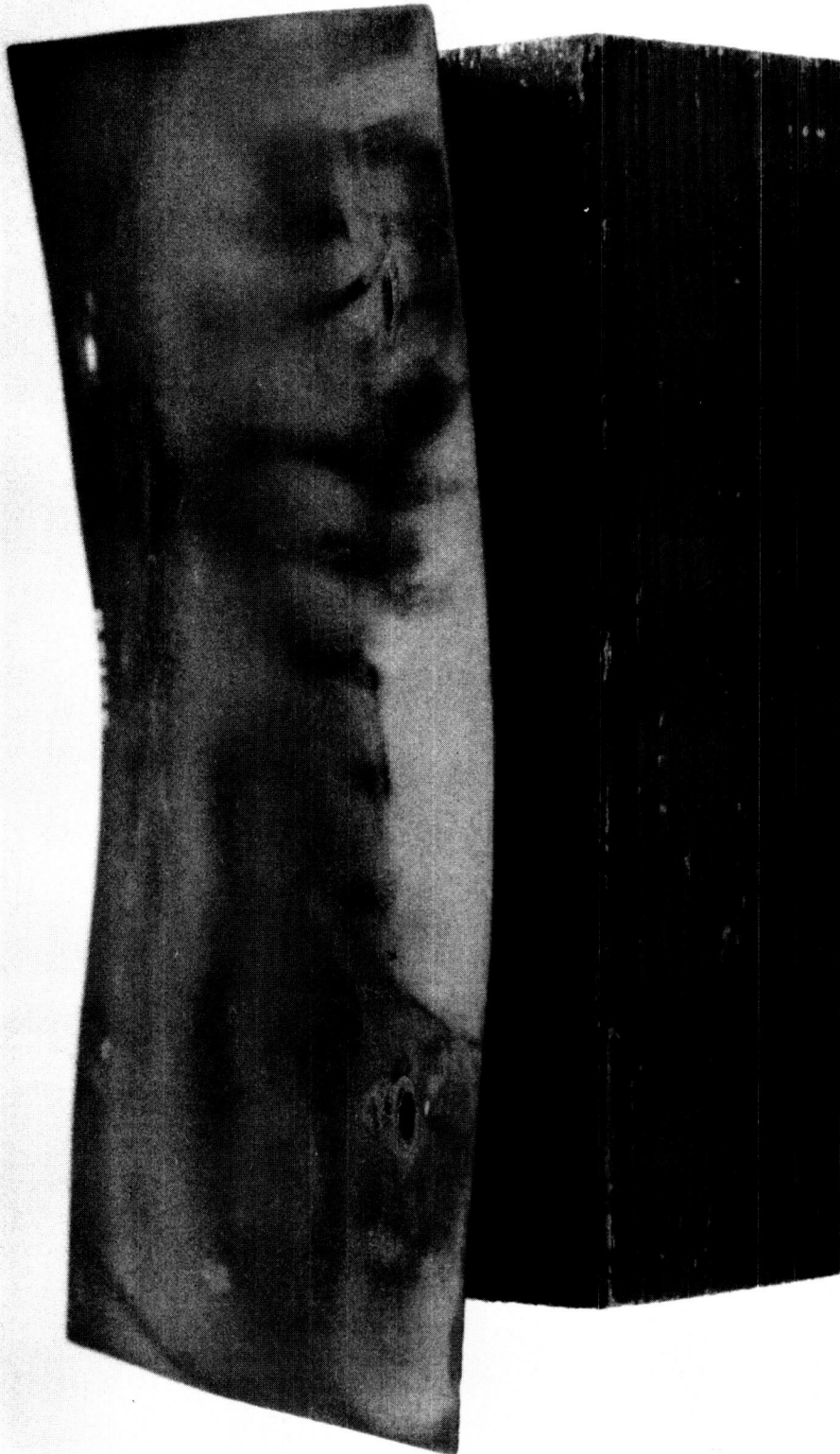


Run Time: 4451 sec  
Start/Stop Cycles: 23

FD 358247

*Figure 3-26. Gas-Path Environment Side of R512-E Coated C-103 Test Panel — Run Time: 4451 seconds — Start/Stop Cycles: 23*

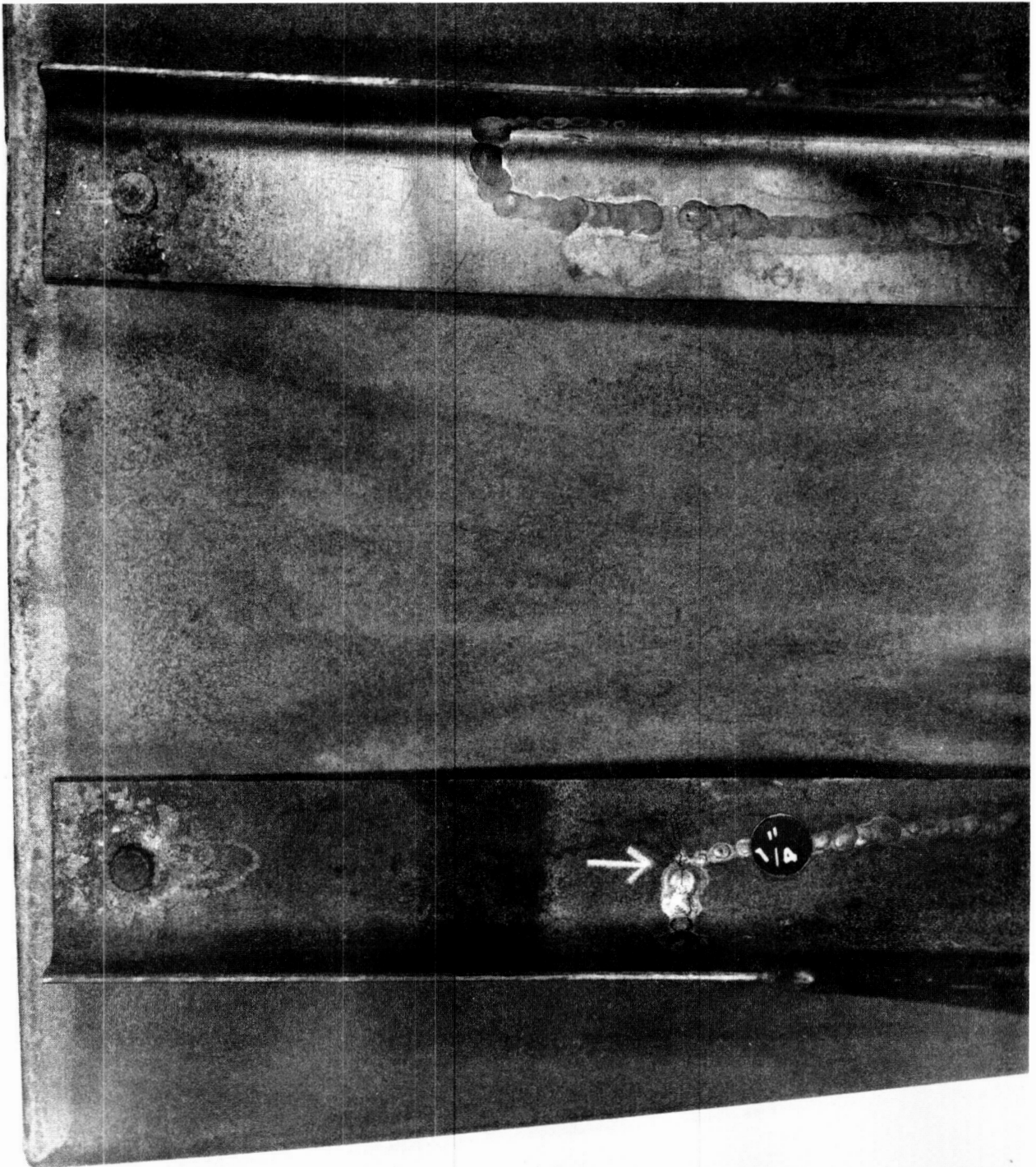
ORIGINAL PAGE IS  
OF POOR QUALITY



FD 358248

*Figure 3-27. Downstream View of R512E Coated C-103 Test Panel (Note the Cooling Tube Spacing Pattern Shown by the Surface Scale of the Panel)*





FD 358249

*Figure 3-28. Bracket Crack (Arrow Shows Crack in Support Bracket Which May Have Reduced Constraining Stresses, Thus Minimizing Warping)*



FD 358250

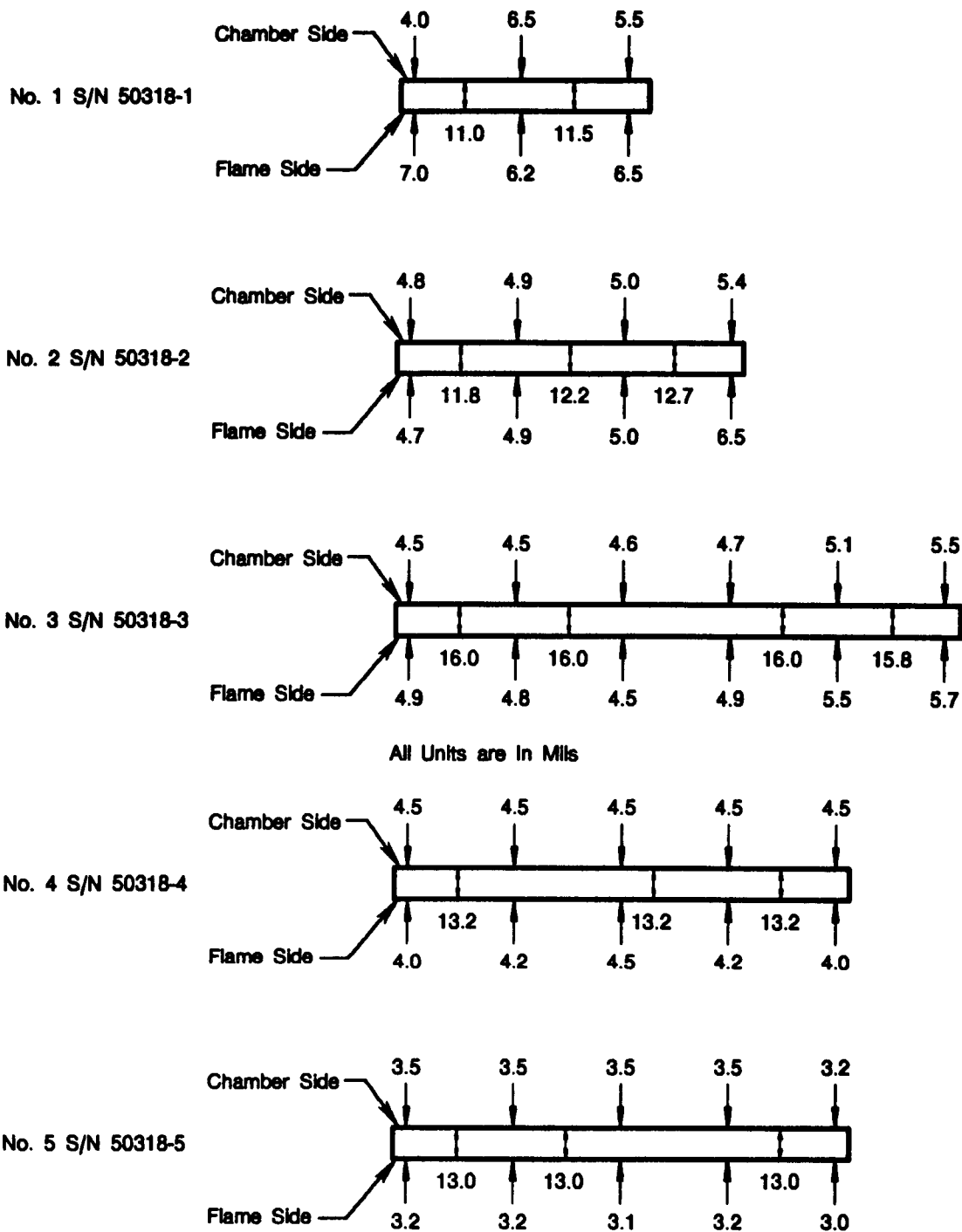
*Figure 3-29. Chamber Environment Side of R512-E Coated C-103 Test Panel (Arrow Locates a Coating Chip at Exit Plane) — Run Time: 4451 seconds — Start/Stop Cycles: 23*



FD 358401

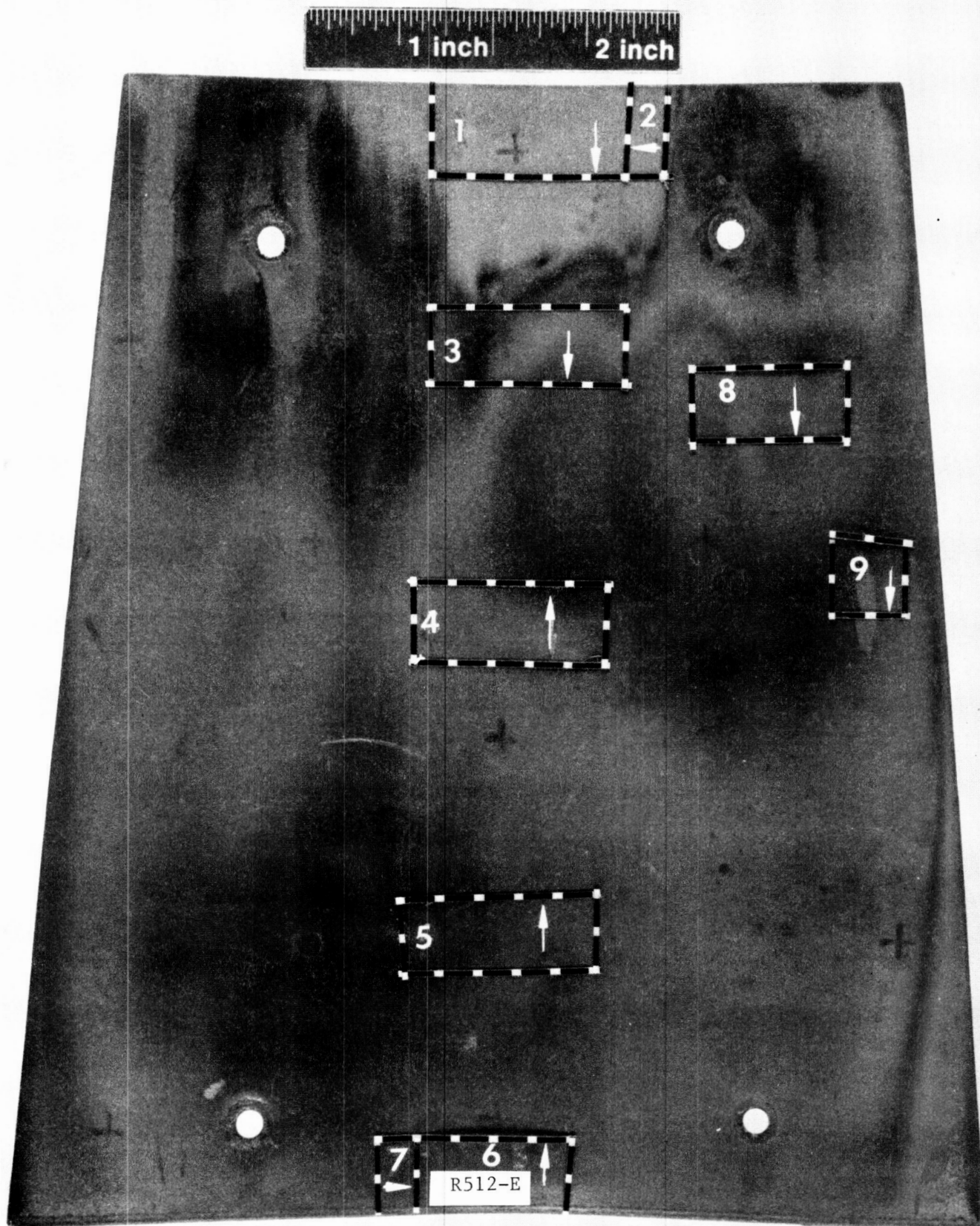
*Figure 3-30. Close-Up View of Coating Chip on Figure 3-29*





FDA 358402

Figure 3-31. As-Coated R512-E Thickness Distribution of  $5.0 \pm 1.0$  mil Coating

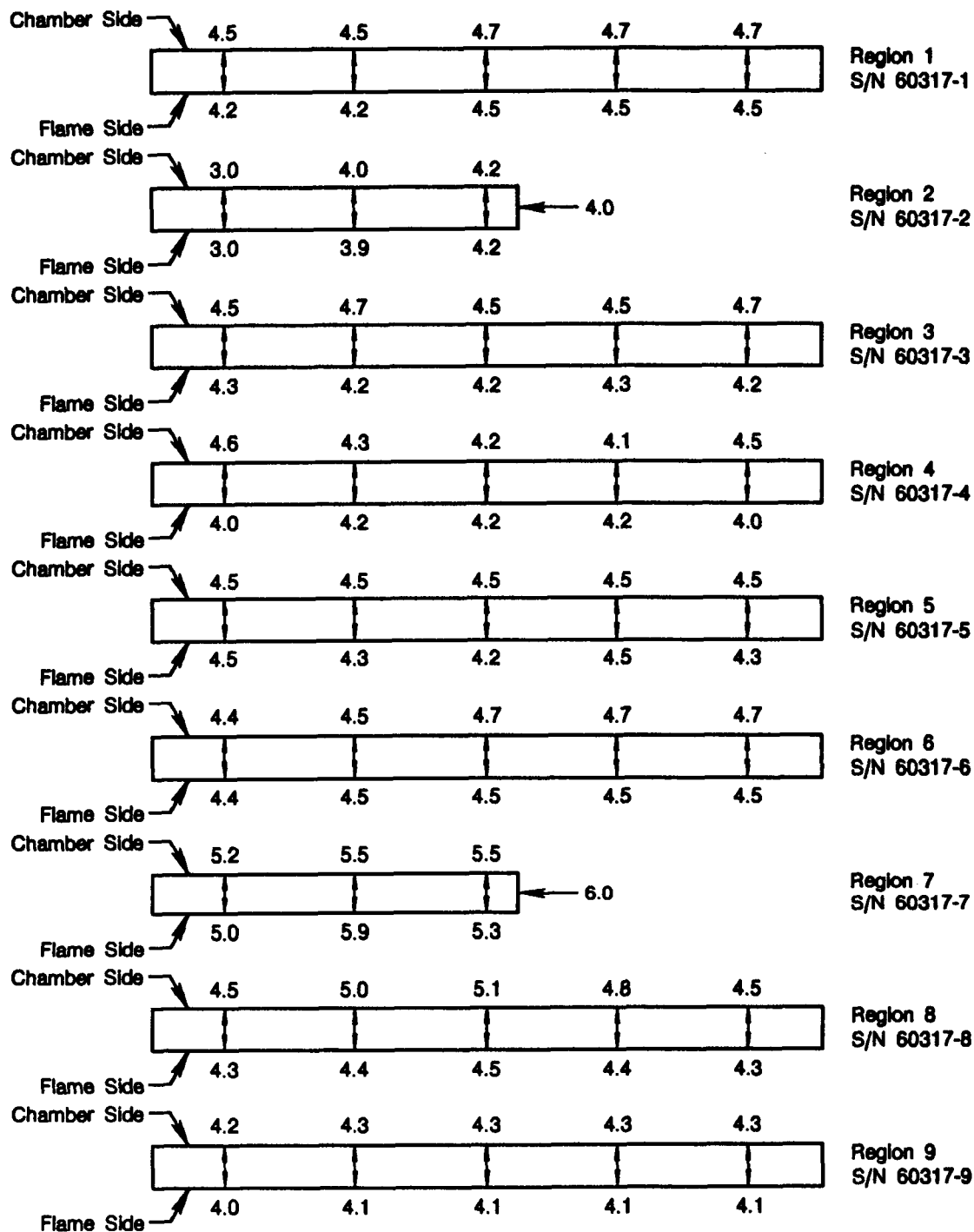


Run Time: 4451 sec  
Start/Stop Cycles: 23

FD 358403

**Figure 3-32.** Sectioning Pattern of Gas Path (Flame) Side of R512-E Coated C-103 Test Panel — Run Time: 4451 seconds — Start/Stop Cycles: 23

Run Time: 4451 sec  
Start/Stop Cycles: 23



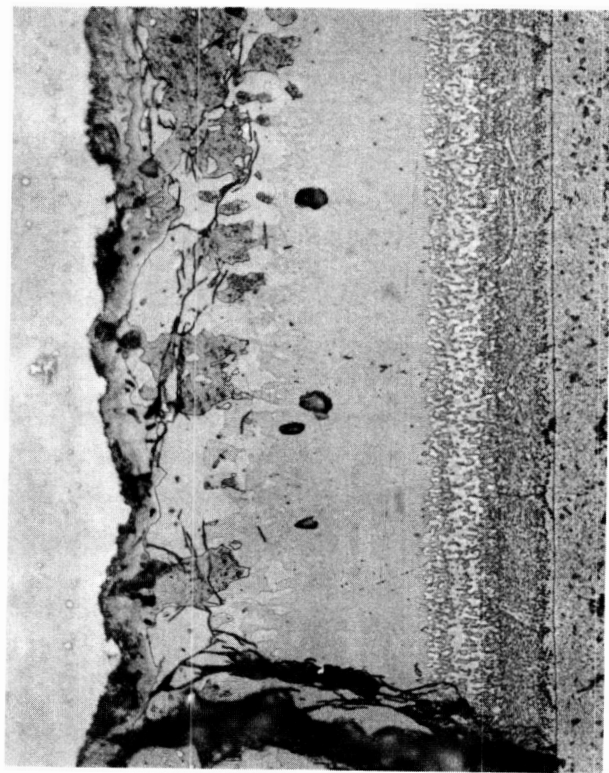
FDA 358404

Figure 3-33. Coating Thickness Distribution Diagram of R512-E Coated C-103 Test Panel  
— Run Time: 4451 seconds — Start/Stop Cycles: 23



Gas Path Side

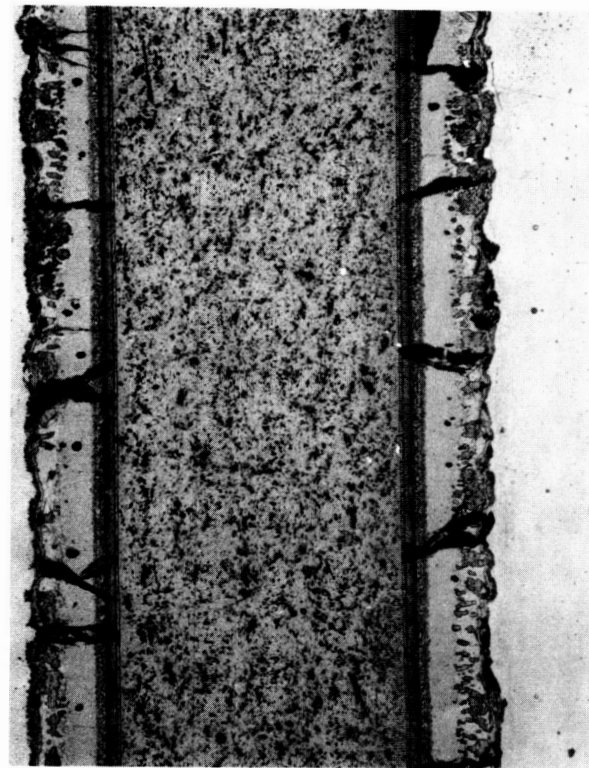
Mag: 500X



Chamber Side

Mag: 500X

Gas Path Side



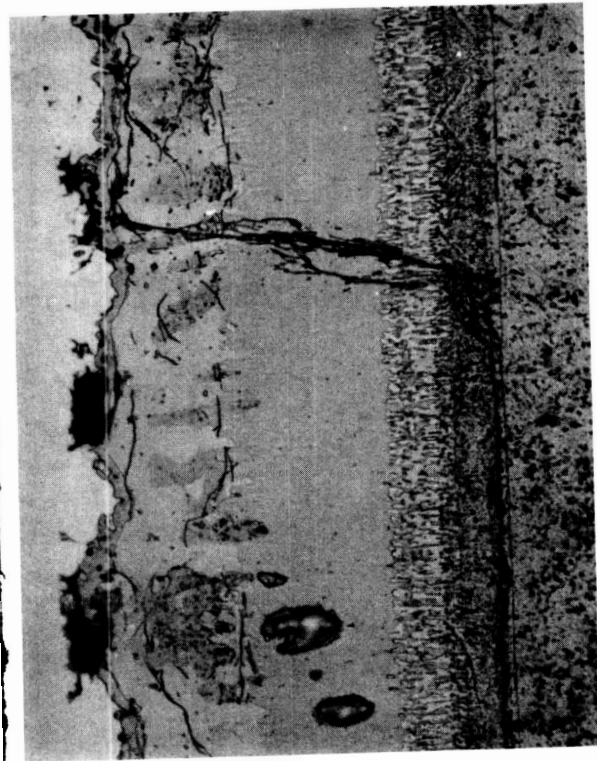
Chamber Side

Mag: 100X

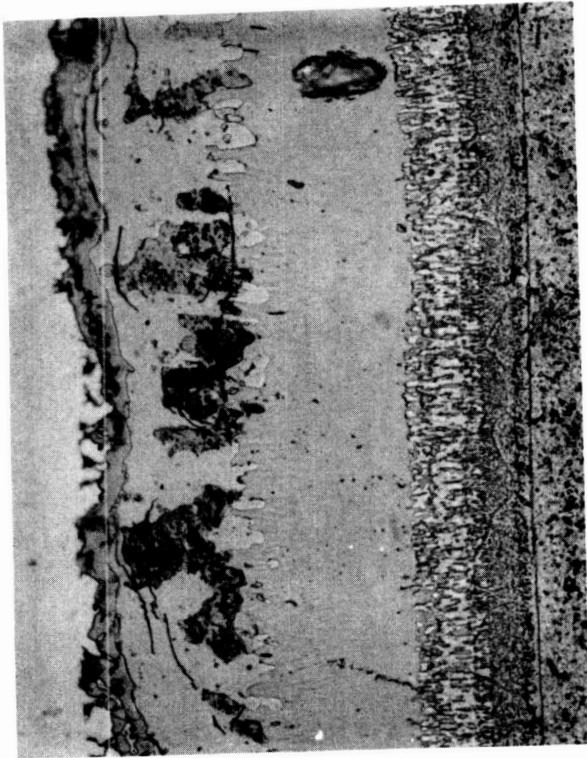
Run Time: 4451 sec  
Start/Stop Cycles: 23

Figure 3-34. R512-E Coating Microstructure at Region 1 (S/N 60317-1) — Run Time: 4451 seconds — Start/Stop Cycles: 23

FD 358405



Gas Path Side  
Mag: 500X



Chamber Side  
Mag: 500X

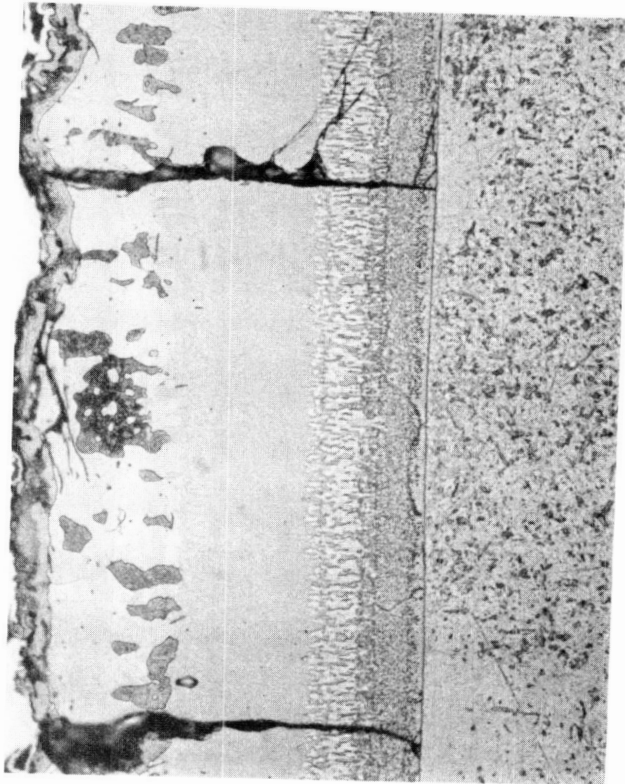


Chamber Side  
Mag: 100X  
FD 358406

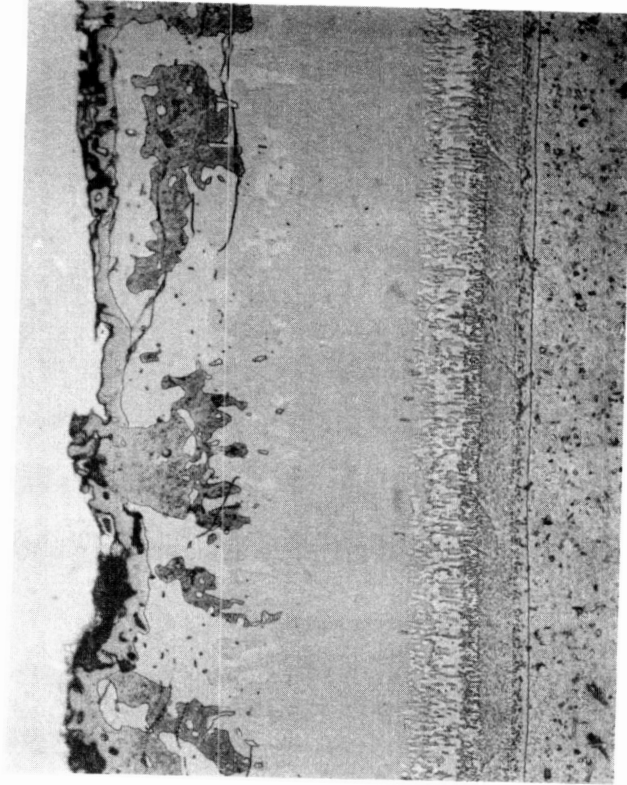
Run Time: 4451 sec  
Start/Stop Cycles: 23

Figure 3-35. R512-E Coating Microstructure at Region 3 (S/N 60317-3) — Run Time: 4451 seconds — Start/Stop Cycles: 23

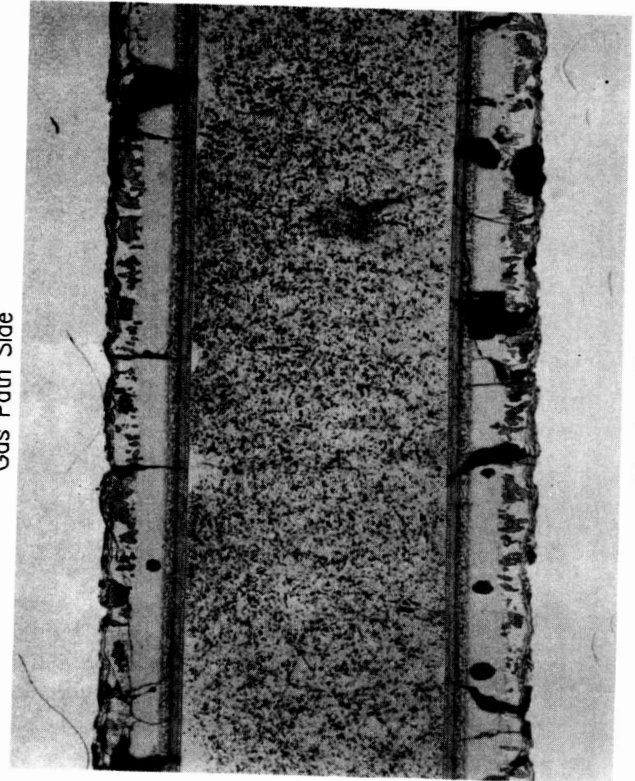




Gas Path Side  
Mag: 500X



Chamber Side  
Mag: 500X

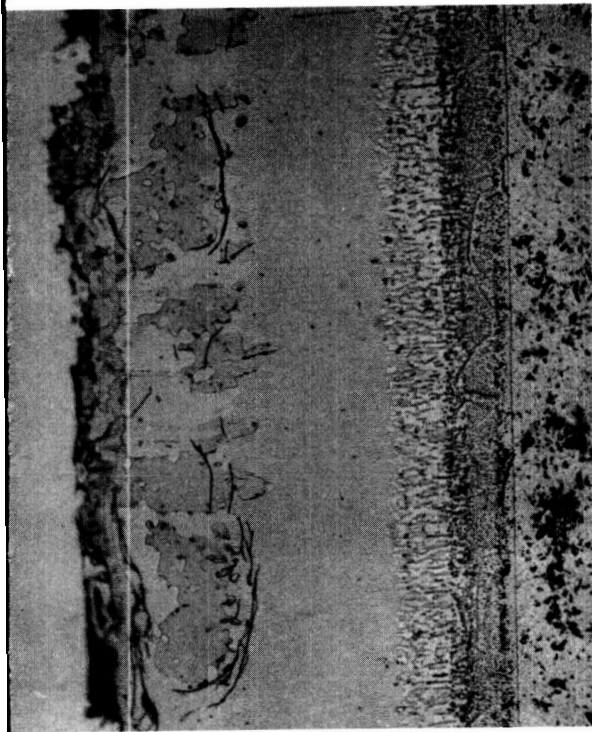


Chamber Side  
Mag: 100X  
FD 358407

Run Time: 4451 sec  
Start/Stop Cycles: 23

Figure 3-36. R512-E Coating Microstructure at Region 4 (S/N 60317-4) — Run Time: 4451 seconds — Start/Stop Cycles: 23

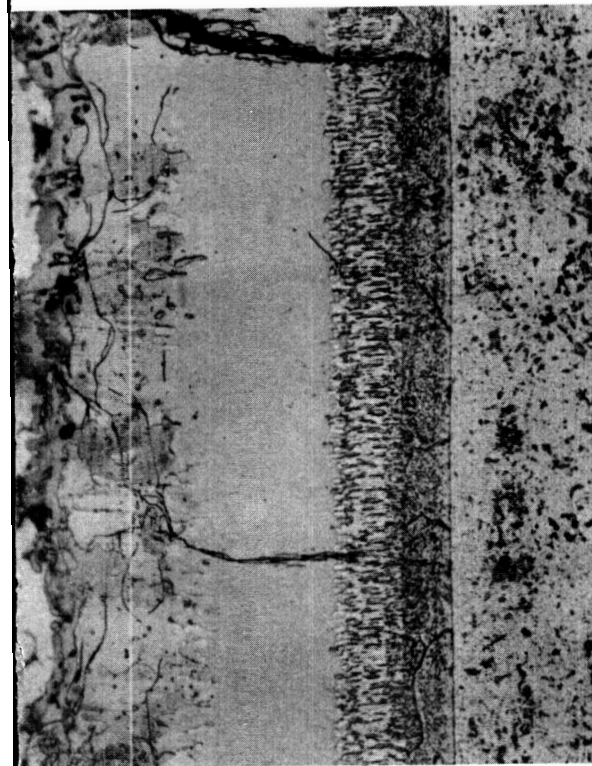
ORIGINAL PAGE IS  
OF POOR QUALITY



Mag: 500X

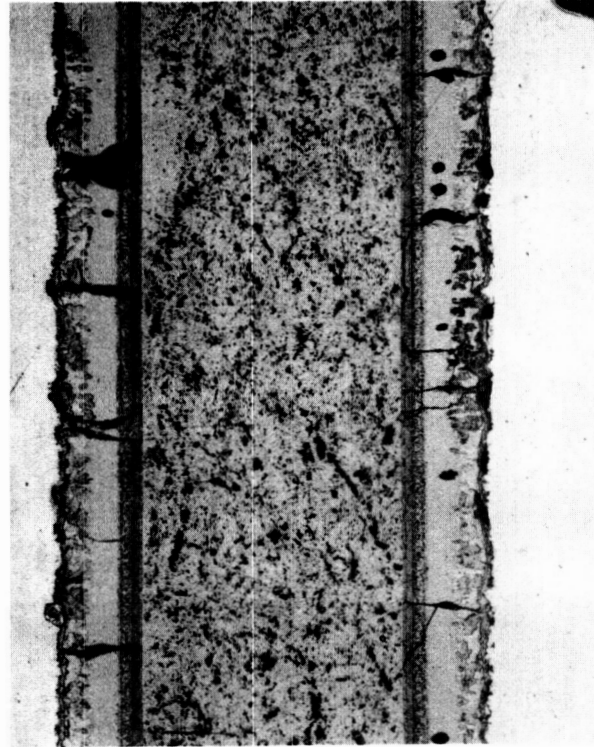
Chamber Side

Gas Path Side



Mag: 500X

Gas Path Side



Mag: 100X

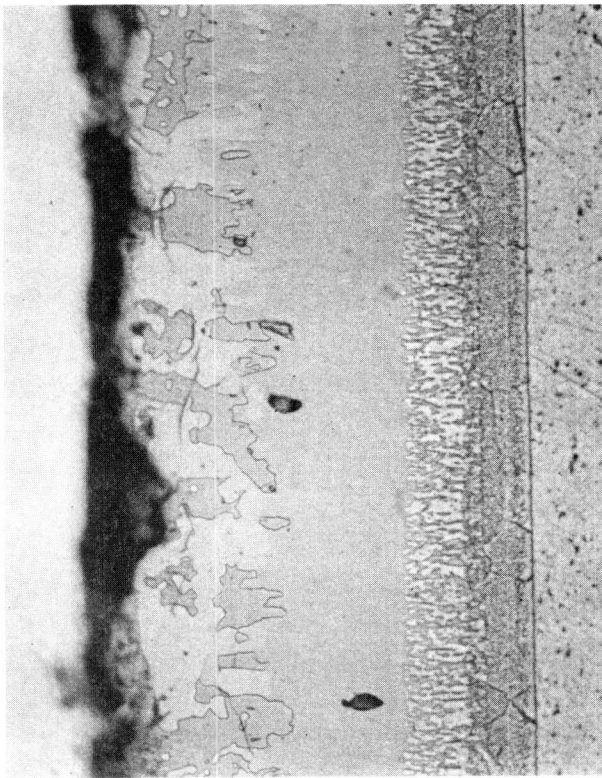
Chamber Side

FD 358408

Run Time: 4451 sec  
Start/Stop Cycles: 23

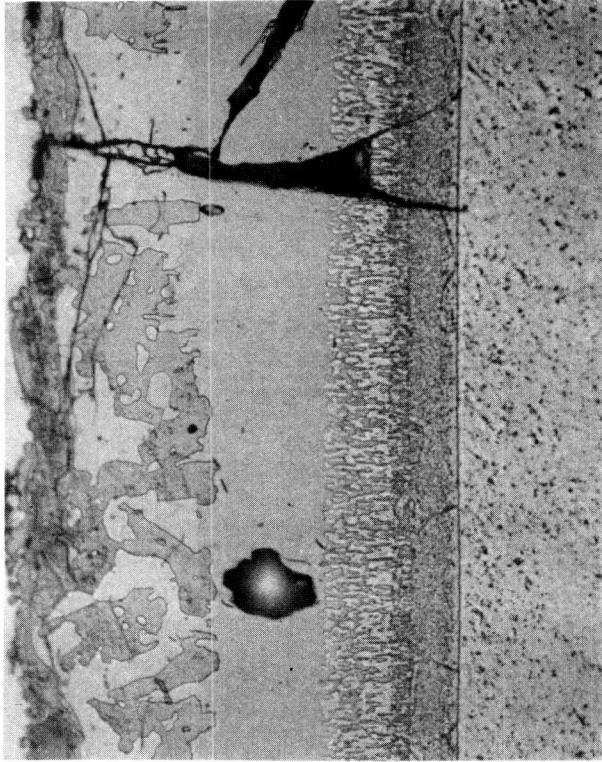
Figure 3-37. R512-E Coating Microstructure at Region 5 (S/N 60317-5) — Run Time:  
4451 seconds — Start/Stop Cycles: 23





Gas Path Side

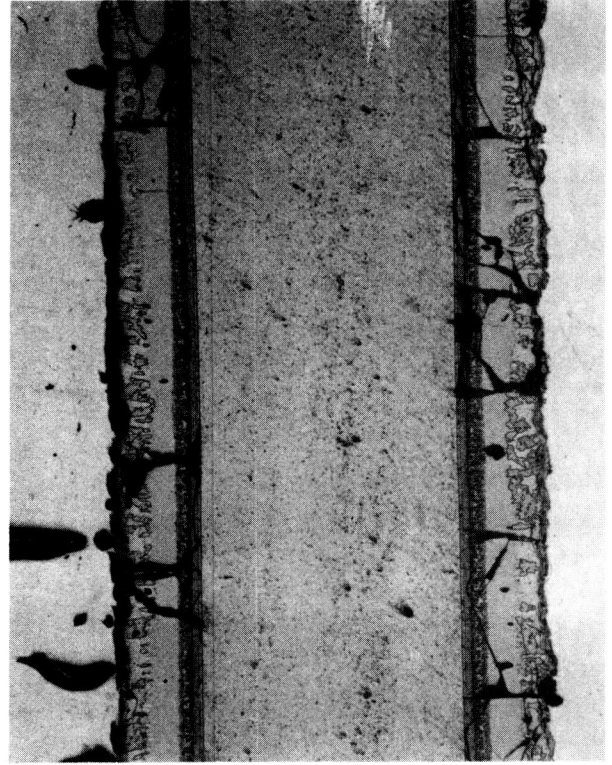
Mag: 500X



Chamber Side

Mag: 500X

II-54



Chamber Side

Mag: 100X

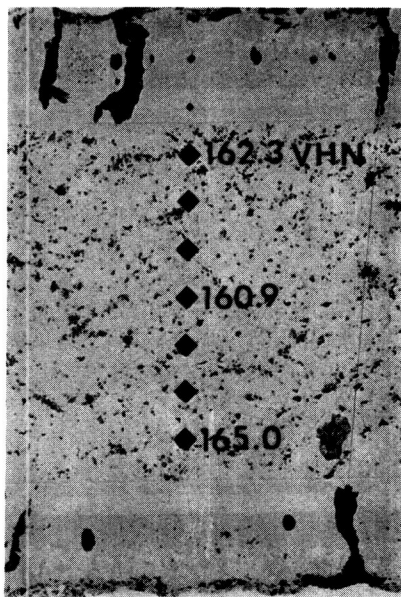
FD 358409

Run Time: 4451 sec  
Start/Stop Cycles: 23

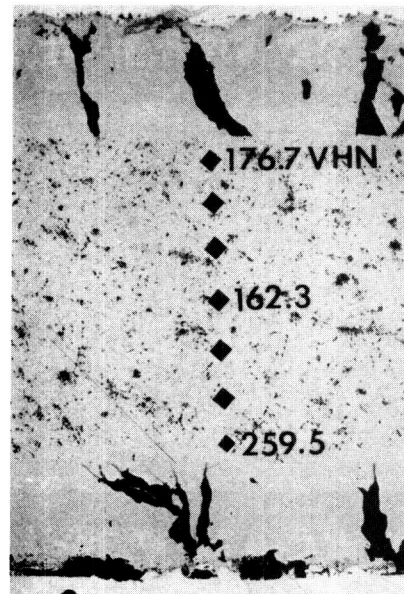
Figure 3-38. R512-E Coating Microstructure at Region 6 (S/N 60317-6) — Run Time: 4451 seconds — Start/Stop Cycles: 23

ORIGINAL PAGE IS  
OF POOR QUALITY

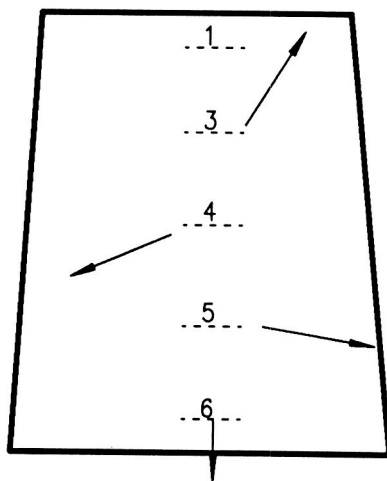
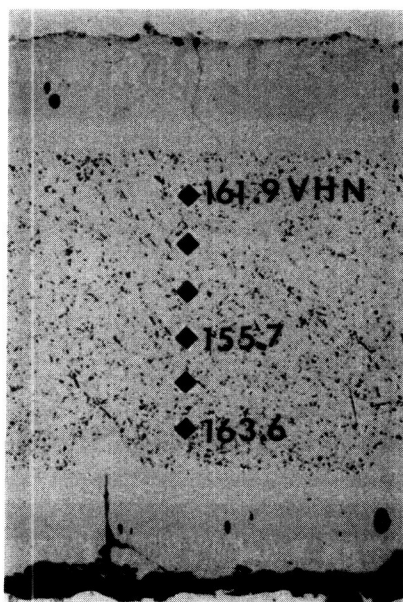
Chamber Environment



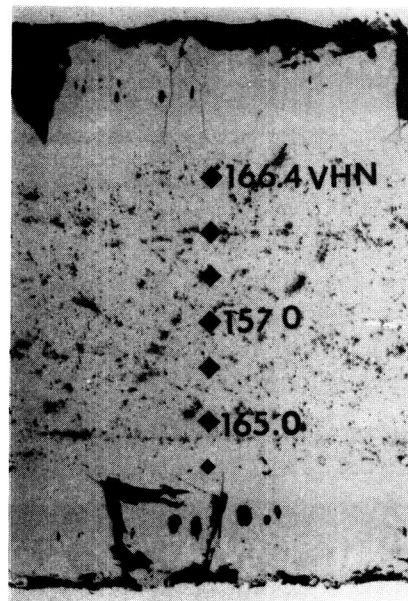
Chamber Environment



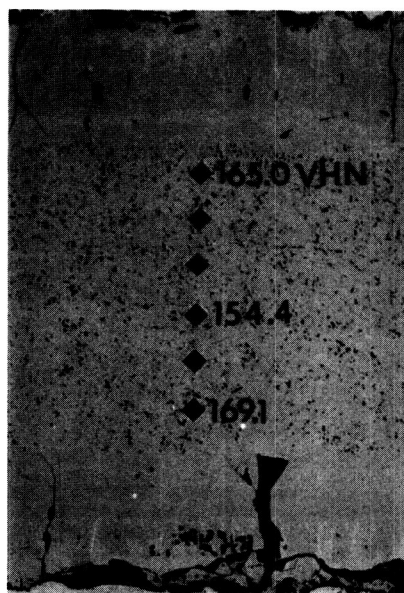
Chamber Environment



Chamber Environment



Chamber Environment



FD 358410

Figure 3-39. Microhardness Measurements Through the Thickness of R512-E Coated C-103 Test Panel — Run Time: 4451 seconds — Start/Stop Cycles: 23

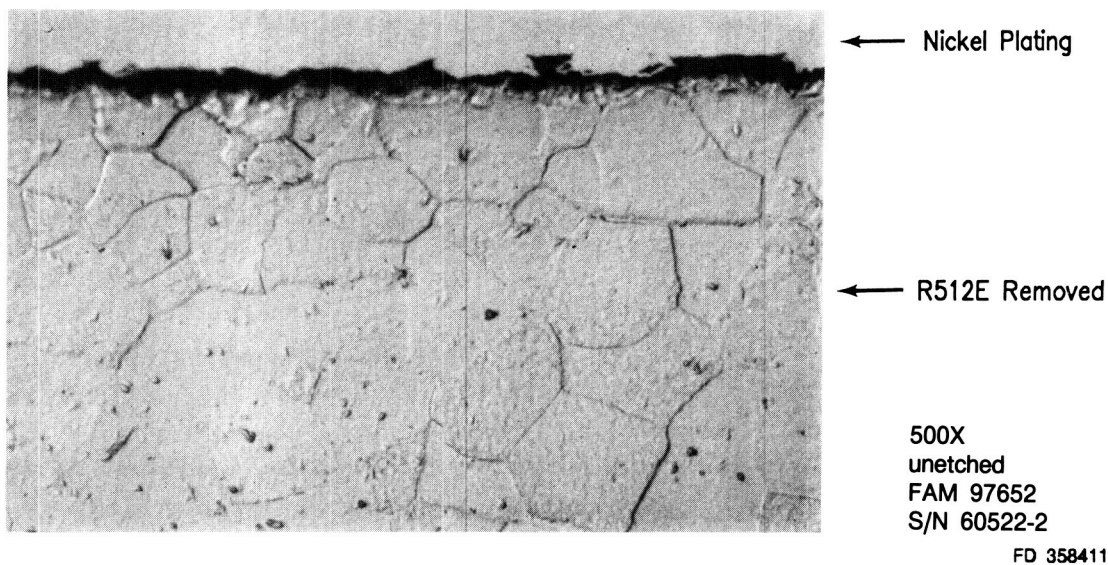
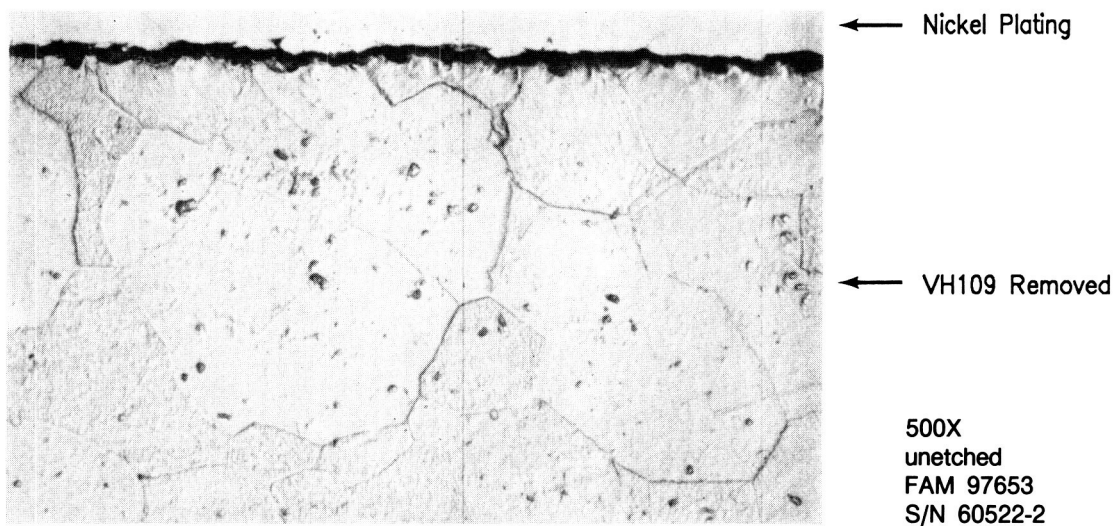
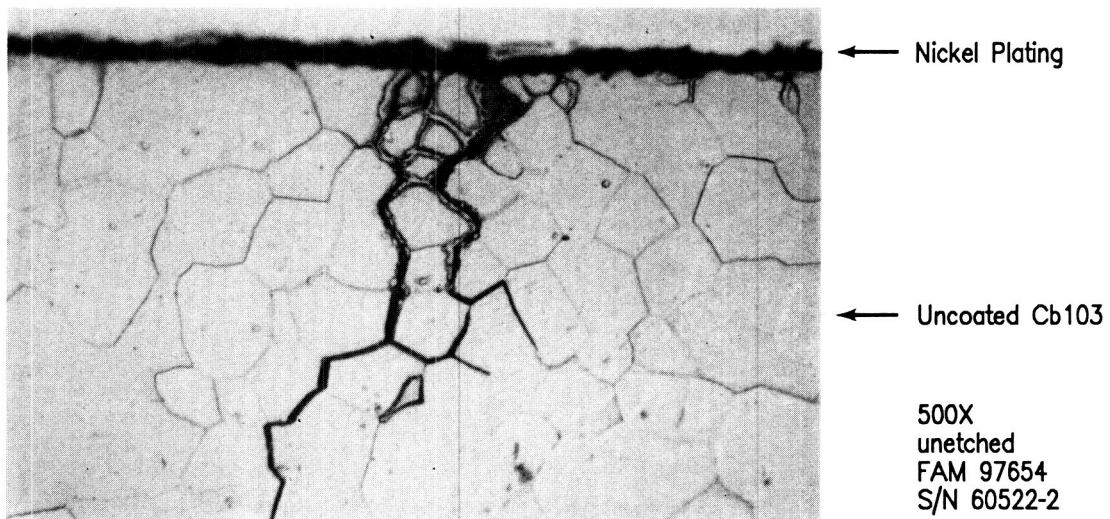
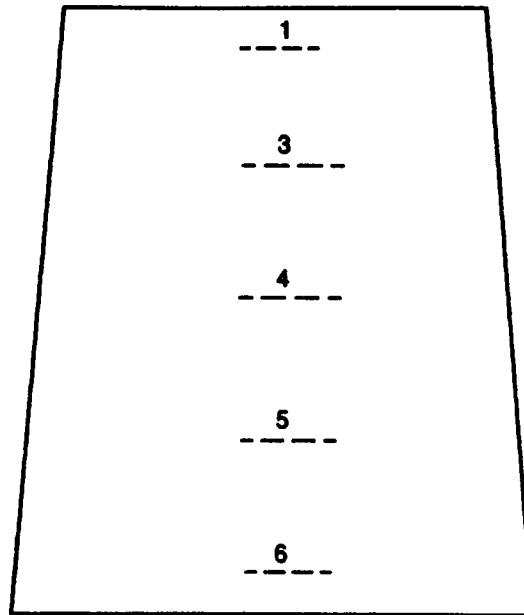
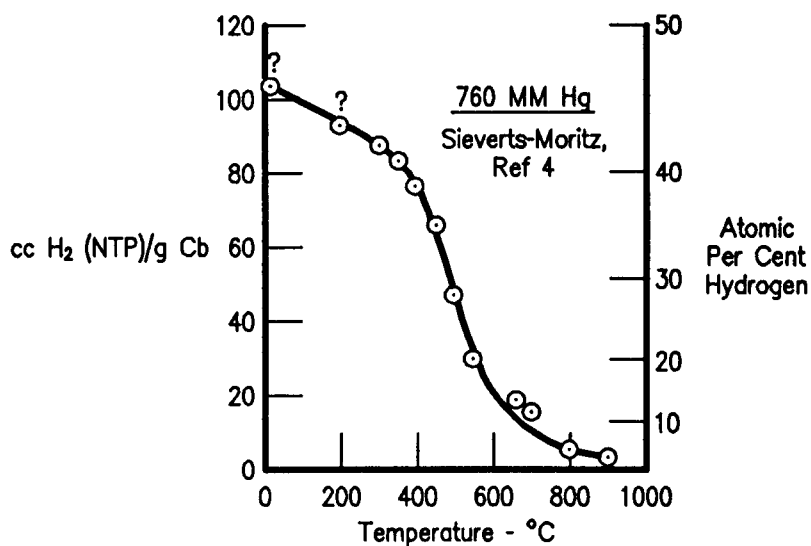


*Figure 4-1. Cross Sections After Grit Blasting to Remove Surface Oxides and Coating*

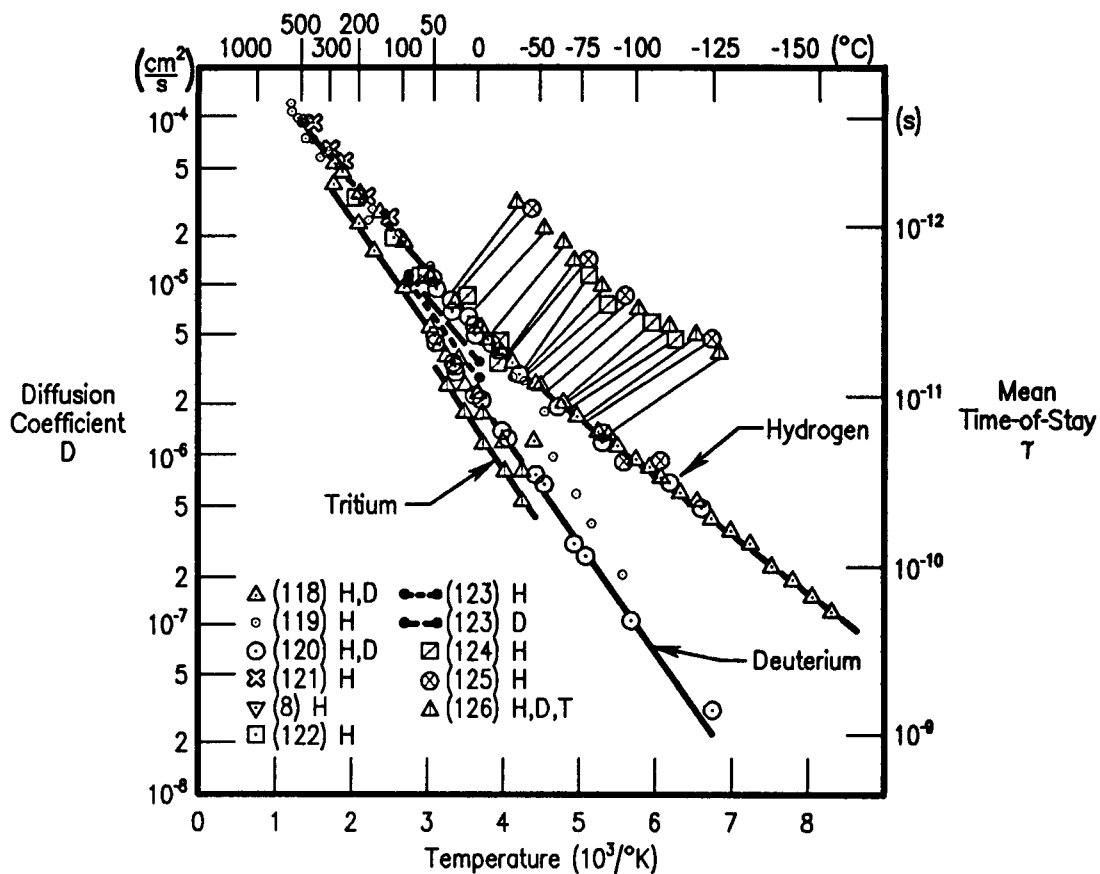


FDA 358412

*Figure 4-2. Schematic of Gas Analysis Locations*



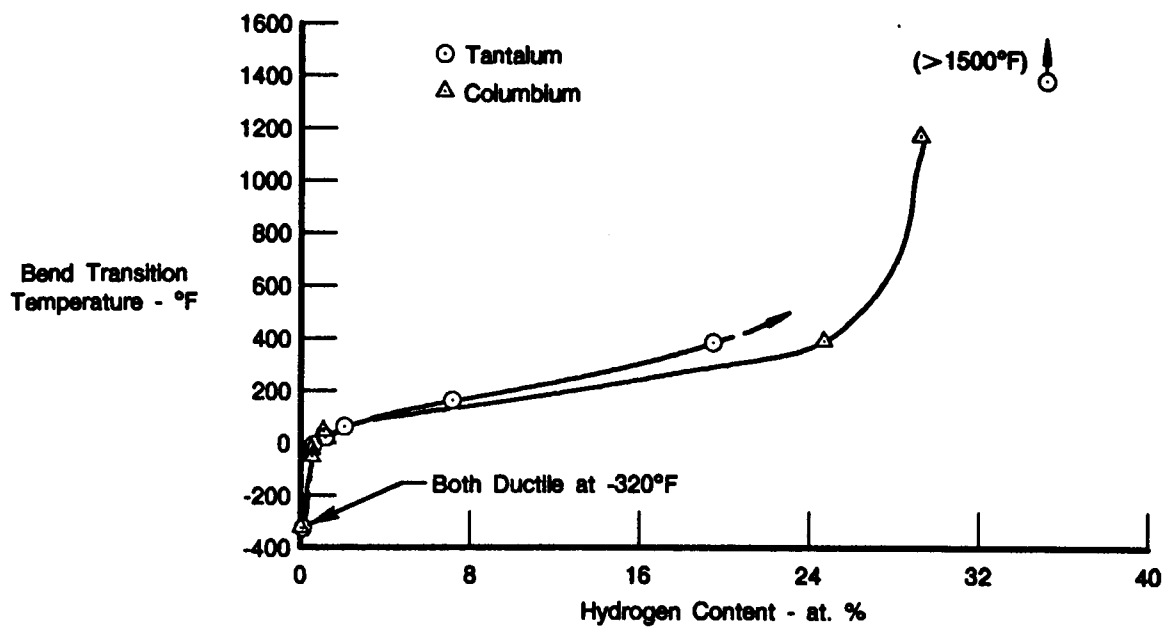
(a) H Solubility in Cb vs Temperature<sup>4</sup>



(b) H Diffusion Coefficient in Cb vs Temperature<sup>5</sup>

FDA 358413

Figure 4-3. Hydrogen/Columbium Data



FDA 358414

Figure 4-4. The Effect of Hydrogen Content on the Ductile-to-Brittle Transition Temperature of Columbium<sup>6</sup>





Mag: 200X  
FD 358415

VH 109

S/N 60321-4



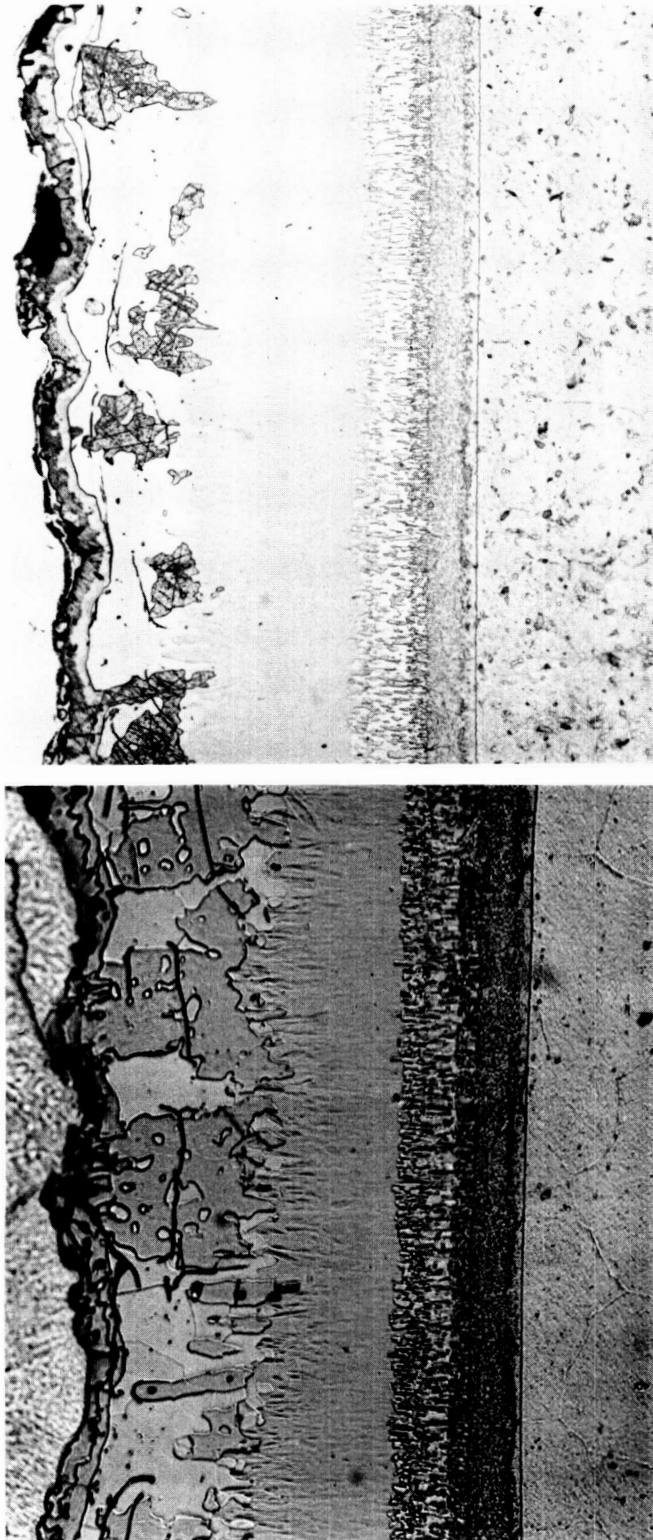
Mag: 200X

R512E

S/N 60317-4

*Figure 4-5. Equivalent Flame-Side Microstructures of R512-E and VH-109 After Engine Exposure — Run Time: 4451 seconds — Start/Stop Cycles: 23*

ORIGINAL PAGE IS  
OF POOR QUALITY

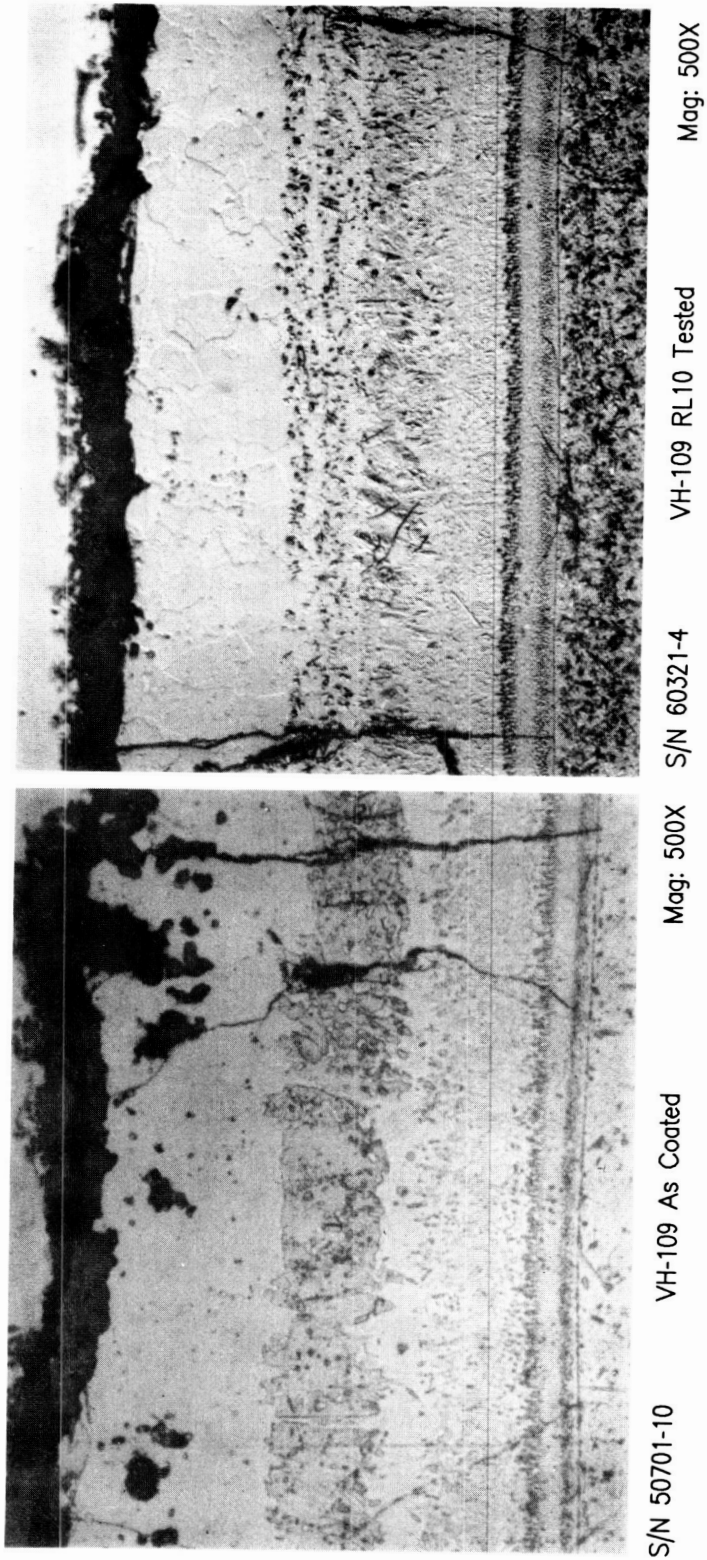


Mag: 500X  
FD 358416

R512E RL10 Tested

S/N 60317-4

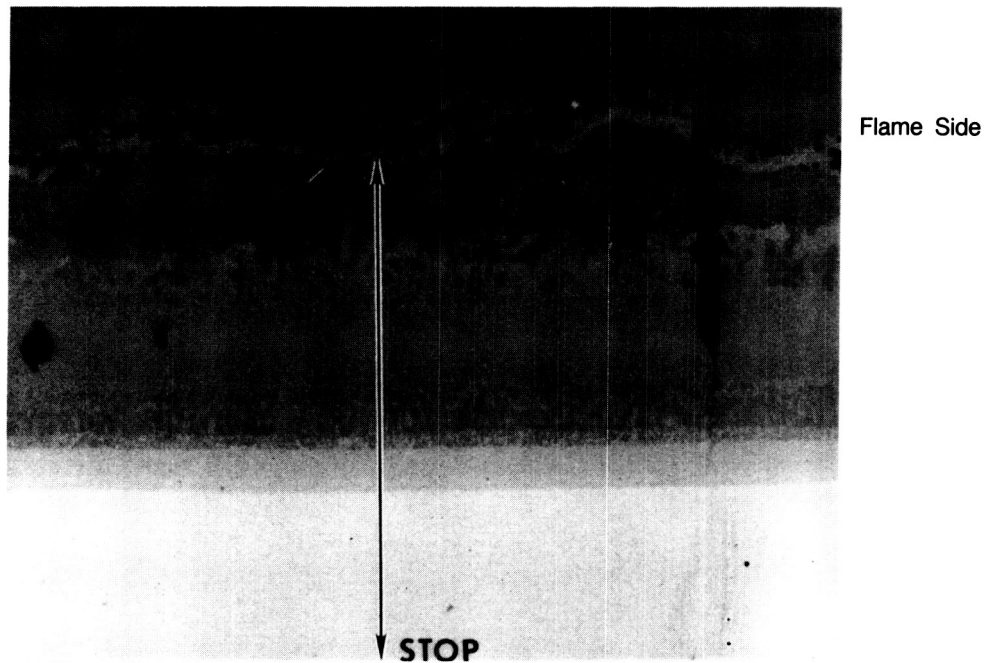
*Figure 4-6. Pretest and Post Test Flame-Side Microstructures of R512-E*



FD 358417

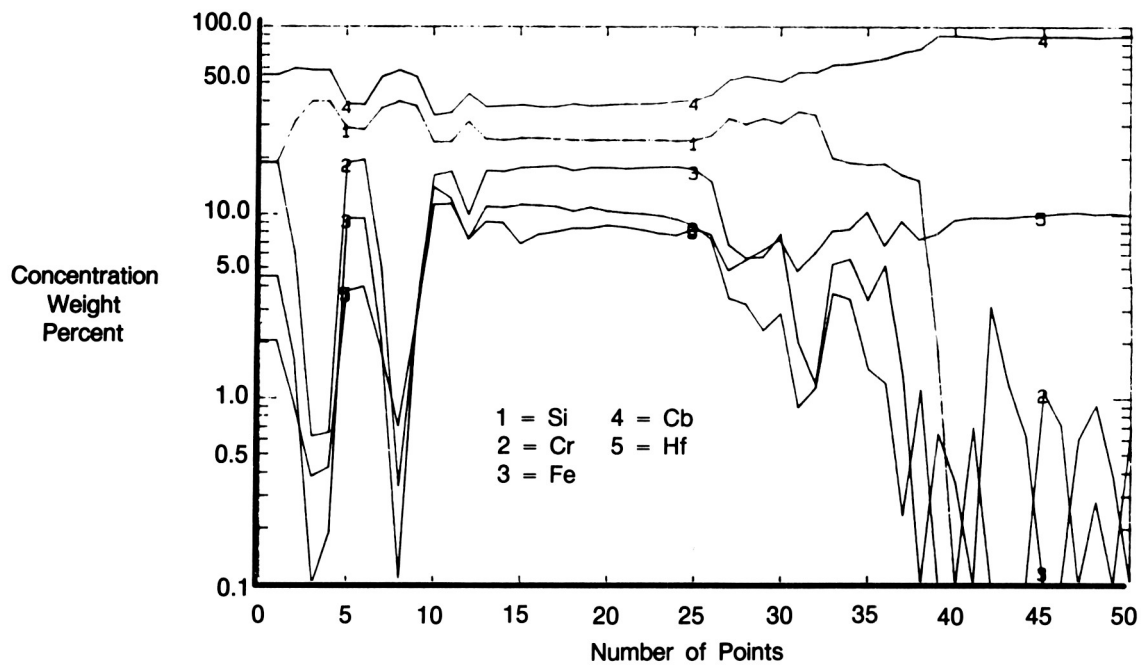
*Figure 4-7. Pretest and Post Test Flame-Side Microstructures of VH-109*

ORIGINAL PAGE IS  
OF POOR QUALITY



S/N 50318-4

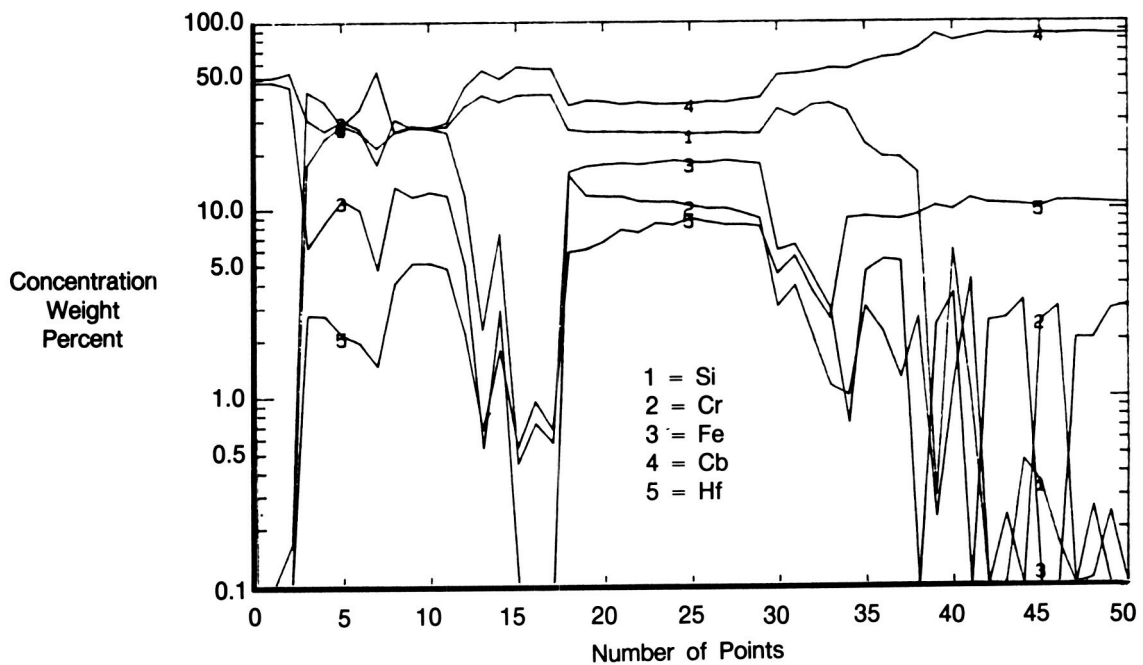
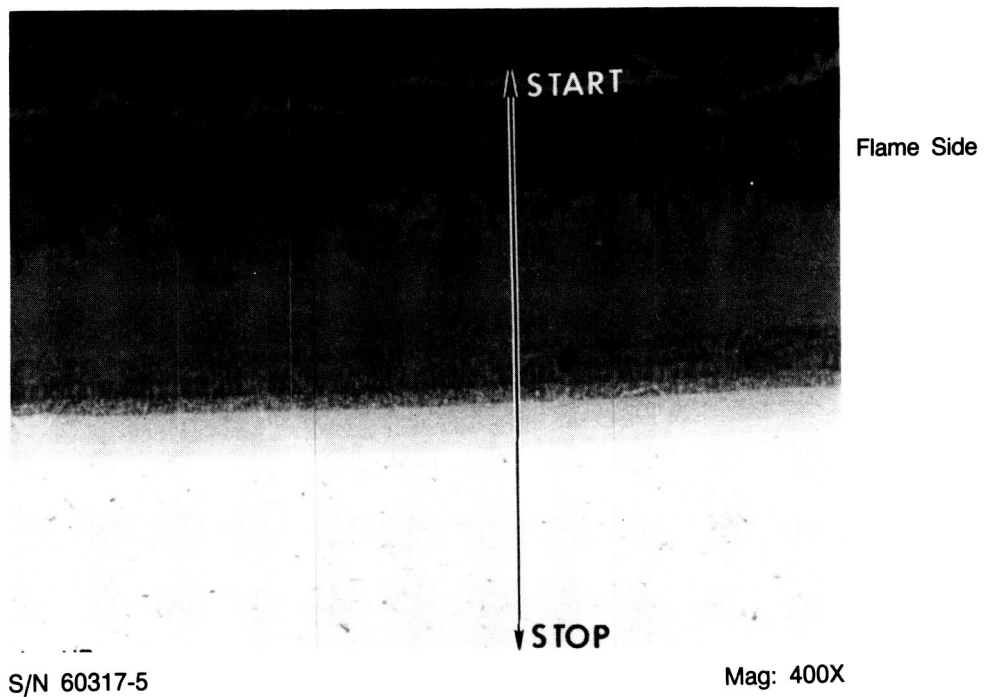
Mag: 200X



FD 358418

Figure 4-8. As-Coated R512-E Composition Profile

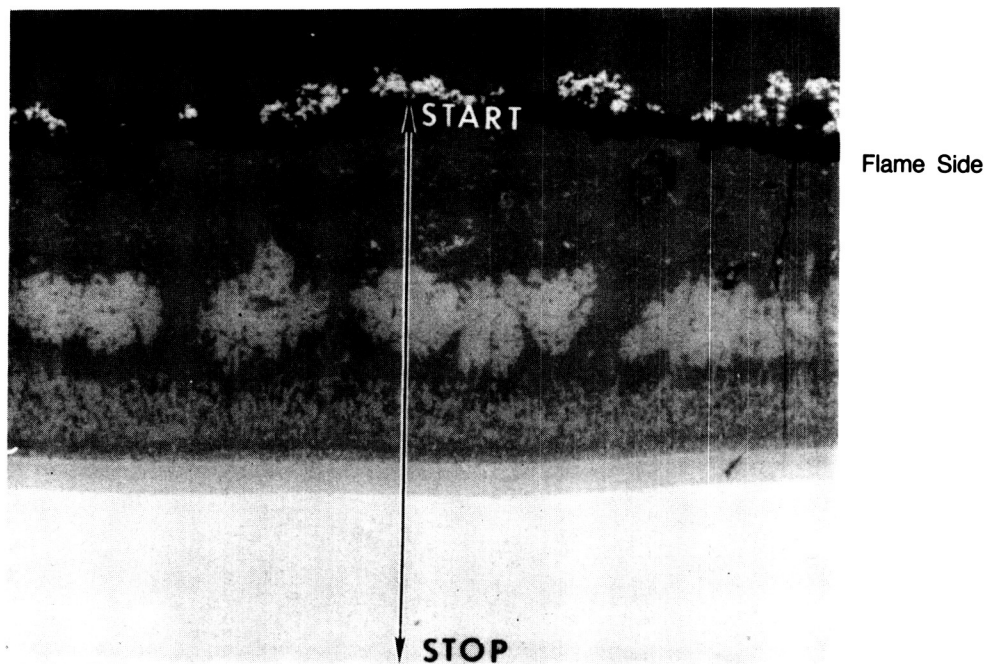
Run Time: 4451 sec  
Start/Stop Cycles: 23



FD 358419

Figure 4-9. Engine Tested R512-E Composition Profile of Region 5 — Run Time: 4451 seconds — Start/Stop Cycles: 23

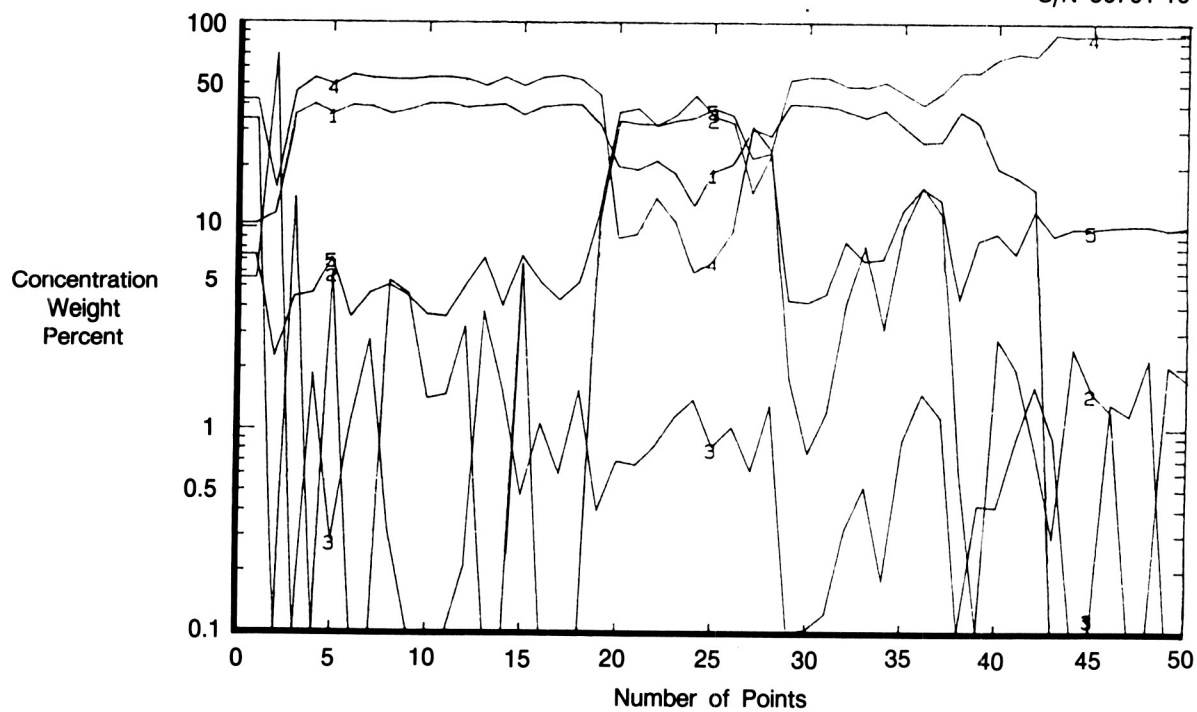
ORIGINAL PAGE IS  
OF POOR QUALITY



Mag: 400X

1 = Si    4 = Cb  
2 = Cr    5 = Hf  
3 = Fe

S/N 50701-10

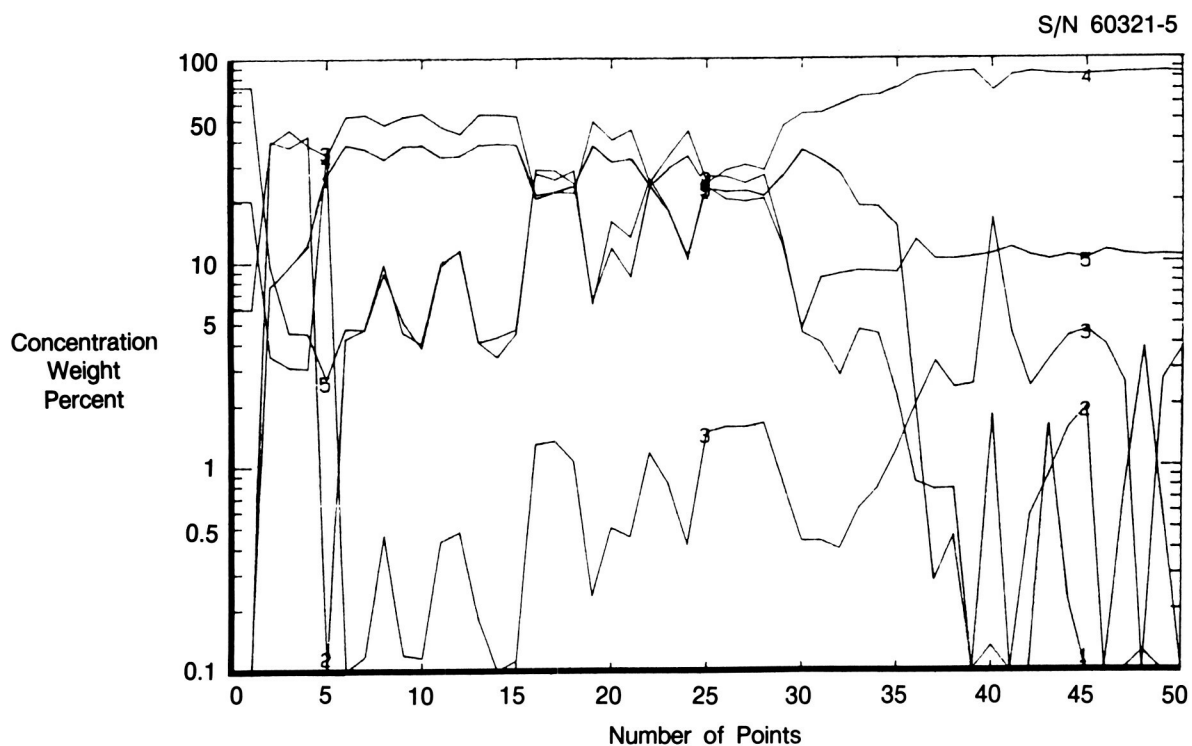
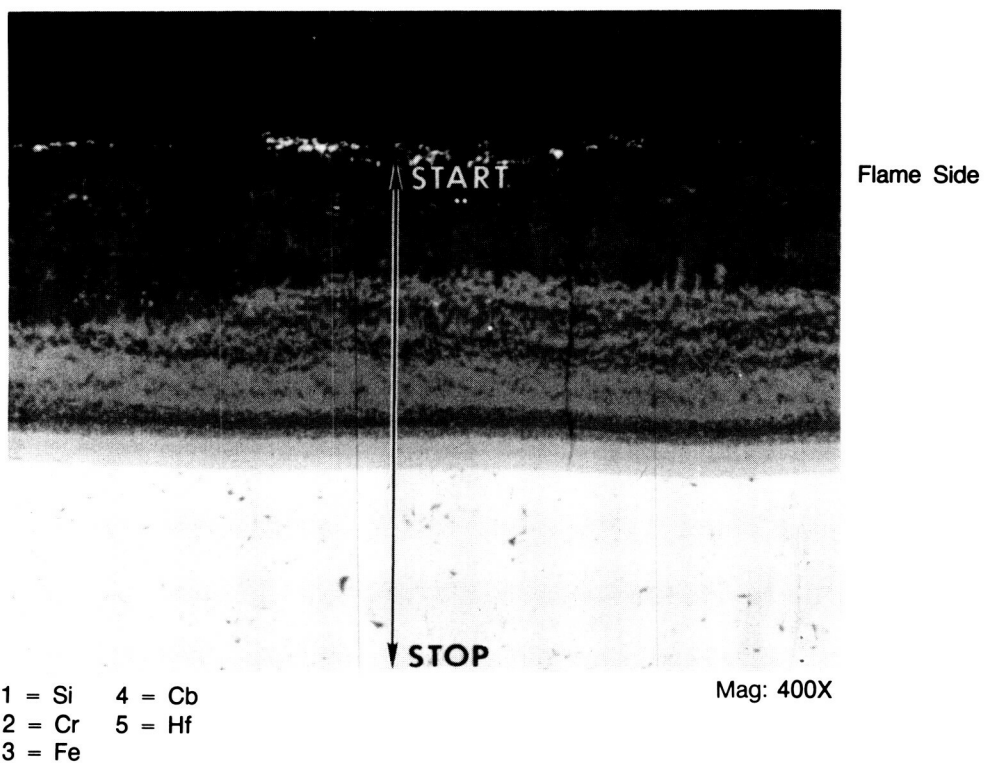


FD 358420

Figure 4-10. As-Coated VH-109 Composition Profile

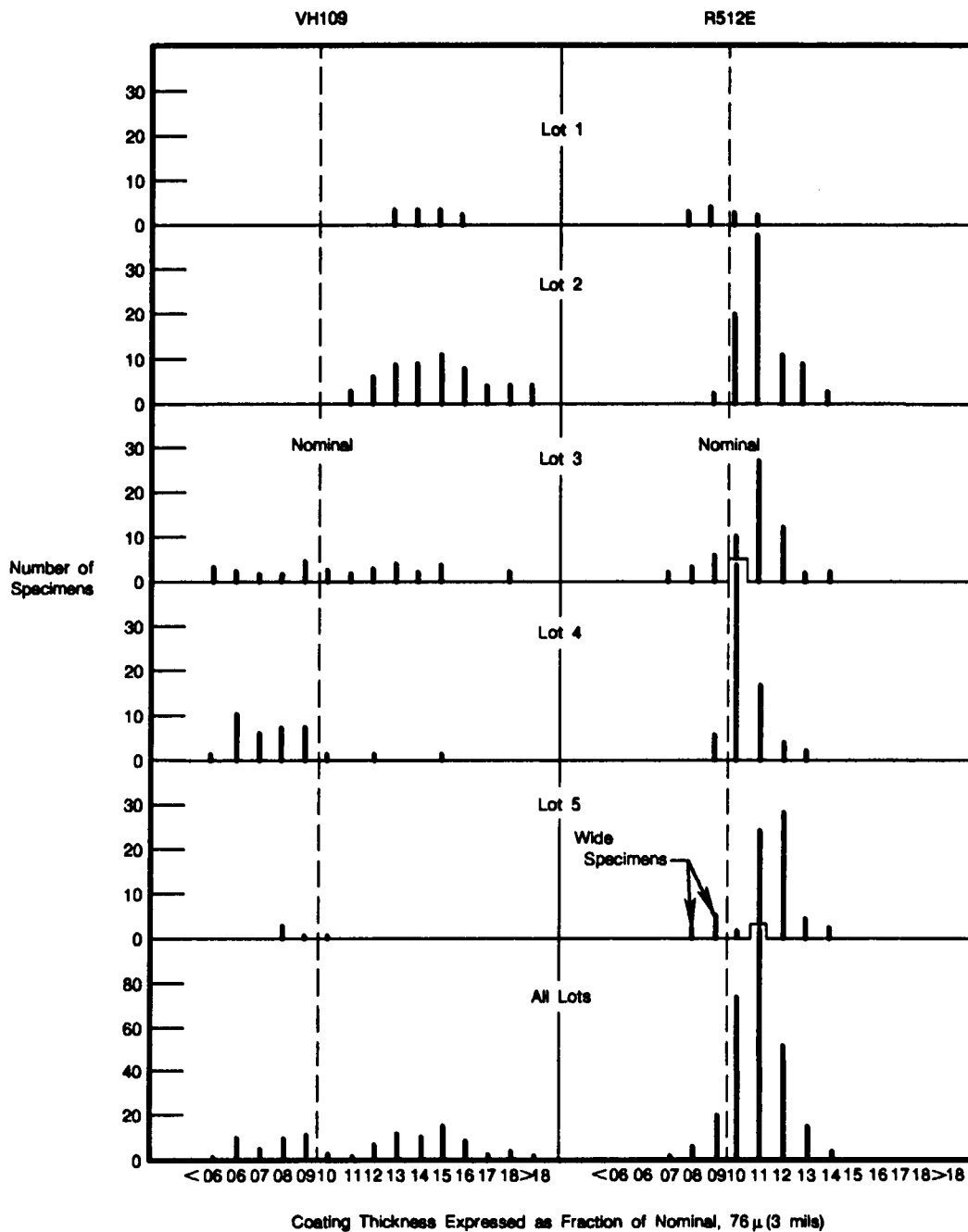


ORIGINAL PAGE IS  
OF POOR QUALITY.



FD 358421

Figure 4-11. Engine Tested VH-109 Composition Profile of Region 5 — Run Time: 4451 seconds — Start/Stop Cycles: 23



FDA 358422

Figure 5-1. Coating Thickness Reproducibility Assessment for VH-109 and R512-E<sup>6</sup>

1. Report No. CR-180809		2. Government Accession No.		3. Recipient's Catalog No.	
4. Title and Subtitle Evaluation of Coated Columbium Test Panels Having Application to a Secondary Nozzle Extension for the RL10 Rocket Engine System; Parts I and II				5. Report Date December 1988	
				6. Performing Organization Code L-27272 L-28198	
7. Author(s) Kenneth S. Murphy				8. Performing Organization Report No.	
				10. Work Unit No.	
9. Performing Organization Name and Address Pratt and Whitney Aircraft P. O. Box 109600 West Palm Beach, FL 33410-9600				11. Contract or Grant No. NAS3-24238 NAS3-25052 NAS3-24738	
				13. Type of Report and Period Covered Topical Report 1/85 - 8/86	
12. Sponsoring Agency Name and Address NASA Lewis Research Center 21000 Brookpark Road Cleveland, OH 44135				14. Sponsoring Agency Code	
15. Supplementary Notes Program Technical Monitor: Richard L. DeWitt, NASA Lewis Research Center, Cleveland Ohio Program Manager: James A. Burkhart, NASA Lewis Research Center, Cleveland, OH					
16. Abstract <p>To increase the specific impulse of the RL10 LH2/O2 rocket engine, a nozzle extension (i.e., secondary nozzle) has been proposed. The extension will translate between stowed and deployed positions. When stowed, the extension will be nested with the cryogenically cooled RL10 nozzle. When extended, it will comprise a smooth continuation of the contour of the regeneratively cooled section of the primary nozzle.</p> <p>A commercially available columbium (niobium) alloy, Cb103, has been chosen as a possible structural material for a secondary nozzle application. This alloy has the necessary high temperature strength properties that are estimated to be required. However, since Cb103 is susceptible to Hydrogen embrittlement as well as high temperature oxidation, a coating must be applied to protect the alloy.</p> <p>Small coated panels, nominally 4 inches by 6 inches, of seven commercially coated Cb103 systems, were screened in an "as received" condition in preparation for the RL10 engine testing of similarly coated panels. Subsequently, panels of two of the systems were fixtured to the exit plane of an RL10 to simulate operating conditions of a radiantly cooled nozzle extension. After 4451 sec of exposure, they were removed and evaluated. One of the two coatings showed no significant change in microstructural features after the engine test; the other showed thickness variability, secondary phase instability, and porosity in the coating.</p>					
17. Key Words (Suggested by Author(s)) Expander Cycle Engine Space Propulsion Systems Variable Thrust Rockets Rocket Nozzles Liquid Propellant Rockets Hydrogen/Oxygen Engine				18. Distribution Statement General Release	
19. Security Classif. (of this report) Unclassified		20. Security Classif. (of this page) Unclassified		21. No. of pages 133	
				22. Price*	

\*For sale by the National Technical Information Service, Springfield, Virginia 22161